ADDIS ABABA UNIVERSITY
ADDIS ABABA INSTITUTE OF TECHNOLOGY
SCHOOL OF MECHANICAL AND INDUSTRIAL ENGINEERING

DESIGN OF SMALL SCALE WIND TURBINE BLADE FOR RURAL VILLAGES ELECTRIFICATION

By

KASSAHUN GASHU

Advisor

MULUGETA HABETEMARIAM

(PhD. Candidate)

Addis Ababa, Ethiopia
October, 2014

DESIGN OF SMALL SCALE WIND TURBINE BLADE FOR RURAL VILLAGES ELECTRIFICATION

By

KASSAHUN GASHU

A thesis submitted to the school of Mechanical and Industrial Engineering Addis Ababa institute of Technology in partial fulfillment of the Degree of Master of Science in Mechanical Engineering (Specialization Mechanical Design)

Advisor

MULUGETA HABETEMARIAM

(PhD. Candidate)

Addis Ababa, Ethiopia

October, 2014

ADDIS ABABA UNIVERSITY
ADDIS ABABA INSTITUTE OF TECHNOLOGY
SCHOOL OF MECHANICAL AND INDUSTRIAL ENGINEERING

DESIGN OF SMALL SCALE WIND TURBINE BLADE FOR RURAL VILLAGES ELECTRIFICATION

By

KASSAHUN GASHU

Approved by Board of Examiners:

Dr._____	***_____***	***_____***
Chairman, Department Graduate Committee	***Signature***	***Date***
MULUGETA HABETEMARIAM		
(PhD. Candidate)	***_____***	***_____***
Advisor	***Signature***	***Date***
Dr. _____	***_____***	***_____***
External Examiner	***Signature***	***Date***
Dr. _____	***_____***	***_____***
Internal Examiner	***Signature***	***Date***

Acknowledgment:

First, I would like to express my heartfelt appreciation and gratitude to my advisor Mulugeta Habetemariam (PhD. Candidate), for his continual encouragement and patient guidance throughout the course of this work. I especially thank my advisor for his patience, respectable and trust during the study.

I also would like to thank all my colleagues and friends for their supports especially Ato Behailu Mamo, Ato Yidenkachew Messele , Ato Araya and Ato Andenet Kumella. Their helpful comments during the research and writing of this thesis are appreciated.

Finally, I would like to take this opportunity to thank all my families specially, my mother W/ro Shitaye Adamu, my brother Ato Zewdu Gutema, my fiancée Seble Alemu and my friends for all their help and understanding. Without them encouragement, love and support, this work would never have been accomplished.

Table of Contents:

List of Figures:

List of Tables:

NOMENCLATURE:

D : Drag force

F_x :Axial force

F_θ :Tangential force

L :Lift force, angular moment

p : Pressure

P : Power

Q :Tip loss correction factor

r : radius and radial direction

R :Blade tip radius

R_L : Resultant load

l : blade length

T : Torque

V : Absolute velocity

W : Relative velocity

V : maximum wind speed

x : Axial coordinate

β : Relative flow angle onto blades

λ : Tip speed ratio

λ_r : Local Tip speed ratio

η : Mechanical/electrical efficiency

ρ : Density

σ' : Local Solidity

θ :Tangential coordinate

Ω :Blade rotational speed

ω : Wake rotational speed

γ : Aerofoil inlet angle

C_P : power coefficient of wind turbine rotor

C_T : thrust coefficient of wind turbine rotor

$\dot{m}$: air mass flow rate through rotor plane

A : area of wind turbine rotor

$\mathbf{Z}$: section modulus

I : area moment

N : number of blade elements

B : number of blades of a rotor

a : axial induction factor at rotor plane

a' : angular induction factor

c : blade chord length

ρ : air density

α : angle of attack

$\boldsymbol{Z}$: the position of the maximum camber

M : the maximum camber

XX : the thickness Airfoil

$HAWT$: horizontal-axis wind turbine

$VAWT$: vertical-axis wind turbine

BEM : blade element-momentum theory

TSR : tip-speed ratio

$NACA$: National Advisory Committee for Aeronautics

Abstract:

Designing small scale horizontal-axis wind turbine (HAWT) blade to achieve satisfactory levels of performance starts with knowledge of the aerodynamic forces acting on the blade. In this thesis Blade-element momentum theory (BEM) known as also strip theory, which is the current mainstay of aerodynamic design and analysis of HAWT blade, is used for HAWT blade design.

The blade design program includes blade geometry parameters (chord-length and twist distributions) and design conditions (design tip-speed ratio, design power coefficient and rotor diameter) with the following inputs; power required from a turbine, number of blades, environmental wind velocity at Negele Borana and blade profile type (airfoil type).

This thesis, focused on the design and stress analysis of small scale wind turbine blade which built for the specific environmental conditions of the small rural village for Laga-Gula kebele communities at Negele Borana. First the blade designed from the aspect of aerodynamic view and the basic principles of the aerodynamic behaviors of HAWT studied. Second modeling and stress analysis of the wind turbine blade are very critically for the further design and application of wind turbine. The small-scale wind turbine blade was focused on, considering the E-Glass fiber reinforced plastic material. Based on the parameters of airfoil and the geometrical parameters of blade, the three-dimension and the assembly models of blades were established with the SOLIDWORK modeling software. Then the models were imported into ANSYS-15 WORKBEANCH software analysis. The displacement, Von Misses and principal stress results are determined. These results show that the positions of maximal displacement and maximum stresses, but it is less than the safety displacement and Ultimate tensile strength (UTS) of the

material, and also it shows the environmental wind speed can produced the sufficient power for Laga-Gula rural kebele communities.

CHAPTER 1

1. INTRODUCTION:

Wind is created by the unequal heating of the Earth's surface by the sun. Wind turbines convert the kinetic energy in wind into mechanical power that runs a generator to produce clean electricity. Today's turbines are versatile modular sources of electricity. Their blades are aerodynamically designed to capture the maximum energy from the wind. The wind turns the blades, which spin a shaft connected to a generator that makes electricity[30].

Wind energy is one of the most abundant renewable energy resource on the earth and has been targeted for centuries. It's predicted that human beings have been using wind energy in their daily work [3]. Energy services and appropriate energy technologies are vital for the social and economic development of Ethiopia. However, a few rural inhabitants have access to any kind of electricity. In these regions, energy needs are met by polluting and unhealthy energy sources such as traditional biomass (wood fuel and charcoal) and fossil fuels. Besides that, if electricity is available, most commonly delivered to the grid, which suffers from power cuts and growing cost [4].

Because of the country's favorable wind regimes, small wind turbines are a relevant option to electrify rural areas with sufficient wind resources. This option is especially attractive for regions where it is out of grid. The technology is available in a whole range of sizes and can fulfill rural energy needs at all levels of society. Smaller wind systems (<1.5kW) are suitable for household usage, small businesses and farmers. Wind energy is the kinetic energy associated with the movement of atmospheric air due to uneven heating and cooling of the earth's surface. This is a renewable energy resource and a popular form for extracting power for humankind. Wind energy is a potential clean energy resource which is currently used to produce energy and will without doubt remain constant in the future. Wind energy contrasts with other forms of energy such as biomass or fossil fuel which have limitations namely, massive carbon dioxide emissions, threat to the atmosphere, and so on which results in a loss of their acceptability for use in energy production [1]. Wind energy which comes from air current flowing across the earth's surface is a source of renewable power. Wind turbines harvest this kinetic energy and convert it into electricity power for homes, farms, schools, or business applications on small or large scales.

Different wind turbines with various capacities are used to extract power from the wind. Horizontal Axis Wind turbine (HAWT) and Vertical Axis Wind turbine (VAWT) are the most common types of wind turbines currently being used for energy production from wind. This study is concerned with a small scale horizontal axis wind turbine blade (HAWT). The classical or horizontal axis wind turbine can be confidently attributed to European designers independent of the oriental vertical axis systems. The first documented historical evidence of horizontal axis wind mills dates back to 1180 which tells of a wind mill called a post or trestle mill present in the Dutch Normandy. From there on the post mill quickly spread throughout Europe and was then further developed into the tower mill two centuries later. In the 16th century the Dutch wind mill was developed in Holland which composed of a mill house with a rotating tower cap and rotor blades. This design is still in practical use today throughout the Netherlands and other European countries for traditional milling processes [1].

For several decades now the wind energy industry has focused on the generation of electricity from large wind turbines located in exposed locations with high mean wind speeds, such as hilltops and coastal waters. In recent years an increasing number of manufacturers have produced small scale wind turbines suitable for use by individual householders or small businesses. Although the definition of 'small wind systems' is generally accepted to include any devices up to a rated power of less than 40kW (typically less than 12m diameter), turbines for domestic applications are generally less than a few meters in diameter and generate $0.5-1.5$ kW of power [1]. It can be mounted on roof-tops or free-standing poles and are usually connected to the user's distribution board (fuse box). The electricity that is generated can be used directly on site, with any surplus being fed into the electricity for small villages.

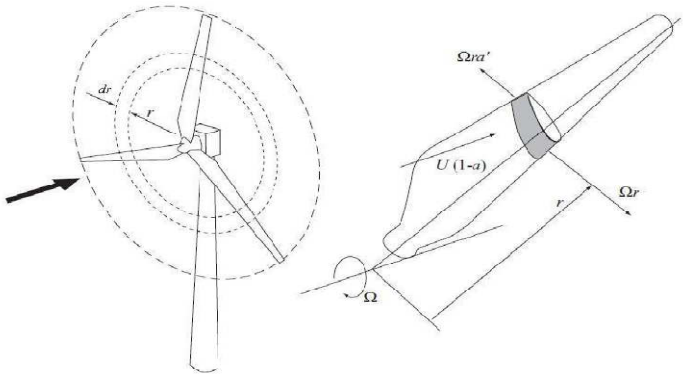

Figure 1.1 A blade element sweeps out an annular ring (Source: Burton *et al.*, 2001)

The need for electricity in the rural villages of Ethiopia is a prime importance due to the sort of evolved life mankind leads. The production of power using traditional methods has taken its toll on the environment and the earth has been polluted to degrees beyond imagination. Alternative energy and green energy from natural recourses is the need of the hour. Technology must be used so as to provide human need and luxuries, but still not affect our rural villages. Wind is such a resource available that it just blows everywhere, from large areas to local winds it just blows. There are various phenomenon's' which makes the flow of wind across the globe. This research envision the design of a small scale wind turbine for rural village electric power generation from $0.5-1.5$ kW. The aim of the research is to design and stress analysis of a wind energy converter comprising of a rotor system, by selecting a gearbox, tower and a generator that will successfully produce the specified electrical power. As wind turbines are not new technology the project will be aimed at proving and Optimizing a system based on existing technology to achieve the desired power output. Considerations are taken in designing the turbine with an effective post life recycling scheme in mind so that there will be minimum wastage of resources once the turbine is made redundant.

Ultimately the aim of this thesis is to make use of a natural resource to supply mankind's energy requirements in a sustainable manner. If a wind turbine can be designed and constructed so that it can produce more power on its life time. It is obvious now that we are facing an oncoming energy shortage. Fossil fuel prices are rising in conjunction with the decrease in their stockpiles and it is vital that alternative methods of energy production be investigated and introduced on a global scale to maintain our standard of life. Wind energy has the potential to meet our requirements and several nations have already begun effectively producing and harvesting this form of green energy.

1.1 OBJECTIVE:

As previously mentioned, the electricity producing wind turbine is an already existing technology in Ethiopia and this thesis is focused on redesigning and adapting mechanical and electrical engineering principles to design new small wind turbine blade and perform stress analysis on the blade by using computer programs on SOLIDWORK and ANSYS 15 WORK BEANCH to realize the specified energy output for rural villages in the country.

Realistically the simplest method to realize the goal in this thesis would be to design an existing turbine because of the environmental wind speed limitation at Negele Borana until its power output fell into the category of $0.5-1.5$ kW. However it is vital that a good understanding of the concepts and principles behind small scale wind turbine design is developed so that existing methods of wind energy production can be improved and made more efficient.

The main objectives of the thesis are:

- To design a suitable small scale wind turbine blade using the Blade Element Momentum (BEM) Theory, it is run by a minimum average environmental wind speed for Laga-Gula rural kebele communities at Negele Borana zone of Oromiya.

The specific objectives of the thesis are:

- To develop a mathematical analysis of stress,
- To collect a mean wind speed data of Negele town from Federal Water and Energy Minister of Ethiopia deepened on the standard at 10m height of tower and to select a composite material arrangement of fiber with matrix.
- To develop a Model, Deformation and Stress analysis on the blade by using computer programs on SOLIDWORK and ANSYS 15 WORK BEANCH.

1.2 STATEMENT OF THE PROBLEM:

Electricity is the basic need for the population and the economy. In Ethiopia, much of the population lives in relative poverty and energy insecurity. As stated above, Laga-Gula rural kebele communities at Negele Borana zone of Oromiya do not have access to electricity. The implementation of small scale wind turbine for electric power generation is feasible alternative to be implemented in the short run to electrify the communities in Laga-Gula kebele.

Small scale wind turbines proposed to provide electric power for residential homes, primary schools, a health center, and for battery charging. This study therefore making design of small scale wind turbines with a capacity of generating power from 0.5 to 1.5 kW; and the affordability of the wind energy systems in rural environment in Laga-Gula kebele; and makes the necessary recommendations for future development.

1.3 ORGANIZATION OF THE PAPER:

This thesis has been divided into six chapters. *Chapter 1* is 'Introduction', which covers a brief account of the current status of wind energy worldwide and in Ethiopia. *Chapter 2* Background and Literature reviews, discussed historical background of small scale wind turbines, and the methods of previous thesis, journals and books related to small scale wind turbine blades. *Chapter 3*, the aerodynamic and design behaviors of horizontal-axis wind turbines are dealt with in detail. All theories on aerodynamic of horizontal-axis wind turbines are examined under separate subtitles for each and the blade design procedure is given based on the BEM theory. How airfoil characteristics affect the performance of a blade is discussed as well. Design procedure is then studied for a designed blade and the validity of an approximation used for determining the optimum relative wind angle for a certain local tip-speed ratio is explained and illustrated with figures. *Chapter 4*, structural design of HAWT blade. *Chapter 5*, covers all the numerical results and discussion of results obtained in the thesis. Finally, *Chapter 6*, gives a conclusion to the thesis, its contribution and possible future research directions.

CHAPTER 2
BACKGRAOUND AND LITERATURE REVIEW

2.1 BACKGRAOUND:

Energy is vital for economic and social development of the world, according to international energy agency- world energy outlook (2012) [3], the traditional use of biomass for cooking, but there are also around 400 million people that rely on coal for cooking and heating purposes, which causes air pollution and has serious potential health implications when used in traditional stoves to satisfy to its energy demand they consume in inefficient open fire mechanism, it is environmentally unfriendly, the populations are lives in China, South Africa and India) [3].

Some of the sources of energy are: Nuclear power plant, Fossil fuel power plant, Hydroelectric Power plant, Wind power and Solar power

A wind turbine utilizes the power from the wind to generate electric power. Several wind turbines can be sited in the same area to form a wind farm.

Figure2.1 Adama Wind power plant

2.1.1 Large scale vs. small scale wind turbines:

The definition of “small” and “large” scale windmill has remained vague in the literature of wind energy. Small wind turbine was initially defined on the basis of its capability to produce electrical power sufficient enough to cover individual household electricity demands. But the problem lies in the fact that the consumption of electricity by a household itself is very debatable because it varies with time and place. For example, an average American family needs a 10 kW turbine to cover their full consumption, while a European household requires a 4 kW turbine, which further reduces to a 1.5 kW turbine for an average Chinese household. Lacking any credible unanimous definition, the range for the rated power capacity of small scale wind turbines vary from few watts to few hundred kilowatts [2] . The size of the wind turbine need depends on application. Small turbines range in size from 20 watts to 100 kilowatts (kW). The smaller or “micro” (20- to 500-watt) turbines are used in a variety of applications such as charging batteries for recreational vehicles and sailboats[30]. To bring consistency in discussion, we define a nomenclature in this report based on the size of the horizontal axis wind turbine rotors as follows:

Table 2.1 Scale classification of wind turbines[2]

Scale	Rotor Diameter	Power Rating
Small	Less than 12 m	Less than 40kW
Medium	12 m to 45 m	40kW to 999kW
Large	46 m and larger	1.0 MW and larger

Access to modern energy is a key element in rural development .However, despite all attention given to energy issues in Ethiopia in the past rural communities continue to be deprived of basic energy services. Modern forms of energy are simply not available in rural areas while traditional sources are rapidly being depleted like traditional biomass energy (wood fuels, crop residues, and cattle dung), there by deepening the rural energy crises.

According to (Nation Master; 2013), Ethiopia has one of the lowest levels of electric power consumption per capital in the world, which is 32.675kWh per capital[3].

According to the World Energy Outlook (2010)estimated national electricity access at 17% of the population in 2009 of the Ethiopian population has access to electricity[3].

The energy consumption of the country is dominated by a heavy reliance on traditional biomass energy (wood fuels, crop residues, and cattle dung), which accounts for 92 % of total energy consumption in Ethiopia by 2009,Petroleum and electricity contribute only 7% and 1% respective[3].

According to the World Bank report on 2012, 82.4% of Ethiopian population lives in rural areas and the remaining 17.6 % in urban areas, there is a significant bias between the power supply of urban and rural population. According to the World Energy Outlook (2012), urban electricity access is estimated at 80 % while only 2% of rural households have access to electricity[3].

The Energy Sector in Ethiopia is expanding rapidly; the problem of water level fluctuating will not be solved completely even with the construction of large scale hydro power plants. Most of the dams faced shortage of water due to hydrological problems resulted from climate change. Hence, the power generation system has to be diversified. In the short-run it is necessary to increase the current power generation mix, to cover increasing and unsatisfied power demand and to avoid dependence on fuel imports. To overcome this effect modernizing the use small scale wind turbines can generate 0.5 - 1kW at the height of 10-12 m to bring better efficiency shall be advantageous. A study on the environmental impacts of wind energy projects, Environmental Impacts of Wind-Energy Projects (2007, National research council (US)),

[3]. highlights some important positive factors that support the development of wind energy farms. Wind turbines are a viable medium of energy production in that they can produce our energy requirements in place of other methods and do not have the same harmful effects on the environment. Wind turbines do not pollute our air or water with polluted or toxic bi-products of energy production. Directly, their operation only affects the wind speed directly behind the rotor blades. Other organizations have however drawn attention to some adverse environmental effects.

These include the visual effect they have on humans, the interference on the ecosystem; birds and bats –rotor blades, and the increase in transport infrastructure and power lines to the wind farm site

2.1.2 Basic Parts of small wind Turbine:

Small wind turbine generally comprise a rotor, a generator or alternator mounted on a frame, a tail (usually), a tower, wiring, and the "balance of system" components: controllers, inverters, and/or batteries. Through the spinning blades, the rotor captures the kinetic energy of the wind and converts it into rotary motion to drive the generator[30].

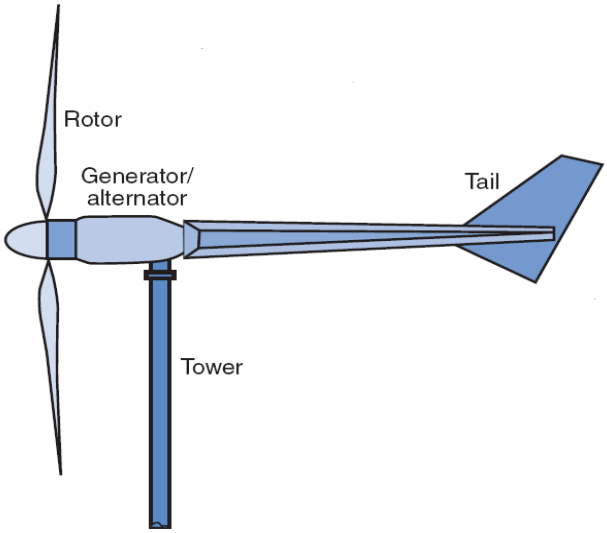

Figure 2.2 Basic Parts of small wind Turbine [30].

i. Turbine:

Most turbines manufactured today are horizontal axis upwind machines with three blades, which are usually made of a composite material such as fiberglass reinforced plastic(GRP). The amount of power a turbine will produce is determined primarily by the diameter of its rotor. The diameter of the rotor defines its "swept area," or the quantity of wind intercepted by the turbine. The turbine's frame is the structure onto which the rotor, generator, and tail are attached. The tail keeps the turbine facing into the wind[30].

ii. Tower:

Because wind speeds increase with height, the turbine is mounted on a tower. In general, the higher the tower, the more power the wind system can produce. The tower also raises the turbine above the air turbulence that can exist close to the ground because of obstructions such as hills, buildings, and trees. A general rule of thumb is to install a wind turbine on a tower with the bottom of the rotor blades at least 9 meters above any obstacle that is within 90 meters of the tower. Relatively small investments in increased tower height can yield very high rates of return in power production. There are two basic types of towers, self-supporting (free standing) and guyed. Most small wind turbine power systems use a guyed tower. Guyed towers, which are the least expensive, can consist of lattice sections, pipe, or tubing (depending on the design), and supporting guy wires. They are easier to install than self-supporting towers. However, because the guy radius must be one-half to three-quarters of the tower height, guyed towers require enough space to accommodate them[30].

iii. Balance of System:

The parts in addition to the turbine and the tower, or the balance of system parts, will depend on the application. The balance of system required will depend on whether the system is grid-connected, standalone, or part of a hybrid system. For a residential grid-connected application, the balance of system parts may include a controller, storage batteries, a power conditioning unit (inverter), and wiring[30].

iv. Stand-Alone Systems:

Stand-alone systems (systems not connected to the utility grid) require batteries to store excess power generated for use when the wind is calm. They also need a charge controller to keep the batteries from overcharging. Deep-cycle batteries, such as those used for golf carts, can discharge and recharge 80% of their capacity hundreds of times, which makes them a good option for remote renewable energy systems.

Automotive batteries are shallow-cycle batteries and should not be used in renewable energy systems because of their short life in deep-cycling operations. Small wind turbines generate direct current (DC) electricity. In very small systems, DC appliances operate directly off the batteries. Use standard appliances that use conventional household alternating current (AC), must install an inverter to convert DC electricity from the batteries to AC. Although the inverter slightly lowers the overall efficiency of the system, it allows the home to be wired for AC, a definite plus with lenders, electrical code officials, and future homebuyers. For safety, batteries should be isolated from living areas and electronics because they contain corrosive and explosive substances. Lead-acid batteries also require protection from temperature extremes[30].

V. Grid-Connected Systems:

In grid-connected systems, the only additional equipment required is a power conditioning unit (regulation and conversion) that makes the turbine output electrically compatible with the utility grid[30].

2.1.3 Negele Borana :

Negele Borana is a town and separate woreda in southern Ethiopia. Located in the Gujii Zone of the Oromia region on the road connecting Addis Aaba to Dolo Odo, it is the largest town in the region traditionally inhabited by the Borana Oromo. It has a attitude and longitude of $5^0$20'N $39^0$35'E / 5.333N 39.583^{0}E with an altitude of about 1,475 meters (4,839 ft) above sea level. The town is reported the electrical power was introduced by a branch of the Ethiopian Electric Light and Power (EELPA), and in January 1961 a diesel- driven 120kW electric power plant for the town was completed. A 2004 report states that Negele Borana is supplied with electricity by only the Ethiopian Electric Power Corporation(the successor utility to the EELPA) from the national grid but there is no wind power plant[8].

Figure 2.3 Location of Negele Borana within Ethiopia[8].

2.1.4 Laga-Gulla Kebele:

Laga-Gulla is an rural kebelle in Negele wereda. The 2007 national census of Ethiopia, Statistical Report for Oromiya Region reported a total population of this kebele of 1195, of whom 776 were men and 419 were women and the number of households in the kebele is 193[28].

This rural kebele has high access to wind but the communities do not have access to electricity, for electrification purpose the consumption of wood fuel has far exceeded its supply to the communities .

According to Federal Water and Energy Minister data report this kebele has an average wind speed in the range of 6.13m/s to 8.26m/s at 10m elevation so the implementation of small scale wind turbine is best way to solve the problems of the kebele comunities and also to prevent desert.

2.2 LITERATURE REVIEW:

The contents are an overview of the available literature and a number of authors have written on design and stress analysis of small scale wind turbine blade. Many papers had been published to present the results obtained. Since the late listed, there has been great interest in small scale wind turbine. Therefore, including review of static analysis, and dynamic loading conditions is of paramount importance.

Siraj Ahmed [10] studied design and analysis of horizontal axis wind turbine rotor**.** In his paper, an optimization model for rotor design of 750 kW horizontal axis wind turbine having the blade length of 21.0 m was presented and airfoil type for the blade was S809. The result obtained from ANSYS was compared with the existing design.

Verónica Cabanillas [11] studied blade performance analysis and design improvement of a small wind turbine for rural areas. In his paper, electrification projects based on renewable energy technology was demonstrated to be suitable for providing electricity to rural communities. The turbine was built for the specific environmental conditions of the mountainous region of the Andes rural village in Peru. This thesis focused on the performance identification of the current blades of the IT-PE-100. His result was the optimum combination of the modifications yielded approximately 20% more energy annually produced with high performance in high wind ranges.

Peter J. Schubel and Richard J. Crossley [12], studied wind turbine blade design. They presented that the detailed review of the current state-of art for wind turbine blade design is presented, including theoretical maximum efficiency, propulsion, practical efficiency, HAWT blade design, and blade loads. The review was provided a complete picture of wind turbine blade design and shows the dominance of modern turbines almost exclusive use of horizontal axis rotors. The aerodynamic design principles for a modern wind turbine blade are detailed, included blade plan shape/quantity, aerofoil selection and optimal attack angles, described aerodynamic, gravitational, centrifugal, gyroscopic and operational conditions.

Mulugeta Biadgo [13], studied computer-aided aerodynamic and structural design of horizontal axis wind turbine blades. In his paper detailed review of the designing horizontal-axis wind turbine(HAWT) blades to achieve satisfactory levels of performance starts with knowledge of the aerodynamic forces acting on the blades and HAWT blade design was studied from the aspect of aerodynamic view and the basic principles of the aerodynamic behaviors HAWTs was investigated.

Fadi Abdulhadi [14], studied design and characterization of a Small wind turbine model equipped with a pitching system**.** In this paper detailed a small pitch-controlled wind turbine with a 0.58m rotor diameter was designed, constructed and tested in the wind tunnel. The blade was a prototype of a larger blade that was constructed in an earlier project. His paper concerned two main tasks. First, careful characterization of the small wind turbine was carried out at different wind velocities and pitch setting angles. Second, a pitch control system was implemented to control the power output of the turbine at wind speeds above the rated speed.

Andrew Corbyn [15], studied fiber glass wind turbine blade manufacturing guide. In his paper was revised in blade is comprised of two main halves (both made from fibre glass), a wooden core at the root and a 'stringer' along the inside from root to tip. Once the blade has been constructed and stuck together, a two-part expanding foam is used to fill the structure of the blade helping to add strength and rigidity to the blades

Ravi Anant Kishore [16], studied small-scale wind energy portable turbine (SWEPT). In this paper was provided the first systematic effort towards design and development of SSWTs (rotor diameter<50 cm) targeted to operate at low wind speeds (<5 m/s). An inverse design and optimization tool based on Blade Element Momentum theory was proposed. The utility and efficacy of the tool was validated by demonstrating a 40 cm diameter small-scale wind energy portable turbine (SWEPT) operating in very low wind speed range of 1 m/s−5 m/s with extremely high power coefficient.

Qiyue Song [17], studied design, fabrication, and testing of a new small wind turbine blade. In his paper a small wind turbine blade was designed, fabricated , tested and the power performance of small horizontal axis wind turbines was simulated in detail using modified blade element momentum methods (BEM). Various factors such as tip loss, drag coefficient, and wake were considered. The simulation was validated by experimental data collected from a small wind turbine Bergey XL 1.0. A new blade was designed for the Bergey XL 1.0 after comparing three types of aerodynamic blade structures and their related performance, and then the detailed blade structure was determined. The performance of the new rotor at different additional pitch angles was simulated and compared with the original Bergey XL 1.0 rotor.

Jason R.etal.2011 [18], studied design and experimental testing of small-scale wind turbines. They presented that the increasing environmental and economic cost of fossil fuels, alternative sources of energy were needed. Much of the current wind turbine research focused on large-scale wind turbines. An alternative approach is small-scale wind turbines designed specifically to produce power at low wind speeds. This thesis investigated the design and testing of these turbines. Concerned specific to small-scale design, such as low Reynolds number flow, separation, and low wind speed power generation were addressed. A test apparatus was developed to validate the design procedure, and specific methods to increase power generation under these conditions, such as span wise and axial roughness, two, three, and four-bladed systems and tip-speed ratios of 1, 3, and 7, were investigated.

Student nr: 1333186 [19], studied small wind turbines in Kenya, rural electrification has been a long-standing goal in Kenya, but there is still a long way to go with only 4% rural access to electricity. On top of that, if electricity is available, it is most commonly delivered by the grid, which suffers from power failures and growing costs. Therefore, there lies a large potential in small wind turbines (SWT) for the rural electrification of Kenya in areas endow with sufficient wind resources. Their research analyses the status of the SWT sector by using Strategic Niche Management and the Multi-Level Perspective as its theoretical frameworks.

The results of this analysis serve as input for developing strategy recommendations for all niche practitioners and for a start-up company, RIWIK, in particular. This research finds that the obstacles for sector growth go much beyond the low public awareness and high upfront cost of small wind turbines. This thesis also suggests possible ways in which the theory and methodology could be enhanced.

F.W. Perkins and D.E. Cromack [20], studied wind turbine blade stress analysis and natural frequencies, there were many problems to be addressed with respect to the design of wind turbine blades. Foremost among these are aerodynamic performance, structural integrity and cost. The subject of aerodynamic performance, at least in the steady state condition, has been dealt with at some length by various investigators. The cost of a blade system was beyond the scope of this paper. The structural integrity of wind turbine blades must be insured in both the static and dynamic load cases. The critical static load has been determined to be a hurricane wind perpendicular to the blade plan form. The dynamic loads included the fluctuating component due to the wind and all blade-support interactions.

Youm. I , etal.2005 [21], studied analysis of wind data and wind energy potential along the northern coast of Senegal. The main purpose of this paper was to present and to perform an investigation on the wind energy potential of the northern coast of Senegal along the Atlantic Ocean. Therefore, in this study, wind data collected over a period of two years at five different locations in this region of Senegal were evaluated in order to figure out the wind energy potential along the northern coast of Senegal. The data from selected stations were analyzed using the two-parameter Weibull probability distribution function. With an annual mean wind speed of 3.8 m/s, an annual energy of 158 kWh/m^2 could be extracted. It is found that the potential uses of wind energy in these locations are for water pumping in rural areas. The study presented here is also an attempt to promote wind energy in Senegal and to bridge the gap in order to create prospective Wind Atlas of Senegal.

Jean-Jacques chattot [22], studied design and analysis of wind turbines using helicoidally vortex model. The design corresponds to the maximum power output for a given thrust and the distributions of circulation, induced velocities, chord and twist of two- and three-bladed rotors are obtained. The analysis of turbines at off-design conditions is based on the same helicoidally vortex model, however, the power was not prescribed and an iteration was needed to insure that the vortex system was consisted with the resulting power extracted from the air. 2-D data from experiments or viscous codes are used to correct for viscous effects. Comparisons with published cases indicate that the method produces useful results very efficiently.

Xinzi T. etal.2011 [23], studied Anthony Ian broad, design and finite element analysis of mixed aerofoil wind turbine blades. This paper presented the design and finite element analysis (FEA) of a 10kW fixed-pitch variable-speed wind turbine blade with five different thickness of aerofoil shape along the span of the blade. The main parameters of the wind turbine rotor and the blade aerodynamic geometry shape were determined based on the principles of the blade element momentum (BEM) theory. Based on the FE method, deflections and strain distributions of the blade under extreme wind conditions are numerically predicted. The results indicated that the tip clearance is sufficient to prevent collision with the tower, and the blade material is linear and safe.

Hao W.etal.2011 [24], studied the modeling and stress analysis of wind turbine blade. They used modeling and stress analysis of the wind turbine blade were very critical for the further design and the application of wind turbine blade. The small-scale wind turbine blade was focused on, considering the glass fiber reinforced plastic material. Based on the parameters of airfoil and the geometrical parameters of blade, the three-dimension model of blade was established with the modeling software. Then the model was introduced into ANSYS software to carry out the FEM analysis. According to the displacement solution of blade, the maximal displacement occurs in the blade tip while working, but it is less than the safety displacement of wind turbine. And the stress concentration occurs in the center of the blade, which corresponds to the comprehensive stress from the elastic stress solution of the wind turbine blade.

Serhat Duran [25], studied computer- aided design of horizontal- axis wind turbine blades. In this paper, HAWT blade design was studied from the aspect of aerodynamic view and the basic principles of the aerodynamic behaviors of HAWTs are investigated. Blade-element momentum theory (BEM) known as also strip theory, which is the current mainstay of aerodynamic design and analysis of HAWT blades, is used for HAWT blade design in this paper. Firstly, blade design procedure for an optimum rotor according to BEM theory is performed. Then designed blade shape was modified such that modified blade will be lightly loaded regarding the highly loaded of the designed blade and power prediction of modified blade was analyzed. When the designed blade shape was modified, it has seen that the power extracted from the wind was reduced about 10%and the length of modified blade was increased about 5% for the same required power.

Almost all the above projects of small and medium scale wind turbine blade had been done by different types of software's like, ANSYS 12, CATIA V5 R16, FEM, GAMBET, etc. The working area wasn't specified, and the papers focused on an aerodynamically analysis like, the actuator disk theory and the betz limit, the general momentum theory, blade element theory, blade element-momentum (BEM) theory, but this thesis of small scale wind blade for some specific small rural area in the country. Using blade element-momentum (BEM) theory, to determined the forces on the blade and also the blade modeling by SOLIDWORK and ANSYS 15 WORKBEANCH, is used the stresses on the blade. The wind blade is running by small average environmental wind speed. The final output of the thesis project is to provide electricity for small rural villages like Laga-Gulla Kebele in Negele Borana zone (as mentioned earlier).

CHAPTER 3

AERODYNAMICS OF HORIZONTAL AXIS SMALL WIND TURBINE

Wind turbine power production depends on the interaction between the rotor and the wind. The wind may be considered to be a combination of the mean wind and turbulent fluctuations about that mean flow[9]. Experience has shown that the major aspects of wind turbine performance (mean power output and mean loads)are determined by the aerodynamic forces generated by the mean wind. Periodic aerodynamic forces caused by wind shear, off-axis winds, rotor rotation, randomly fluctuating forces induced by turbulence and dynamic effects are the source of fatigue loads and are a factor in the peak loads experience by a wind turbine. These are, of course, important, but can only be understood once the aerodynamics of steady state operation has been understood. Accordingly this chapter focuses primarily on steady state aerodynamics. General aerodynamic concepts are then introduced. The details of momentum theory and blade-element theory are developed. The combination of two theories, called blade-element momentum theory (BEM)[9]. This method can be used for design of new wind blade and can be carried out using a spreadsheet and lift and drag curves for the chosen airfoil.

More sophisticated treatments are available but this method has the advantage of being simple and easy to understand[9].

3.1 Blade Element Momentum Theory (BEM):

Blade Element Momentum Theory equates two methods of examining how a wind turbine operates. The first method is to use a momentum balance on a rotating annular stream tube passing through a turbine. The second is to examine the forces generated by the airfoil lift and drag coefficients at various sections along the blade. These two methods then give a series of equations that can be solved [5].

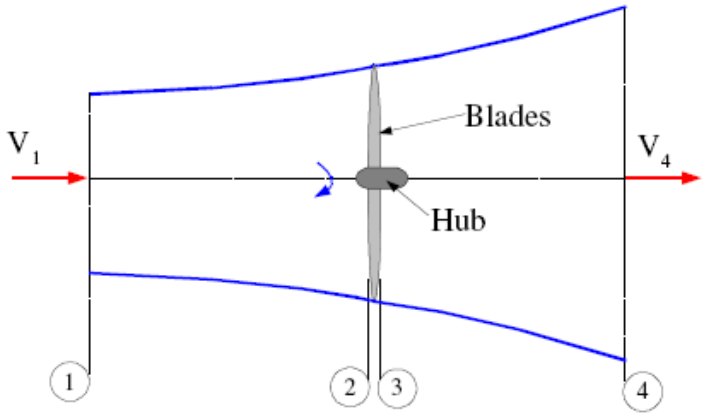

Figure 3.1: Axial Stream tube around a Wind Turbine[5].

3.1.1 Momentum Theory:

i. Axial Force:

Consider the stream tube around a wind turbine shown in Figure 3.1. Four stations are shown in the diagram 1, some way upstream of the turbine, 2 just before the blades, 3 just after the blades and 4 some way downstream of the blades. Between 2 and 3 energy is extracted from the wind and there is a change in pressure as a result.

Assume $p_1 = p_4$ and that $V_2 = V_3$. We can also assume that between 1 and 2 and between 3 and 4 the flow is frictionless so we can apply Bernoulli's equation. After some algebra:

$$p_2 - p_3 = \frac{1}{2}\rho(V_1^2 - V_4^2) \quad \text{3.1}$$

Noting that force is pressure times area we find that:

$$dF_X = (p_2 - p_3)dA \quad \text{3.2}$$

$$dF_X = \frac{1}{2}\rho(V_1^2 - V_4^2)dA \quad \text{3.3}$$

Define a the axial induction factor as:

$$a = \frac{V_1 - V_2}{V_1} \quad \text{or} \quad a = \frac{1}{2}\left(\frac{V_1 - V_4}{V_1}\right) \quad \text{3.4}$$

It can also be shown that:

$$V_2 = V_1(1 - a) \quad \text{3.5}$$

$$V_4 = V_1(1 - 2a) \quad \text{3.6}$$

Substituting yields:

$$dF_X = \frac{1}{2}\rho {V_1}^2[\,4a\,(\,1-a)]\pi r dr \quad \text{.....3.7}$$

ii. Rotating Annular Stream tube:

Consider the rotating annular stream tube shown in Figure 3.2. Four stations are shown in the diagram 1, some way upstream of the turbine, 2 just before the blades, 3 just after the blades and 4 some way downstream of the blades. Between 2 and 3 the rotation of the turbine imparts a rotation onto the blade wake[6].

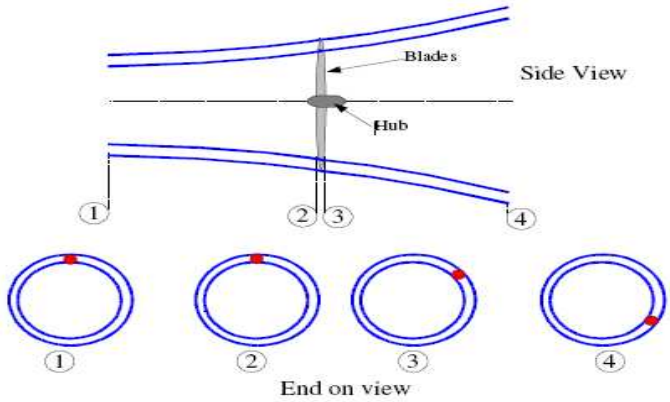

Figure 3.2: Rotating Annular Stream tube[6].

Consider the conservation of angular momentum in this annular stream tube. An "end-on" view is shown in Figure 3.2. The blade wake rotates with an angular velocity ω and the blade rotate with an angular velocity of Ω. Recall from basic physics that:

Moment of Inertia of an annulus, $I = mr^2$ 3.8

Angular Moment, $L = I\omega$ 3.9

Torque, $T = \frac{dL}{dt}$ 3.10

$$T = \frac{dI\omega}{dt} = \frac{d(mr^2\omega)}{dt} = \frac{dm}{dt}\, r^2\omega \quad \text{.....3.11}$$

So for a small element the corresponding torque will be:

$$dT = d\dot{m}\, r^2\omega \quad \text{.....3.12}$$

For the rotating annular element:

$$\dot{m} = \rho A V_2 \quad \text{.....3.13}$$

$$d\dot{m} = \rho 2\pi r dr V_2 \quad \text{.....3.14}$$

$$dT = \rho 2\pi r dr V_2 r^2 \omega = \rho V_2 \omega r^2 2\pi r dr \quad \text{.....3.15}$$

Define angular induction factor a':

$$a' = \frac{\omega}{2\Omega} \quad \text{.....3.16}$$

Recall that $V_2 = V_1(1 - a)$ so :

$$dT = 4a'(1 - a)\rho V \Omega r^3 \pi dr \quad \text{.....3.17}$$

Momentum theory has therefore yielded equations for the axial (Equation 3.7) and tangential force (Equation 3.17) on an annular element of fluid.

3.1.2 Blade Element Theory:

Blade element theory relies on two key assumptions:

- There are no aerodynamic interactions between different blade elements.
- The forces on the blade elements are solely determined by the lift and drag coefficients

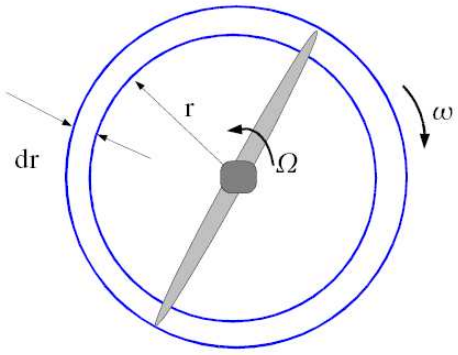

Figure 3.3: Rotating Annular Stream [7].

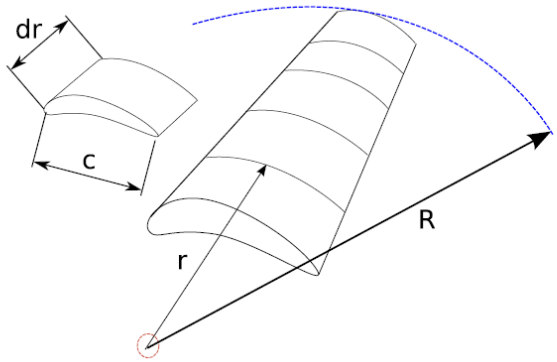

Figure 3.4: The Blade Element Mode[7].

Consider a blade divided up into *N* elements as shown in Figure 3.4. Each of the blade elements will experience a slightly different flow as they have a different rotational speed (Ω*r*), a different chord length (*c*) and a different twist angle (γ). Blade element theory involves dividing up the blade into ten elements and calculating the flow at each one. Overall performance characteristics are determined by numerical integration along the blade span.

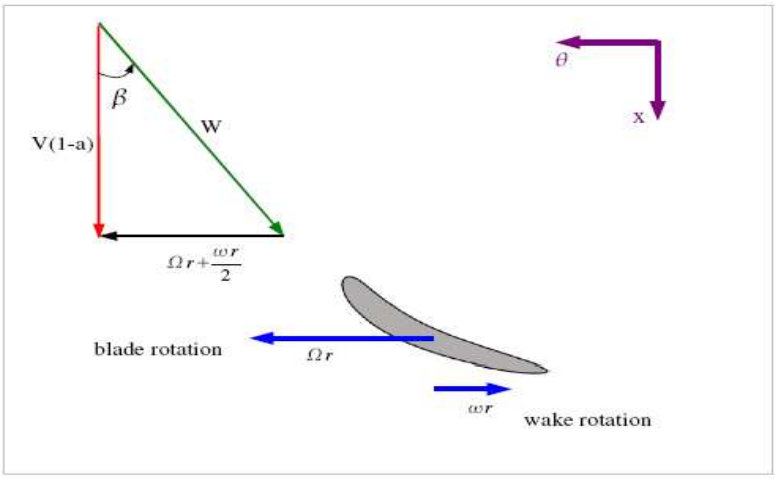

Figure 3.5: Flow onto the turbine blade[7].

i. Relative Flow:

Lift and drag coefficient data are available for a variety of airfoils from wind tunnel data. Since most wind tunnel testing is done with the airfoil stationary need to relate the flow over the moving airfoil to that of the stationary test. To do this use the relative velocity over the airfoil. More details on the aerodynamics of wind turbines and airfoil selection can be found in [9].

In practice the flow is turned slightly as it passes over the airfoil so in order to obtain a more accurate estimate of airfoil performance an average of inlet and exit flow conditions is used to estimate performance. The flow around the blade starts at station 2 in Figures 3.1 and 3.2 and ends at station 3. At inlet to the blade the flow is not rotating, at exit from the blade row the flow rotates at rotational speed ω. That is over the blade row wake rotation has been introduced. The average rotational flow over the blade due to wake rotation is therefore $\omega/2$. The blade is rotating with speed Ω. The average tangential velocity that the blade experiences is therefore $\Omega r + \frac{1}{2}\omega r$. This is shown in Figure 3.5.

Examining Figure 3.5 can immediately note that:

$$\Omega r + \frac{\omega r}{2} = \Omega r(1 + a') \quad \text{..... 3.18}$$

Recall that (Equation 3.5) : $V_2 = V_1(1 - a)$ and so:

$$\tan\beta = \frac{\Omega r(1 + a')}{V(1 - a)} \quad \text{..... 3.19}$$

Where V is used to represent the incoming flow velocity V_1. The value of β will vary from blade element to blade element. The local tip speed ratio λ_r is defined as:

$$\lambda_r = \frac{\Omega r}{V} \quad \text{..... 3.20}$$

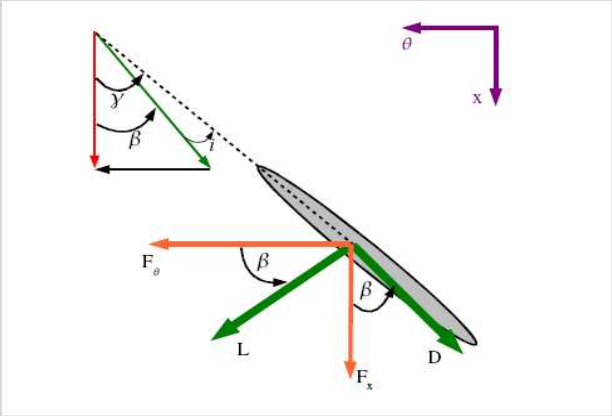

Figure 3.6: Forces on the turbine blade[9].

So the expression for tanβ can be further simplified:

$$\tan\beta = \frac{\lambda_r(1+a')}{(1-a)} \quad \text{..... 3.21}$$

From Figure 3.5 the following relation is apparent:

$$W = \frac{V(1-a)}{cos\beta} \quad \text{..... 3.22}$$

ii. Blade Elements:

The forces on the blade element are shown in Figure 3.6, note that by definition the lift and drag forces are perpendicular and parallel to the incoming flow. For each blade element one can see:

$$dF_\theta = dL\ cos\beta - dDsin\beta \quad \text{..... 3.23}$$

$$dF_X = dL\ sin\beta + dDcos\beta \quad \text{..... 3.24}$$

Where dL and dD are the lift and drag forces on the blade element respectively. dL and dD can be found from the definition of the lift and drag coefficients as follows:

$$dL = \frac{1}{2}\ C_L\rho W^2 cdr \quad \text{..... 3.25}$$

$$dD = \frac{1}{2}\ C_D\rho W^2 cdr \quad \text{..... 3.26}$$

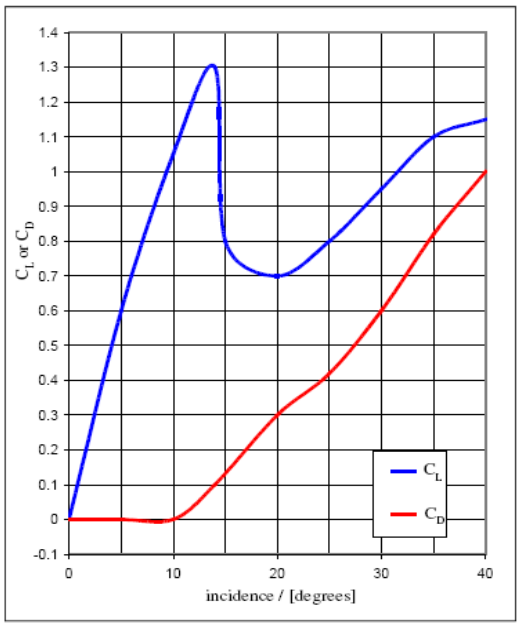

Figure 3.7: Lift and Drag Coefficients for a NACA 4412 Airfoil[9].

Lift and Drag coefficients for a *NACA 4412* airfoil are shown in Figure 3.7, this graph shows that for low values of incidence the airfoil successfully produces a large amount of lift with little drag. At around $i \approx 14^0$ a phenomenon known as stall occurs where there is a massive increase in drag and a sharp reduction in lift.

If there are *B* blades, combining Equation 3.23 and equation 3.25 it can be shown that:

$$dF_X = \frac{1}{2} B\rho W^2 (C_L\, sin\beta + C_D cos\beta) cdr \quad \text{..... 3.27}$$

$$dF_\theta = \frac{1}{2} B\rho W^2 (C_L\, cos\beta - C_D sin\beta) cdr \quad \text{..... 3.28}$$

The Torque on an element, dT is simply the tangential force multiplied by the radius.

$$dT = \frac{1}{2} B\rho W^2 (C_L\, cos\beta - C_D sin\beta) crdr \quad \text{..... 3.29}$$

The effect of the drag force is clearly seen in the equations, an increase in thrust force on the blade and a decrease in torque (and power output). These equations can be made more useful by noting that β and W can be expressed in terms of induction factors etc. (Equations 3.21 and 3.22). Substituting and carrying out some algebra yields:

$$dF_X = \sigma' \pi\rho \frac{V^2(1-a)^2}{cos^2\beta}(C_L sin\beta + C_D cos\beta) r dr \quad \text{3.30}$$

$$dT = \sigma' \pi\rho \frac{V^2(1-a)^2}{cos^2\beta}(C_L\, cos\beta - C_D sin\beta) r^2 dr \quad \text{3.31}$$

Where σ' is called the local solidity and is defined as:

$$\sigma' = \frac{Bc}{2\pi r} \quad \text{3.32}$$

3.1.3 Tip Loss Correction:

At the tip of the turbine blade losses are introduced in a similar manner to those found in wind tip vortices on turbine blade. These can be accounted for in BEM theory by means of a correction factor.

This correction factor *Q* varies from 0 to 1 and characterizes the reduction in forces along the blade.

$$Q = \left(\frac{2}{\pi}\right) \cos^{-1}\left[\exp\left(\frac{-\frac{B}{2}\left(1-\frac{r}{R}\right)}{\frac{r}{R}cos\beta}\right)\right] \quad \text{3.33}$$

The results from cos^{-1} must be in radians. The tip loss correction is applied to Equation 3.7 and Equation 3.17 which become:

$$dF_X = Q\rho\, V_1^2\, [\,4a\,(1-a)]\,\pi r dr \quad \text{3.34}$$

$$dT = Q4a'\,(1-a)\,\rho V \Omega r^3 \pi dr \quad \text{3.35}$$

Now there are four equations, two derived from momentum theory which express the axial thrust and the torque in terms of flow parameters (Equations 3.34 and 3.35), and also have two equations derived from a consideration of blade forces which express the axial force and torque in terms of the lift and drag coefficients of the airfoil (Equations 3.30 and 3.31).

To calculate rotor performance Equations 3.34 and 3.35 from a momentum balance are equated with Equations 3.30 and 3.31. Once this is done the following useful relationships arise.

$$\frac{a}{1-a} = \frac{\sigma'\,[C_L sin\beta + C_D cos\beta\,]}{4Q cos^2\beta} \quad \text{3.36}$$

$$\frac{a'}{1-a} = \frac{\sigma'\,[C_L cos\beta - C_D sin\beta\,]}{4Q\lambda_r cos^2\beta} \quad \text{3.37}$$

Equation 3.36 and 3.37 are used in the blade design procedure.

3.1.4 Power Output:

The contribution to the total power from each blade span is:

$$dP = \Omega dT \quad \text{..... 3.38}$$

The total power from the rotor is:

$$P = \int_{r_h}^{R} dP dr = \int_{r_h}^{R} \Omega dT dr \quad \text{..... 3.39}$$

Where r_h and R are the hub and the rotor radius respectively. The airfoil profile of NACA 4412 was generated using NACA coding. Specifications of the blade are[27]. Power= 0.5−1.5 kW, root chord length *(s)* = 334mm, tip chord length= 182.1mm, blade length *(l)* = 1500mm, hub diameter = 90mm, hub length = 150mm, hub to blade (neck) length= 150mm.

The power coefficient C_P is given by:

$$C_P = \frac{P}{P_{wind}} = \frac{\int_{r_h}^{R} \Omega dT}{\frac{1}{2}\rho\pi R^2 V^3} \quad \text{..... 3.40}$$

Using Equation 3.31 it is possible to develop an integral for the power coefficient directly. After some algebra.

$$C_P = \frac{8}{\lambda^2}\int_{\lambda_h}^{\lambda} Q{\lambda_r}^3 a'(1-a)\,[\,1 - \frac{C_D}{C_L}\tan\beta\,]\,d\lambda_r \quad \text{..... 3.41}$$

3.1.5 Performance Parameters of HAWTS:

The power performance parameters of a HAWT can be expressed in dimensionless form, in which the power coefficients, C_P and the tip-speed ratio, λ are used. From equation *3.40* and *3.20* respectively.

$$C_P = \frac{P}{\frac{1}{2}\rho\pi R^2 V^3}$$

$$\lambda = \frac{\Omega R}{V}$$

Note that, tip-speed ratio is defined for a fixed wind speed.

A sample C_P & λ curve is given in Figure 3.8 for a typical HAWT operating at fixed pitch.

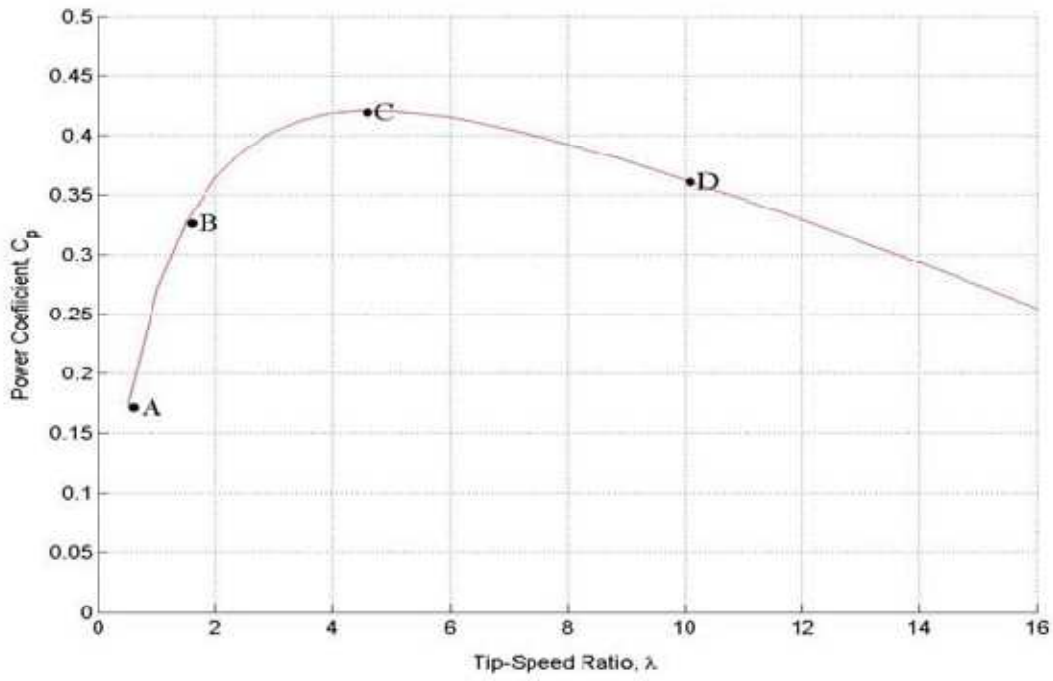

Figure 3.8 Typical plot of rotor power coefficient vs. tip-speed ratio for HAWT with a fixed blade pitch angle[26].

To give a few comments on the operating points A, B, C and D shown in Figure 3.8 will help reading such C_P & λ curves of HAWTs. The left-hand side of Figure 3.8 following the path ABC is controlled by blade stall. Local angles of attack (angles between the relative wind angle and the blade chord line) are relatively large as point A is approached. The right-hand side of the same figure following the path CD is controlled by drag, particularly 'skin friction' because the angles of attack are small as point D is approached. At fixed pitch maximum power occurs in the stall region when the lift coefficient is near its peak value over much of the blade[26].

As a result, for a selected airfoil type and for a specified tip-speed ratio and blade length (i.e. rotor radius), the blade shape can be designed for optimum rotor and from the calculation of power coefficient the maximum power that can be extracted from the wind can then be found for any average wind velocity.

Table 3.1 Blade Chord and Twist Distribution for a Three-Bladed HAWT

(Airfoil NACA 4412, $C_{l\,,design}$=1.074 α_{design} = 5.5^0 γ = 0.0075)

Local tip-speed ratio λ_r	Radial location r/R	Chord-length ratio c/R	Twist angle θ (deg)
0.25	0.025	0.071369	34.143
0.75	0.075	0.10831	29.92
1.25	0.125	0.097031	20.273
1.75	0.175	0.080973	14.33
2.25	0.225	0.067803	10.475
2.75	0.275	0.057746	7.8221
3.25	0.325	0.050049	5.9018
3.75	0.375	0.044051	4.4543
4.25	0.425	0.039279	3.327
4.75	0.475	0.035407	2.4258

As an example, the blade chord-length and twist distribution for an optimum three-bladed rotor at the design tip-speed ratio is tabulated in Table 3.1 for the airfoil NACA 4412 whose lift coefficient and drag coefficient values are taken.

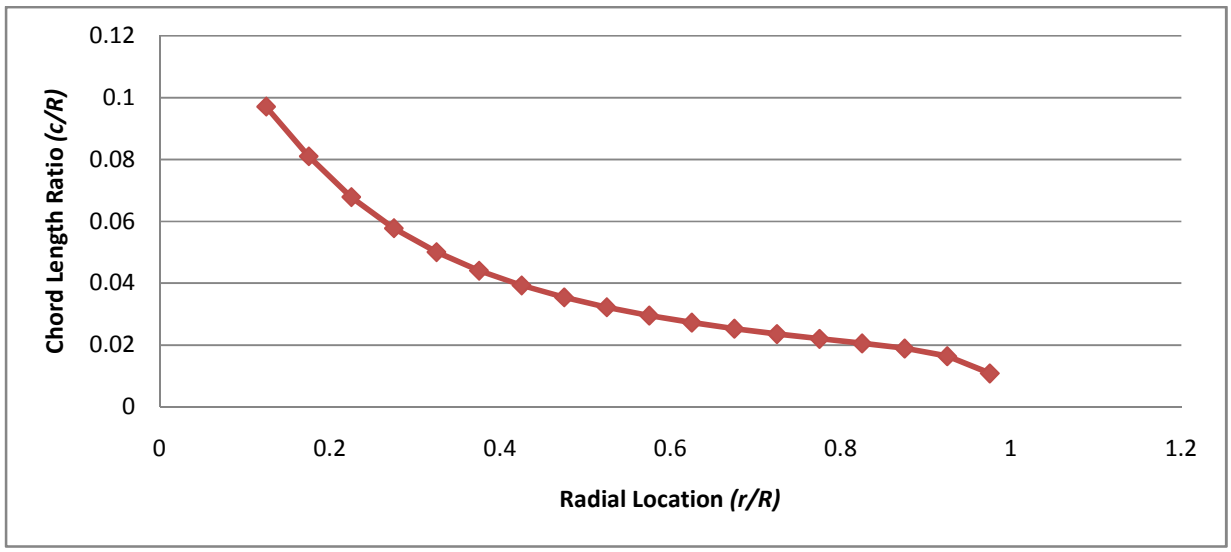

Figure 3.9 Chord-length distribution for the designed blade

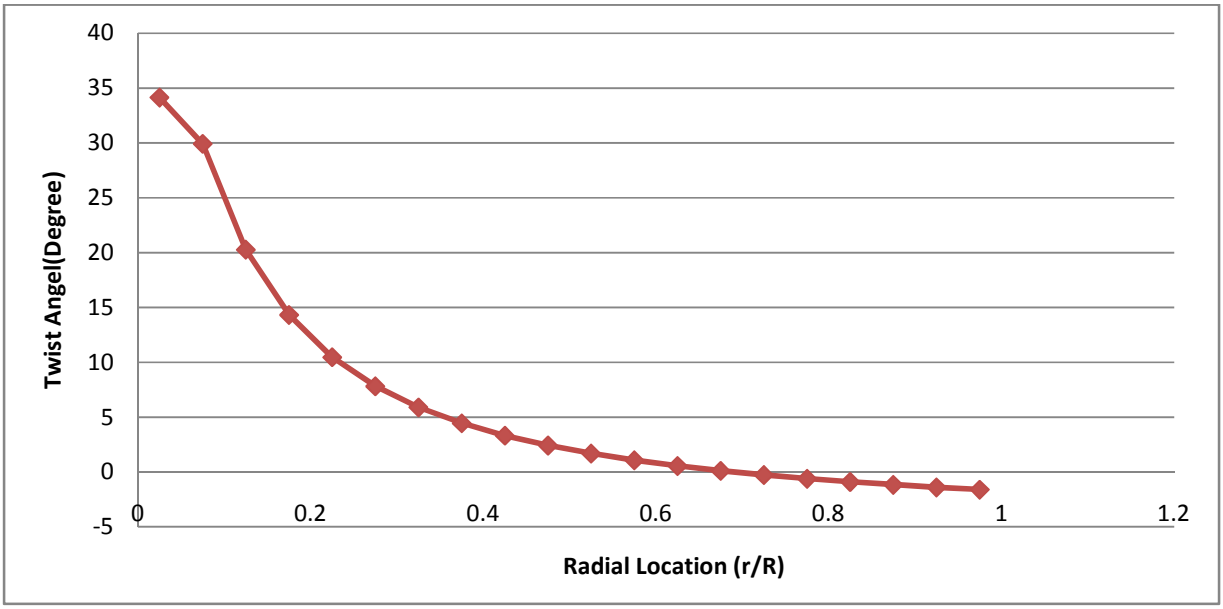

Figure 3.10 Twist distributions for the designed blade

In Figure 3.9 chord-length distribution with respect to radial location of each blade element both of which are normalized with blade radius is shown. Similarly twist distribution with respect to radial location is illustrated in Figure 3.10.

CHAPTER 4

STRUCTURAL DESIGN OF HAWT BLADE

Structural design of HAWT blades is an important as their aerodynamic design. The dynamic structural loads which a rotor will experience play the major role in determining the lifetime of the rotor. Obviously, aerodynamic loads are a major source of loading and the blade geometry parameters are required for dynamic load analysis of wind turbine rotor.

Design of a HAWT blade has been explained and shown the solution method via the equations derived from BEM theory. Tip-loss factor and drag effect have also been considered. The method of determining blade shape for optimum performance of a turbine has been developed, how an optimum blade shape is modified for the best performance has been introduced and finally power performance calculation methods and stresses on blade have been established. And the airfoil NACA 4412 was used while performing these methods.

At the height of 10m tower wind speed range is decided between 6m/s − 9m/s, which can meet the needs of the areas of different wind. Therefore, the mean average wind speed was determined as 8.26m/s. The span was firstly divided into ten sections along the span wise direction from the end of the tip to the first of the root part of the airfoil. There are ten cross-sections in all and each section is 0.013m long. Then the Wilson design method was used to calculate the chord length c and twist angle α of every blade elements [18].

4.1 Blade Design Procedure:

i. Determine the total power from the rotor is :

$$P = C_P \eta \frac{1}{2} \rho \pi R^2 W^3 \quad \text{.....4.1}$$

where:

- P is the power output
- R is the tip radius ($R = 1.5m$)

- W is the expected relative wind velocity ($W = 6.13m/s$)
- C_P is the maximum power coefficient (0.593 for a modern three bladed wind turbine)
- η is the expected electrical and mechanical efficiencies (0.9 would be a suitable value)

$$P = C_P \eta \frac{1}{2} \rho \pi R^2 W^3$$

$$= (0.593) * (0.9) \frac{1}{2} * 1.225 \, {}^{kg}/_{m^3} * \pi \, (1.5m)^2 * (6.13)^3$$

$$P = 532.33 watt$$

This amount of power is produced from a single turbine and can operate 16.131 number of lamps for three hours per day of working time but the power consumption of each lump is 11watt.

The power that produced by the wind at $V = 8.26m/s$ is:

$$P_{wind} = \frac{1}{2} \rho \pi R^2 V^3 = \frac{1}{2} * 1.225 \, {}^{kg}/_{m^3} * \pi \, * (1.5m)^2 * (8.26)^3$$

$$P_{wind} = 2439.937 \, watt$$

This power of wind used to design of blade and to calculate stresses on the blade.

ii. Choose a tip speed ratio for the machine. For water pumping pick $1 < \lambda < 3$ (which gives a high torque) and for electrical power generation pick $4 < \lambda < 10$ [9].

iii. Select an airfoil for $\lambda<3$ curved plates can be used rather than an aerofoil shape and choose a number of blades *B* using table 4.1. The NACA *4* digit airfoil series is controlled by *4* digits such that NACA *4412*, which designate the camber, position of the maximum camber and thickness. If an airfoil number is NACA *MZXX* like NACA *4412* then:

- *M* is the maximum camber divided by 100. In the example *M* = 4 so the camber is 0.04 or 2% of the chord
- *Z* is the position of the maximum camber divided by 10. In the example *Z* = 4 so the maximum camber is at 0.4 or 40% of the chord.

- *XX* is the thickness divided by 100. In the example *XX*=12 so the thickness is 0.12 or 12% of the chord.

The *NACA* airfoil section is created from a camber line and a thickness distribution plotted perpendicular to the camber line. The equation for the camber line is split into sections either side of the point of maximum camber position (*Z*). In order to calculate the position of the final airfoil envelope later the gradient of the camber line is also required. The equations are:

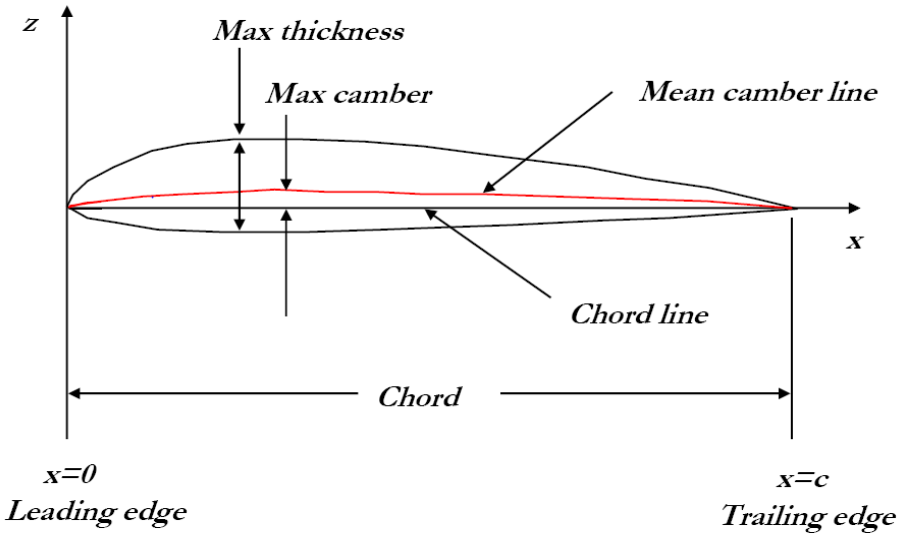

Figure 4.1 *NACA* airfoil section[9].

Table 4.1: Number of Blades[9].

λ	*B*
1	8−24
2	6−12
3	3−6
4	3−4
more than 4	1 − 3

Table 4.2 NACA *4412* equations

Position	Front ($0 \leq x < Z$)	Back($Z \leq x \leq 1$)
Camber	$y_c = \frac{M}{Z^2}(2Zx - x^2)$	$y_c = \frac{M}{(1-Z)^2}(1 - 2Z + 2Zx - x^2)$
Gradient	$\frac{dy_c}{dx} = \frac{2M}{Z^2}(Z - x)$	$\frac{dy_c}{dx} = \frac{2M}{(1-Z)^2}(Z - x)$

The thickness distribution is given by the equation:

$$y_t = \frac{K}{0.2}(a_0 x^{0.5} + a_1 x + a_2 x^2 + a_3 x^3 + a_4 x^4) \quad \text{.....} 4.2$$

Where: $a_0 = 0.2969$ $a_1 = -0.126$ $a_2 = -0.3516$ $a_3 = 0.2843$ $a_4 = -0.1015$ or -0.1036 for a closed trailing edge.

- The constants a_0 to a_4 are for a 20% thick airfoil. The expression $\frac{K}{0.2}$ adjusts the constants to the required thickness.
- At the trailing edge (x=1) there is a finite thickness of 0.0021 chord width for a 20% airfoil. If a closed trailing edge is required the value of a_4 can be adjusted.
- The value of y_t is a half thickness and needs to be applied both sides of the camber line.

Using the equations above, for a given value of x it is possible to calculate the camber line position y_c, the gradient of the camber line and the thickness. The position of the upper and lower surface can then be calculated perpendicular to the camber line.

$$\alpha = a\tan\left(\frac{dy_c}{dx}\right) \quad \text{.....} 4.3$$

Table 4.3 The position of the upper and lower surface

Position	horizontal	vertical
Upper Surface	$x_u = x_c - y_t \, sin\theta$	$y_u = y_c + y_t \, cos\theta$
Upper Surface	$x_1 = x_c + y_t \, sin\theta$	$y_1 = y_c - y_t \, cos\theta$

The most obvious way to plot the airfoil is to iterate through equally spaced values of x calculating the upper and lower surface coordinates. While this works, the points are more widely spaced around the leading edge where the curvature is greatest and flat sections can be seen on the plots. To group the points at the ends of the airfoil sections a cosine spacing is used with uniform increments of β.

Where : ($0 \leq \beta \leq \pi$)

$$x = \frac{(1 - cos\beta)}{2} \quad \text{.....} 4.4$$

iv. Obtain and examine lift and drag coefficient curves for the airfoil in question. Note that different airfoils may be used at different spans of the blade, a thick airfoil may be selected for the hub to give greater strength.

v. Choose the design aerodynamic conditions for each airfoil. Typically select the maximum lift value, this choice effectively fixes the blade twist. On blade a very large degree of twist is required to obtain near the hub. This is not necessarily desirable as the hub produces only a small amount of the power output, a compromise is to accept that the airfoils will have very large angles of attack at the hub.

vi. Choose a chord distribution of the airfoil. There is no easily physically accessible way of doing this but a simplification of blade is given by:

$$c = \frac{8\pi r cos\beta}{3\beta\lambda_r} \quad . \quad \text{4.5}$$

This gives a moderately complex shape and a linear distribution of chord may be considerably easier to make.

vii. Divide the blade into *N* elements or spans. Typically 10 elements or spans would be used.

viii. Assumed the blade shape derived with wake rotation, zero drag and zero tip losses. Note that these equations provide a new design.

The equations are given as follows:

$$\beta = 90^0 - \frac{2}{3}\tan^{-1}(\frac{1}{\lambda_r}) \quad \text{4.6}$$

$$a = [1 + \frac{4cos^2\beta}{\sigma' C_L sin\beta}]^{-1} \quad \text{4.7}$$

$$a' = \frac{1-3a}{4a-1} \quad \text{4.8}$$

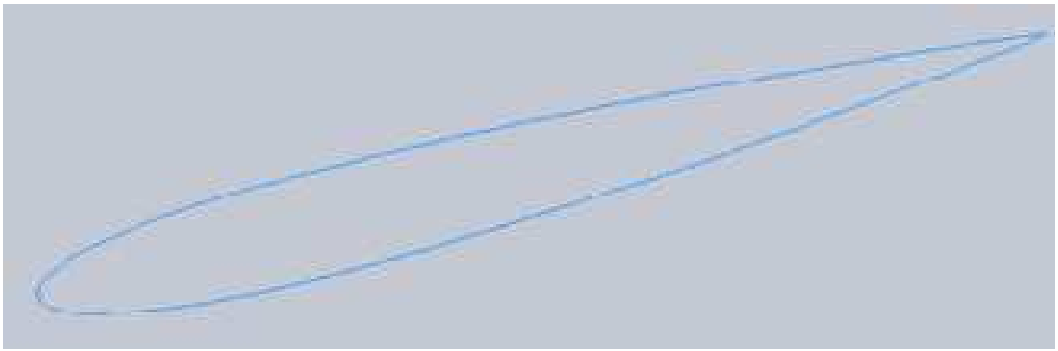

Figure 4.2 The Profile Curve of Blade Element by SOLIDWORK Model.

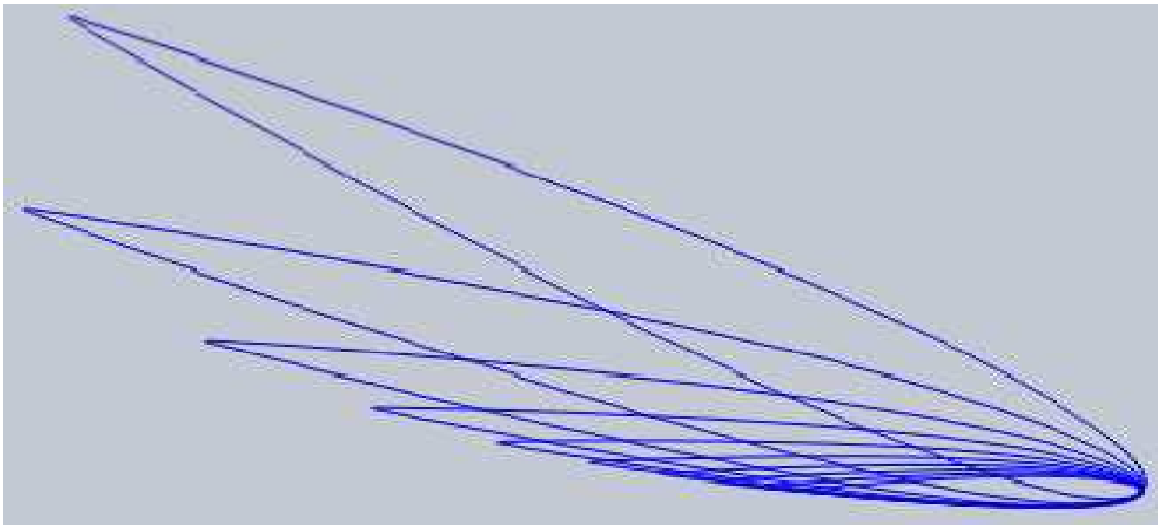

Figure 4.3 Views of blade from root towards tip by SOLIDWORK Mode.

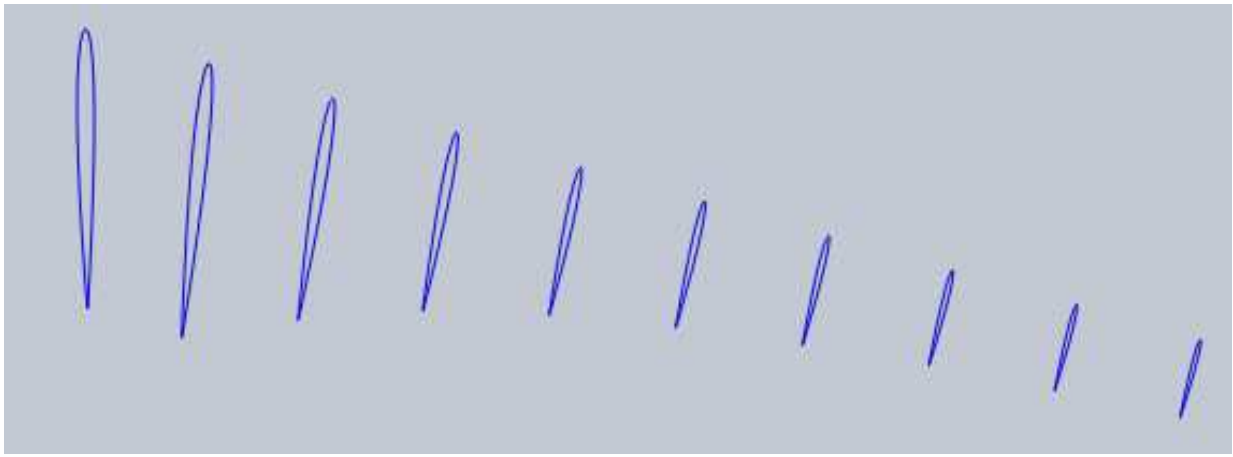

Figure 4.4 Isometric views of the blade elements by SOLIDWORK Model.

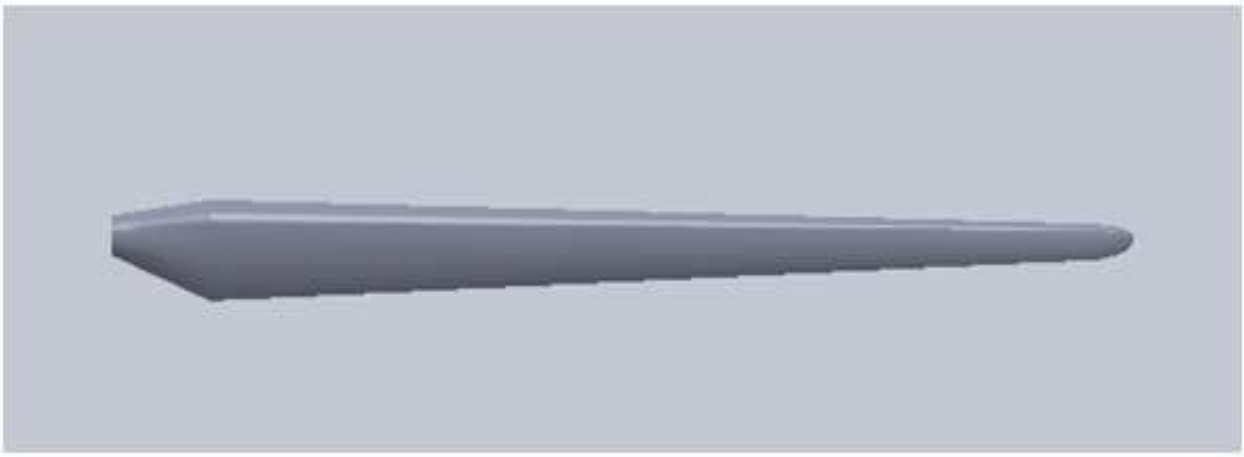

Figure 4.5 3D Model of the blade by SOLIDWORK.

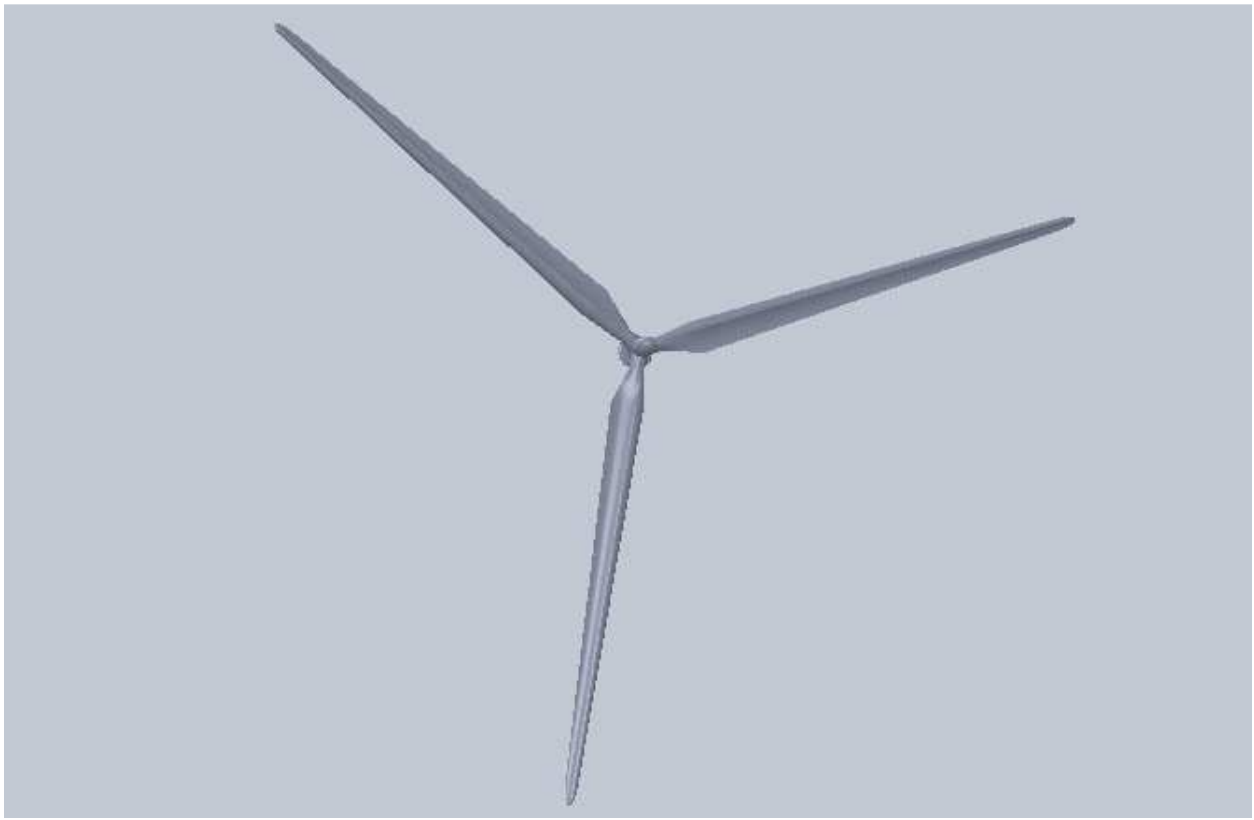

Figure 4.6 Three blades 3D solid model of the design blade by SOLIDWORK Model.

4.2 Load Conditions:

The blade is modeled as a cantilever beam. The loads on the blade in this case are the drag , and gravity. To simplify the design of wind mill structures, it is well to understand the loads which try to break apart these machines. These loads are axial force, lifting and blade weight. These are others, but lesser important.

A structural analysis was then carried out a cantilever beam analysis, with the help of SOLIDWORK and ANSYS 15 WORKBEANCH Software.

4.2.1 Aerodynamic Load:

Aerodynamic load is generated by lift and drag of the blades airfoil section. The turbine has a tip radius of 1.5m, and will operate in a wind speed of 8.26 m/s, a tip speed ratio of 6 and three blades. Assume that the tip loss and the drag coefficient are zero . From Figure 3.7 the drag coefficient is zero at the lift coefficient is one.

The total thrust force on the single blade from Equation 3.27 is:

$$dF_X = \frac{1}{2} B\rho V^2 (C_L\, sin\beta + C_D cos\beta) cdr$$

$$= \frac{1}{2} B\rho V^2 C_L\, sin\beta\; cdr$$

$$= \frac{1}{2} B\rho V^2\, sin\beta\; cdr$$

$$F_X = \frac{1}{2} B\rho V^2\, sin\beta \int_1^{10} cdr$$

From Equation 4.6

$$\beta = 90^0 - \frac{2}{3} \tan^{-1}\left(\frac{1}{\lambda_r}\right)$$

$$= 90^0 - \frac{2}{3} \tan^{-1}\left(\frac{1}{6}\right)$$

$$= 83.64^0$$

Then the total thrust force is:

$$F_X = \frac{1}{2} B\rho W^2 \, sin\, 83.64 \int_1^{10} cdr$$

$$F_X = \frac{1}{2} * 3 * 1.225 \text{kg/m}^3 * (8.26\ \text{m/s})^2 * 0.994 \int_1^{10} cdr$$

$$F_X = 124.616 \int_1^{10} cdr$$

Table 4.4 The positions of airfoils on the blade

Span No.	Chord Length c(mm)	Rotor radius r (mm)
1	334	200
2	319	330
3	294.5	460
4	263.5	590
5	241.2	720
6	224.86	850
7	212.44	980
8	202.82	1110
9	188.2	1240
10	182.1	1370

Summing up the elemental thrust forces along the blade from blade Table4.4 gives the total thrust on the blade.

$$F_X = (124.616 * 25.739037\ )$$

$$F_X = 3207.495835 \text{ N}$$

The total tangential on the single blade from Equation 3.28 is:

$$dF_\theta = \frac{1}{2} B\rho V^2 (C_L\, cos\beta - C_D sin\beta) cdr$$

$$= \frac{1}{2} B\rho V^2 C_L\, cos\beta\ cdr$$

$$= \frac{1}{2} B\rho V^2\, cos\beta\ cdr$$

$$F_\theta = \frac{1}{2} B\rho V^2 \cos\beta \int_1^{10} cdr$$

Then the total tangential force is:

$$F_\theta = \frac{1}{2} B\rho V^2 \cos 83.64 \int_1^{10} cdr$$

$$F_\theta = \frac{1}{2} * 3 * 1.225 \text{kg/m}^3 * (8.26 \text{ m/s})^2 * 0.1107 \int_1^{10} cdr$$

$$F_\theta = 13.878 \int_1^{10} cdr$$

Summing up the elemental tangential forces along the blade from blade Table4.4 gives the total tangential on the blade.

$$F_\theta = (13.878 * 25.739037)$$

$$F_\theta = 357.20635 \text{ N}$$

4.2.2 Gravitational and Centrifugal Loads:

Gravitational and centrifugal forces are mass dependant which is generally thought to increase cubically with increasing turbine diameter [8]. Therefore, turbines under ten meters diameter have negligible inertial loads, which are marginal for 20 meters upward, and critical for 70 meter rotors and above [4]. The gravitational force is defined simply as mass multiplied by the gravitational constant, although its direction remains constant acting towards the centre of the earth which causes an alternating cyclic load case.

$$G = m_b g$$

$$G = 6.3456kg * 9.81 \, {}^{m}/_{s^2}$$

$$G = 62.25N$$

The centrifugal force is a product of rotational velocity squared and mass and always acts radial outward, hence the increased load demands of higher tip speeds. Centrifugal and gravitational loads are superimposed to give a positively displaced alternating condition with a wavelength equal to one blade revolution.

$$F_C = m_b \omega^2 R$$

$$F_C = 6.3456kg * (6.5)^2 * 1.5m$$

$$F_C = 402.152N$$

4.2.3 Resultant Load:

The resultant of all loads on the blade is:

$$R_L{}^2 = (F_X + G)^2 + (F_C - F_\theta)^2$$

$$R_L = \sqrt{(3207.495835 + 62.25)^2 + (402.152 - 357.206355)^2}$$

$$R_L = 3270.05N$$

4.3 Data's of Wind Speed at Negele town:

Negele station is located in the south of Oromia. The wind speed data was collected from National Metrology Agency of Ethiopia. To further verify and analyze numerical simulation result, data from some meteorological station of Negele town. For this detailed position, see Figure 4.6.

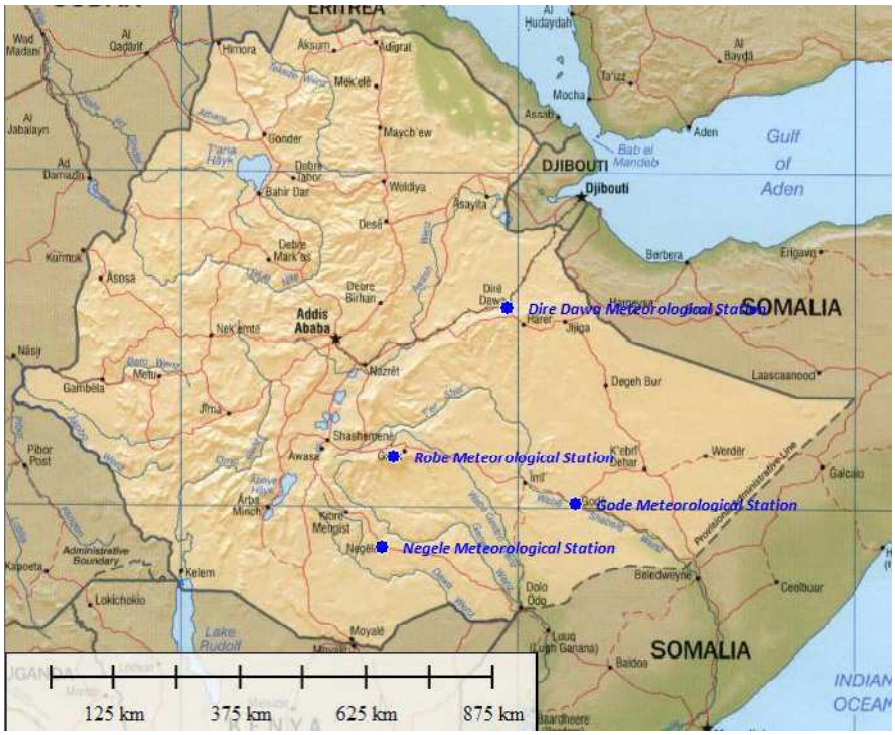

Figure 4.7 Distribution of Some Meteorological Stations in East Ethiopia[29].

4.3.1 Data's of Wind Speed at height of 2m tower:

Table.4.5 Monthly Mean Wind Speed at height of 2m, Negele Station Collected from Federal Water and Energy Minister of Ethiopia.

Month	wind speed (m/s)
1 (JAN)	4.45
2(FEB)	4.83
3(MAR)	3.98
4(APR)	3.36
5(MAR)	4.35
6(JUN)	5.74
7(JUL)	6.28
8(AUG)	6.17
9(SEP)	4.91
10(OCT)	3.45
11(NOV)	4.15
12(DEC)	4.31

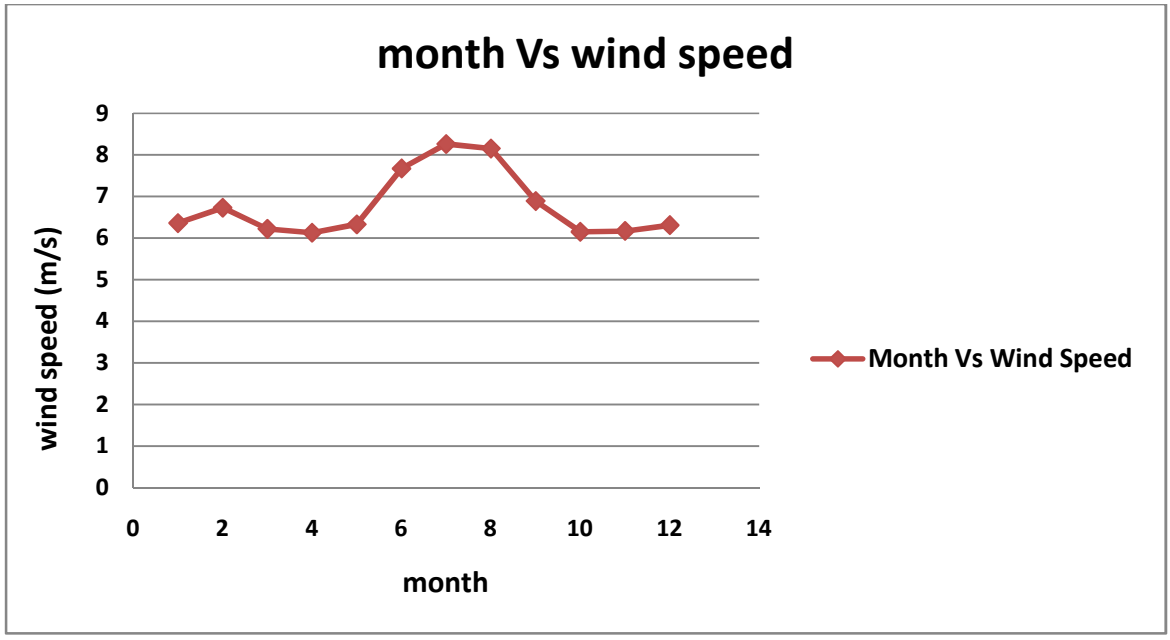

Figure 4.8 curve of monthly mean wind speed at 2m height, Negele station

Seen from the analysis result, wind speed is higher from June to September. There's rich wind resource around Negele station. Annual mean wind speed there is as high as 4.66m/s at the height of 2m. It indicates there is a big ratio of high wind speed weather in the region.

4.3.2 Data's of Wind Speed at height of 10m tower:

Table. 4.6 Monthly Mean Wind Speed at height of 10m, Negele Station Collected from Federal Water and Energy Minister of Ethiopia.

Month	wind speed (m/s)
1 (JAN)	6.36
2(FEB)	6.73
3(MAR)	6.22
4(APR)	6.13
5(MAR)	6.33
6(JUN)	7.67
7(JUL)	8.26
8(AUG)	8.15
9(SEP)	6.89
10(OCT)	6.15
11(NOV)	6.17
12(DEC)	6.31

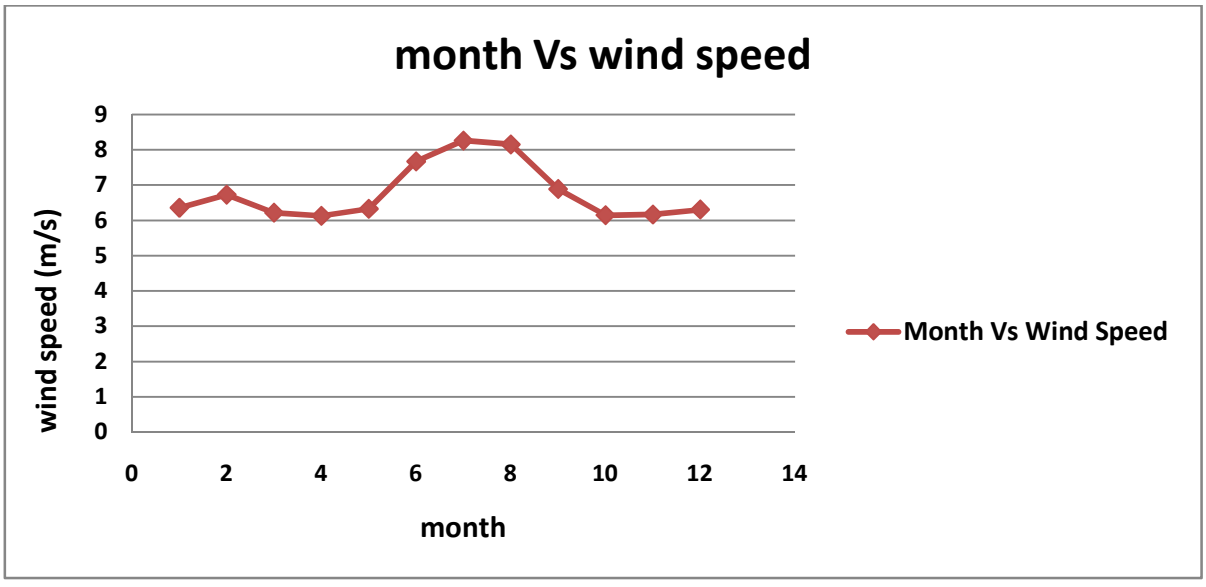

Figure 4.9 curve of monthly mean wind speed at 10m height, Negele station

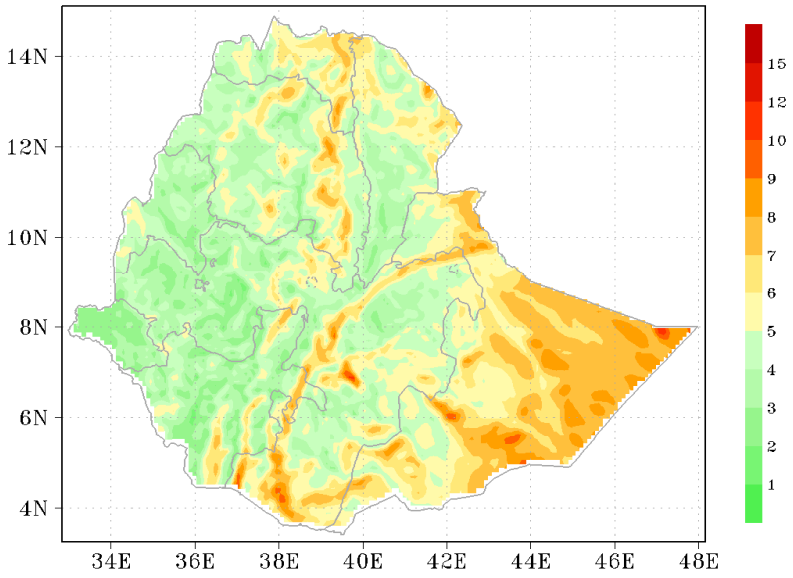

Figure 4.10 Distribution of Average Wind Speed, m/s (Height: 10m, 1980~1989) [29].

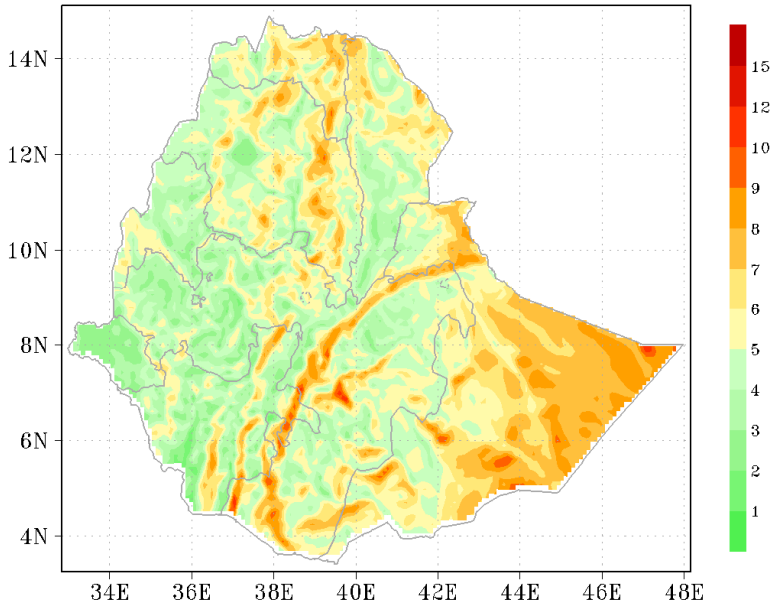

Figure 4.11 Distribution of Average Wind Speed, m/s (Height: 10m, 1990~1999) [29].

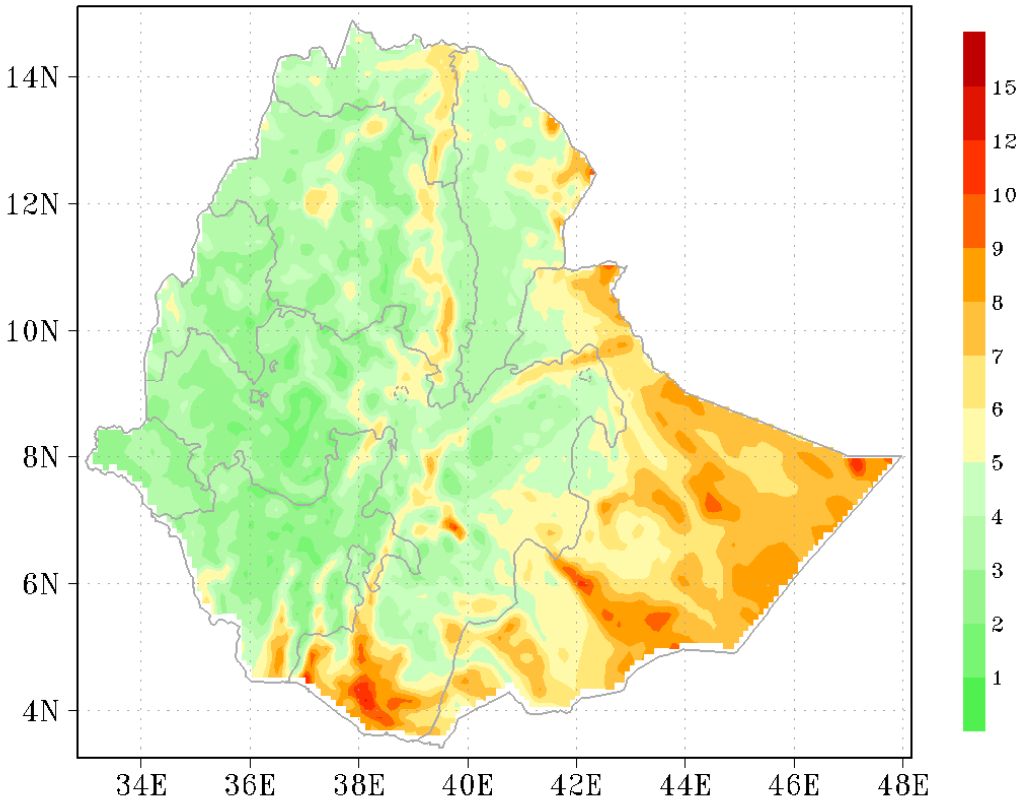

Figure 4.12 Distribution of Average Wind Speed, m/s (Height: 10m, 2000~2009) [29].

4.4 Material for small wind turbine blade:

The blades in a normally operating wind turbine rotor are continuously exposed to loads from wind and gravity. The primary requirements for blade material are high stiffness to ensure aerodynamic performance, low density to minimize mass and long-fatigue. In the wind turbine industry, many materials have been used for blades, including metals, plastics, wood and composites [27].

While various materials have been applied successfully in wind turbine blades, epoxy E-glass fiber- reinforced plastic (GRP) based composites predominate. The important characteristics of GRP are good mechanical properties, good corrosion resistance, high temperature tolerance, ease of manufacture, high tensile strength and favorable cost. More importantly, composite materials enable structures to be designed to provide significant advantages such as weight reduction, over traditional engineering materials, whilst maintaining the required level of performance and reliability. It is also easily knitted and woven into desired textiles to meet different engineering requirements. Usually the fiber glass is embedded within a plastic matrix to form a composite known as glass reinforced plastic (GRP). In composite structures, matrix, also called binder, is the resin used to hold fibers in position and make the blade strong.

For comparative purposes, values are also presented of:

- compressive strength- to - weight ratio,
- fatigue strength as a percentage of compressive strength,
- stiffness- to- weight ratio,

For the material investigation coupon specimens were cut on-axis from a 0°, ±45,90° glass fiber epoxy plate. With similar reason as well stated before the material in case a laminate is built up from 60% (volume) unidirectional glass fiber(all fibers running longitudinally) and 40% epoxy plate lay-up material is selected, and its structural properties are [27]:

Young's modulus : $E_x = 34.412\text{GPa}$; $E_y = E_z = 6.531\text{GP}$

Poisson's ratio : $\upsilon_{xy} = \upsilon_{zx} = 0.217,\ \upsilon_{yz} = 0.336$

Shear modulus : $G_{xy} = G_{zx} = 2.433\text{GPa};\ G_{yz} = 1.698\text{GPa}$

Density : $\rho = 2000\ \text{kg/m}^3$

Ultimate tensile strength (UTS) = 370MPa,

Ultimate compressive strength (UCS) = 235MPa, [27].

4.5 Stresses On Blade:

Power of tapping from wind energy systems has high impact on the economic analysis of this type of energy and capture energy from the wind turbine dependents the blade design and the relevant factors. Wind turbines are exposed to various stresses and loads, and due to the nature of the wind, the loads are highly variable. Design for dynamic loading compared with static loading, due to the emergence of the phenomenon of fatigue is much harder. Since experimental studies are very expensive and time consuming, and also, because of the complex geometry, and analytical methods are lacking in this case, the perfect solution is using numerical methods. In other words, one of the suitable methods to evaluate a new design of wind turbine blades is the numerical modeling.

The blade is modeled as a cantilever, the basis of this calculation is a simplified beam theory model. Each cross-section is therefore divided into three basic geometrical shapes, a rectangle representing the box spar, a half ellipsoid and a triangle representing the leading and trailing edges respectively.

The airfoil profile of *NACA 4412* was generated. Specifications of the blade are; Power= 0.5−1.5 kW, root chord length *(s)* = 334mm, tip chord length= 182.1mm, blade length *(l)* = 1500mm, hub diameter = 90mm, hub length = 150mm, hub to blade (neck) length= 150mm.

To simplify the calculations a symmetrical cross section is assumed. The spar is linearly tapered from the blade root to the tip. All applied loads are transformed along the appropriate axes to find the appropriate stresses along these axes.

By applying the aerodynamic loads, the stress and strain are analyzed. In order to optimization, the chord length and the twist angle of the blade at various radiuses have been calculated by BEM.

The purpose of the analysis is that the stress and strain analysis be done on the blades. Now we want to examine whether the optimized blade, has the ability to withstand the aerodynamic loads? What is the reliability of wind turbine rotor? And the maximum principal stress in the rotor blades is not higher than the yield stress. In order to validate wind turbine blade in stress analysis, at first, blade approximated with a cantilever beam, and non-uniform compressive force applied to the beam. Length of the tapper beam 1500mm and its average mean cross-sectional width and height 49.441mm and 54.6923mm respectively. The following calculations to obtain the maximum stress and displacement end of beam with exact solution, have been performed.

The blade was modeled as a cantilever with one end fully constrained and a uniformly distributed load of $3270.05N$ applied on its upper surface(face). In general operation the blade is not subject to the full loading as experienced in this model due to the variance in the twist angle of the blade. It was chosen to determine an extreme scenario to ensure the blade was of a sufficient standard.

$$I = \frac{bh^3}{12} = \frac{49.441(54.6923)^3}{12} = 674038.2808\, mm^4$$

$$\mathrm{Z} = \frac{bh^2}{6} = \frac{49.441(54.6923)^2}{6} = 24648.37942\, mm^3$$

- Maximum Deformation at the blade Tip:

$$\delta_{max} = \frac{R_L l^4}{8EI}$$

$$\delta_{max} = \frac{3270.05N\ (\,1500mm\,)^4}{8 * 34.412 * 10^9\mathrm{pa} * \ 674038.2808\ \ mm^4}$$

$$\delta_{max} = \ 0.0892144\mathrm{m}$$

$$\delta_{max} = 89.2144\mathrm{mm}$$

- Maximum Stress at Support :

$$\sigma_{max} = \frac{R_L l}{2Z}$$

$$\sigma_{max} = \frac{3270.05 * 1500}{2 * 24648.37942}$$

$$\sigma_{max} = 99.5\ Mpa$$

- Pressure :

$$p = \frac{R_L}{A} = \frac{3270.05N}{(334 * 1500)mm^2}$$

$$p = 6.52704\ kpa$$

CHAPTER 5
RESULT AND DISCUSSION

In this chapter, design of a HAWT blade has been explained and shown the results. Figure 5.1 to Figure 5.3 show the arrangements of different Airfoils, the position of pressure and the model of blade by SLIDWORK software. From Figure 5.4 to figure 5.30 show how the maximum stress distribution around the blade root ,the minimum stress at the blade tip, the maximum deformation at the blade tip and the minimum deformation at the blade root by considering a mean average wind speed data, the maximum and minimum pressure on the blade . The maximum pressure is assumed to be created by considering of resultant load and the power output .

Table 5.1 The values done by ANSYS15 workbench at element mesh size of 1.3979mm

Month	10m height Mean Wind Speed (m/s)	Max. Stress (Mpa)	Min. Stress (pa)	Max.Deformation (m)	Power (Watt)
1 (JAN)	6.36	72.3949	3.19966 E+2	0.060679	594.52
2(FEB)	6.73	76.6066	3.38581E+2	0.064209	704.44
3(MAR)	6.22	70.8013	3.12923E+2	0.059344	556.12
4(APR)	6.13	69.7768	3.08396E+2	0.058485	532.33
5(MAR)	6.33	72.0534	3.18457E+2	0.060393	586.15
6(JUN)	7.67	87.3065	3.85872E+2	0.080031	1042.76
7(JUL)	8.26	94.0224	4.15555E+2	0.088698	1302.38
8(AUG)	8.15	92.7702	4.10020E+2	0.086311	1251.04
9(SEP)	6.89	78.4278	3.46631E+2	0.065736	755.88
10(OCT)	6.15	70.0046	3.09402E+2	0.058676	537.55
11(NOV)	6.17	70.2322	3.10408E+2	0.058867	542.81
12(DEC)	6.31	71.8258	3.17452E+2	0.060202	580.14

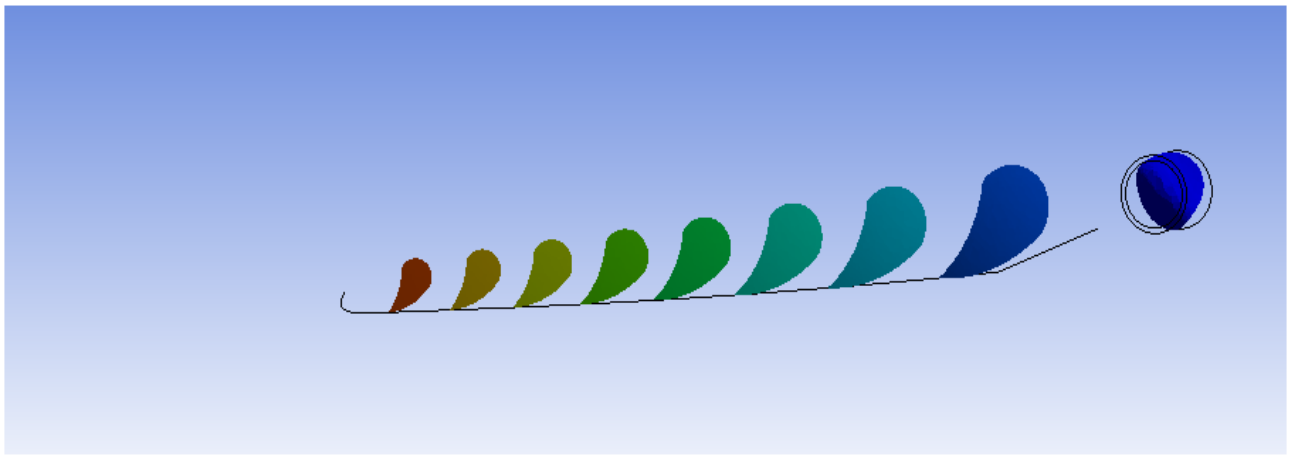

Figure 5.1 Solid work Model of NACA 4412 Airfoil profiles.

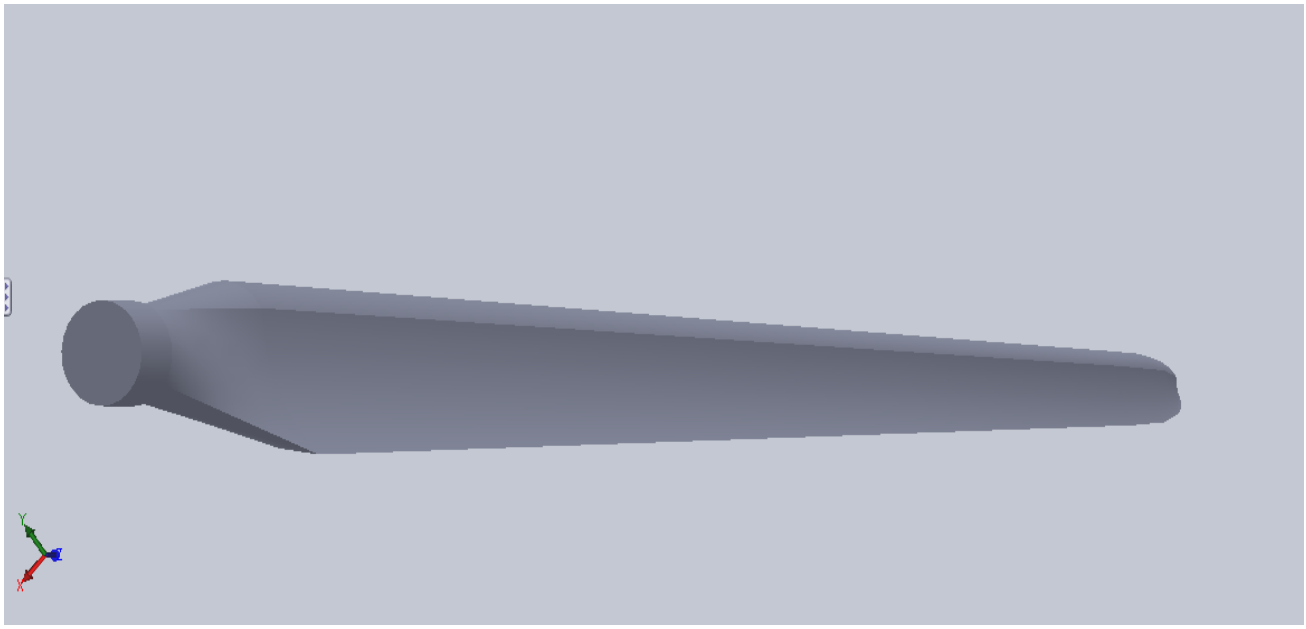

Figure 5.2 Solid work Model of single blade

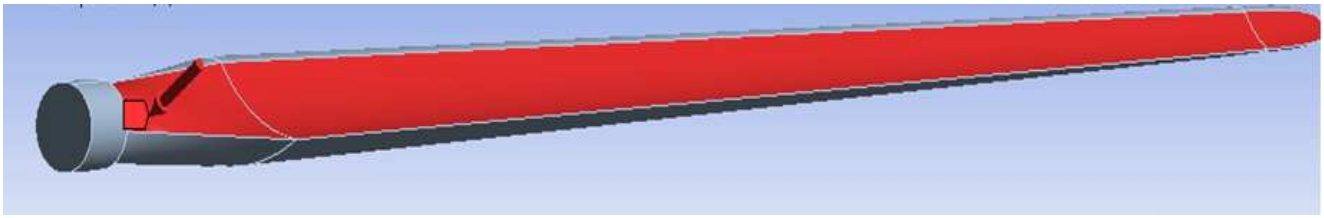

Figure 5.3 Wind pressure at blade

5.1 Minimum wind speed of $V = 6.13\ m/s$ for power production purpose :

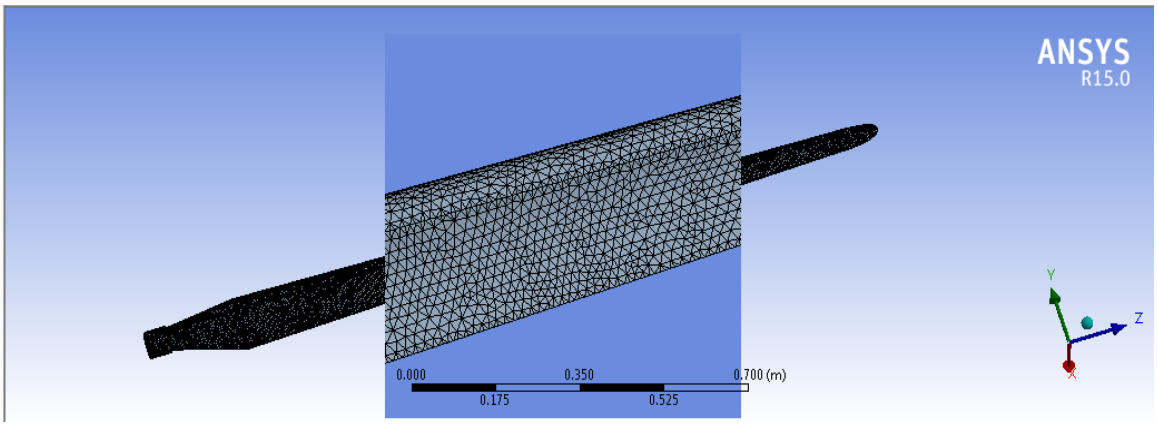

Figure 5.4 A 1.3979mm element size mesh

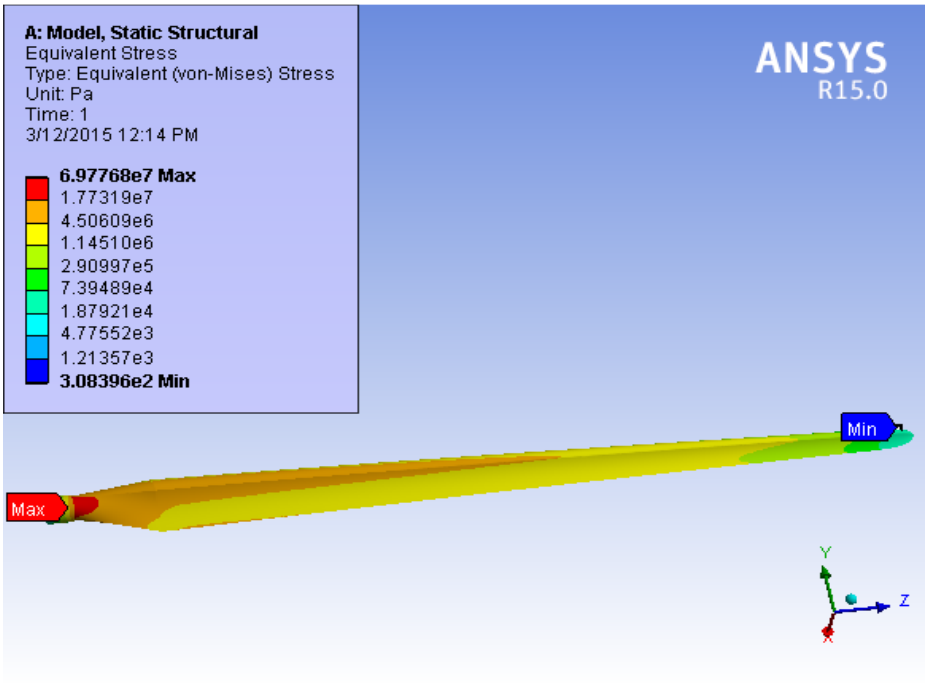

Figure 5.5 Equivalent (von mises) stress at V= 6.13m/s

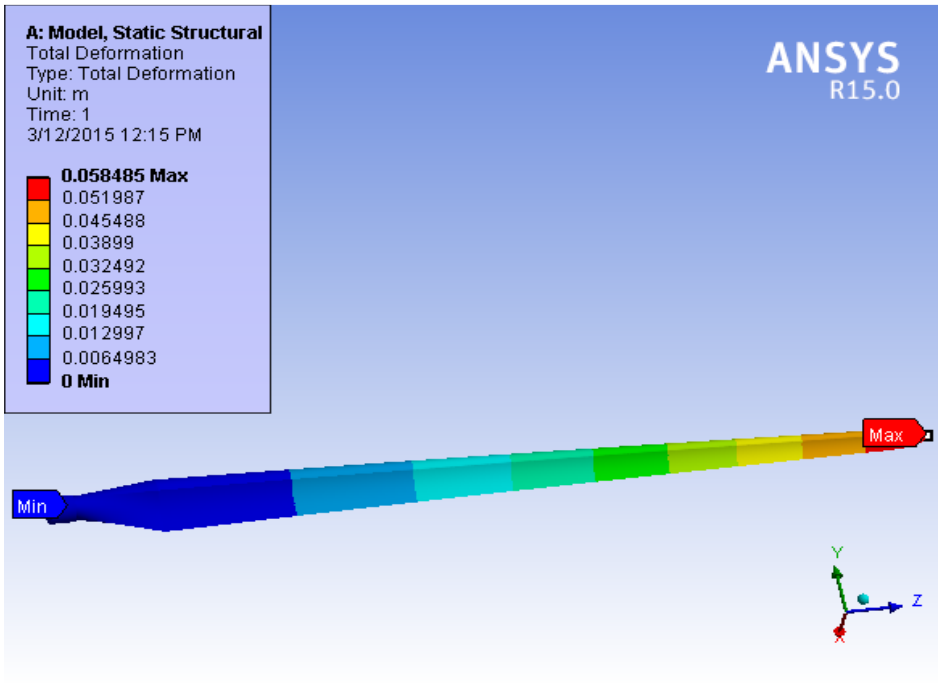

Figure 5.6 Maximum Deformation at the tip at V= 6.13m/s

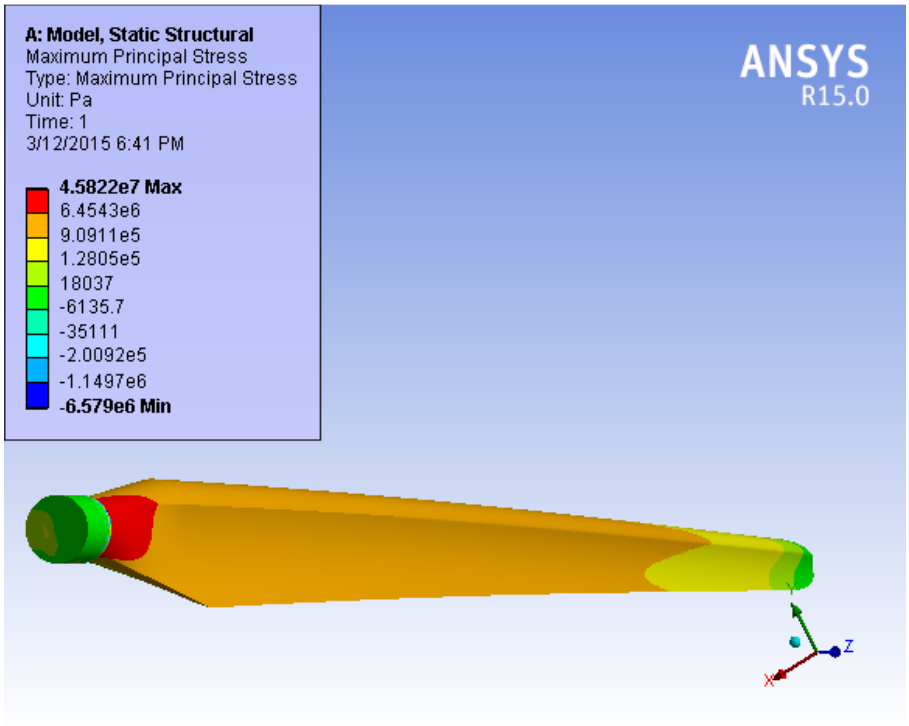

Figure 5.7 Maximum Principal Stress at V= 6.13m/s

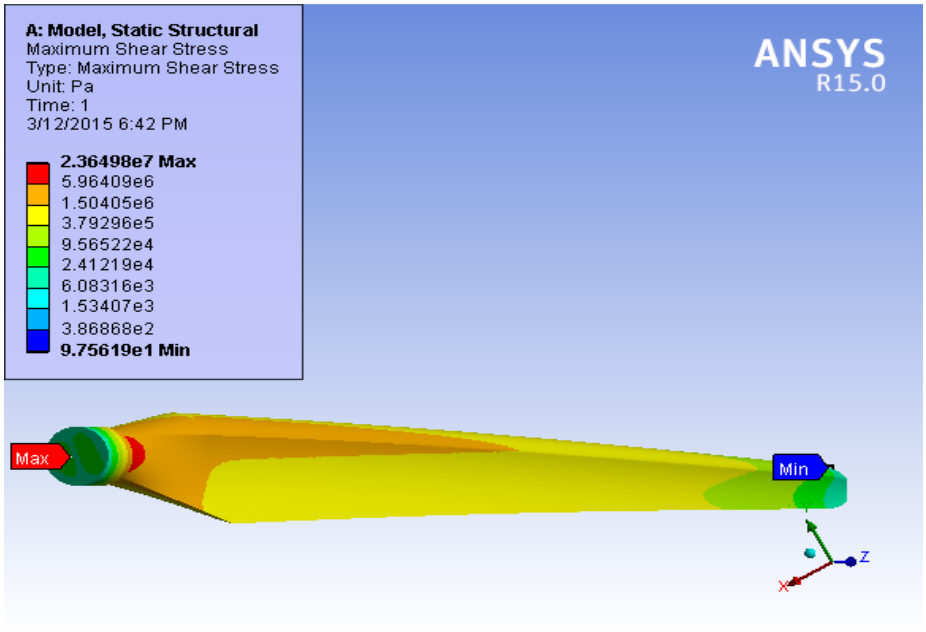

Figure 5.8 Maximum Shear Stress at V= 6.13m/s

Table 5.2 All results at V= 6.13m/s

Object Name	*Equivalent Stress*	*Total Deformation*	*Maximum Principal Stress*	*Maximum Shear Stress*	*Maximum Principal Elastic Strain*	*Maximum Shear Elastic Strain*
State	Solved					
Scope						
Scoping Method	Geometry Selection					
Geometry	All Bodies					
Definition						
Type	Equivalent (von-Mises) Stress	Total Deformation	Maximum Principal Stress	Maximum Shear Stress	Maximum Principal Elastic Strain	Maximum Shear Elastic Strain
Integration Point Results						
Display Option	Averaged		Averaged			
Results						
Minimum	3.084 e-004 MPa	0. m	-6.579e+001 MPa	9.75619 e-005 MPa	1.4678e-008 m/m	6.5677e-008 m/m
Maximum	6.9777e+001 MPa	5.8485e-002 m	4.522+001 MPa	2.36498e+001 MPa	1.1561e-002 m/m	1.751e-002 m/m

In the above figure5.4 to figure5.8the minimum mean average wind speed V= 6.13m/s created an resultant loads of 2426.798N is applied in the positive x- direction. It is possible to apply forces in the local direction specified by the user. The output power at this wind speed is 532.33watt. This amount of power is produced from a single turbine blades and can operate 16.1312 number of lamps for three hours per day of working time but the power consumption of each lump is 11watt.

In the Table 5.2 listed all results after applying displacement and load boundary conditions and computing, the analysis can be run. The resulting Von Misses stress, Directional Deformation, Maximum Principal Stress, Maximum Shear Stress, Maximum Principal Elastic Strain and Maximum Shear Elastic Strain are displayed above, the maximum Von Misses stress value in ANSYS 15 Workbench is 69.7768MPa at the root and the maximum deformation is 0.058485m occur at the tip of blade.

5.2 wind speed of $V = 8.26\ m/s$ for design purpose:

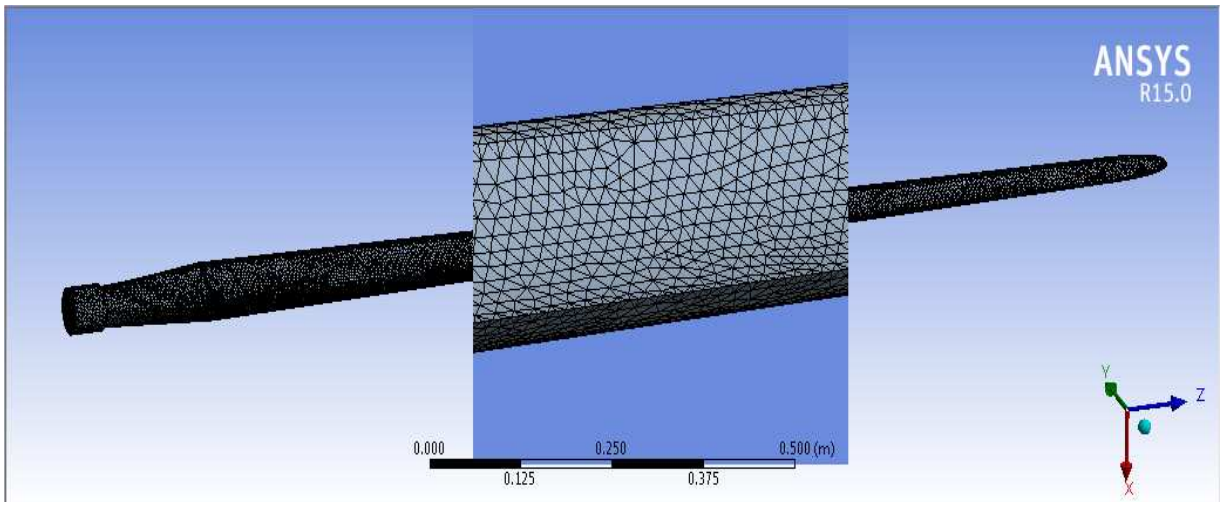

Figure 5.9 A 1.3979mm element size mesh

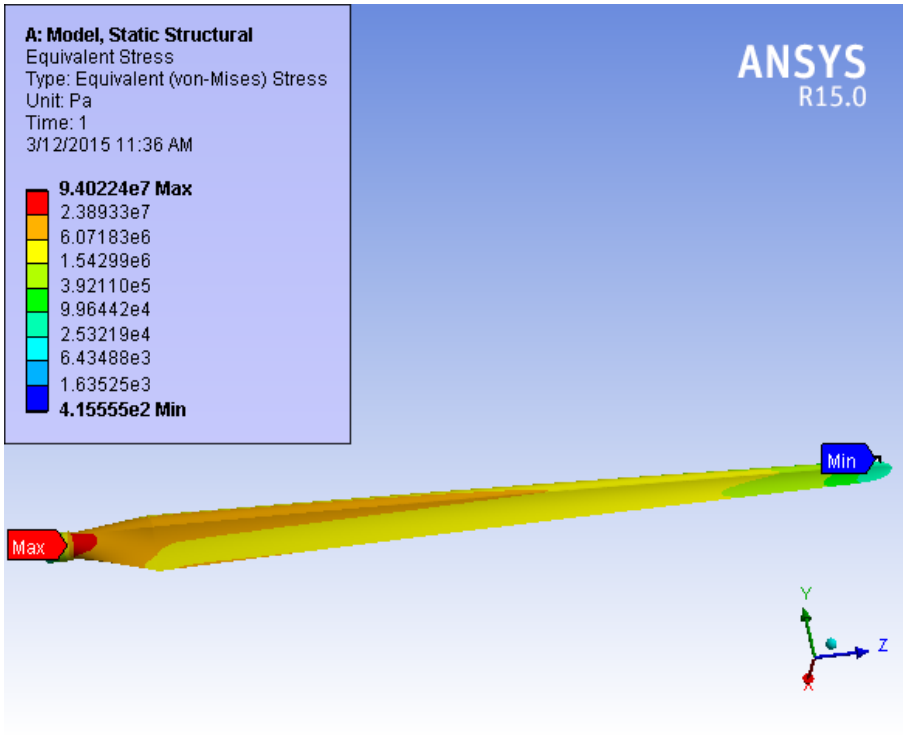

Figure 5.10 Equivalent(von messes)stress at V= 8.26m/s

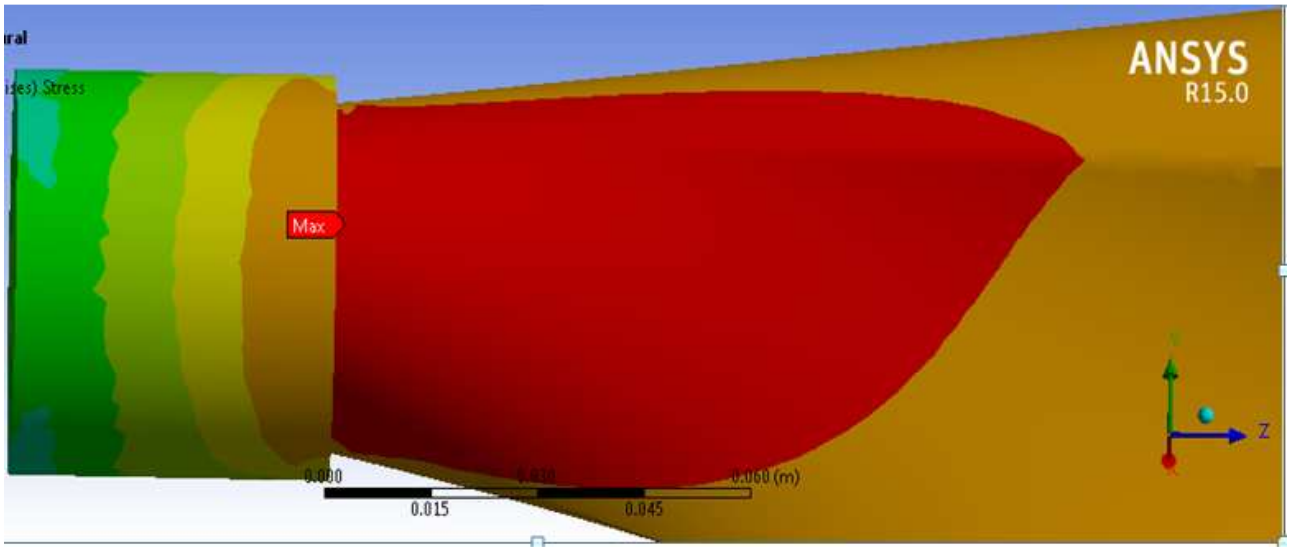

Figure 5.11 Maximum stress at the root at V= 8.26m/s

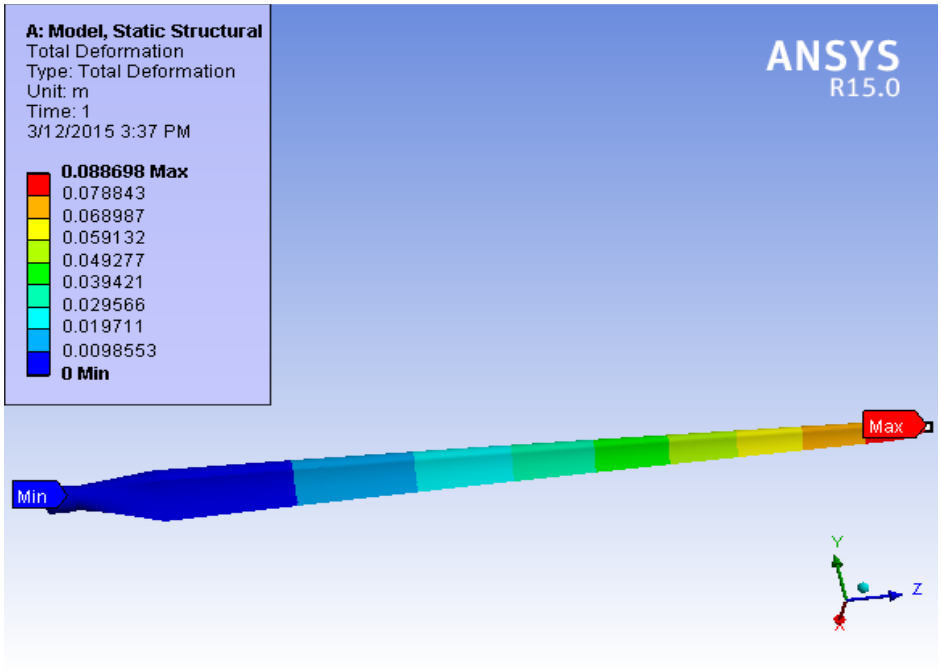

Figure 5.12 Maximum deformation at tip at V= 8.26m/s

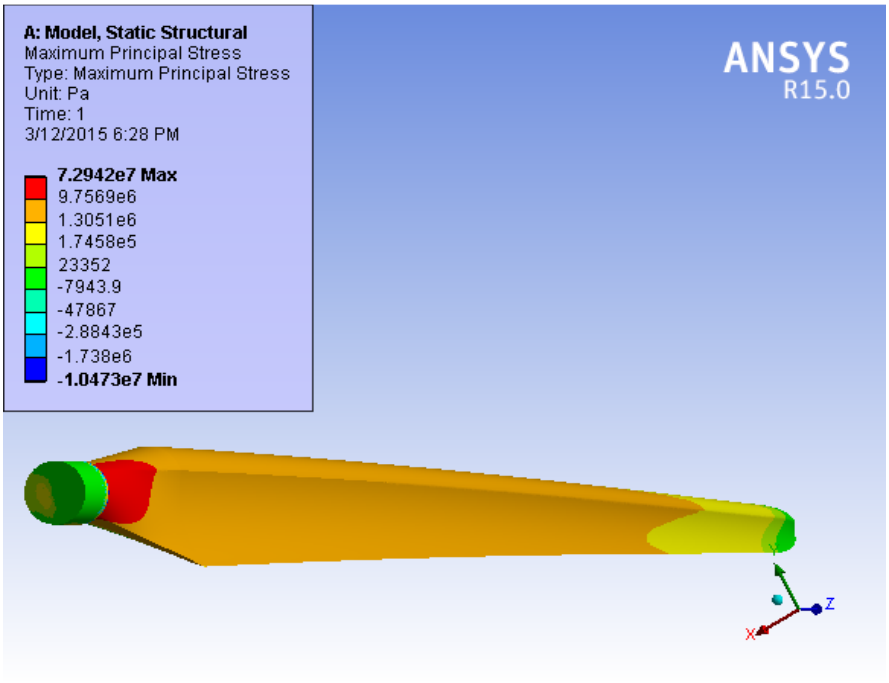

Figure 5.13 Maximum Principal Stress at V= 8.26m/s

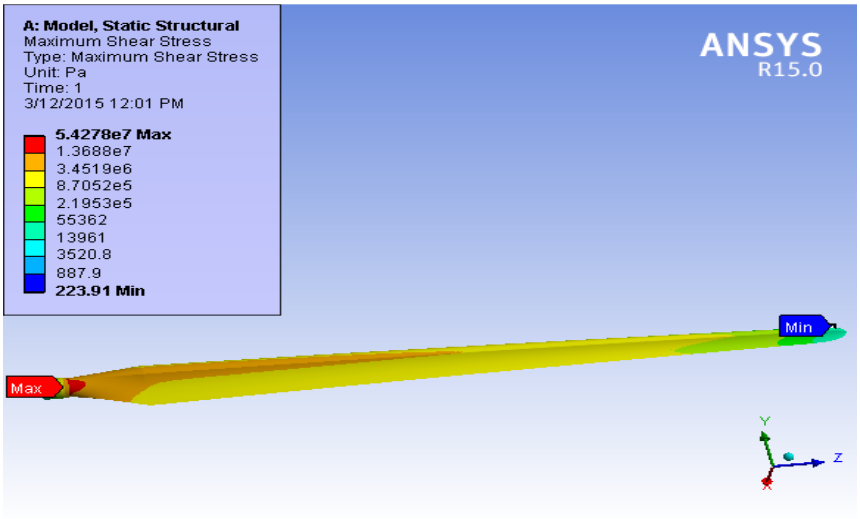

Figure 5.14 Maximum Shear Stress at V= 8.26m/s

Table 5.3 All results at V= 8.26m/s

Object Name	*Equivalent Stress*	*Total Deformation*	*Maximum Principal Stress*	*Maximum Shear Stress*	*Maximum Principal Elastic Strain*	*Maximum Shear Elastic Strain*
State	Solved					
Scope						
Scoping Method	Geometry Selection					
Geometry	All Bodies					
Definition						
Type	Equivalent (von-Mises) Stress	Total Deformation	Maximum Principal Stress	Maximum Shear Stress	Maximum Principal Elastic Strain	Maximum Shear Elastic Strain
Integration Point Results						
Display Option	Averaged		Averaged			
Results						
Minimum	4.15e-004 MPa	0. m	-10.473 MPa	2.2391e-004 MPa	1.9778e-008 m/m	8.8497e-008 m/m
Maximum	94.022 MPa	8.86987e-002 m	72.942 MPa	5.4278e+007 MPa	1.5578e-002 m/m	2.3595e-002 m/m

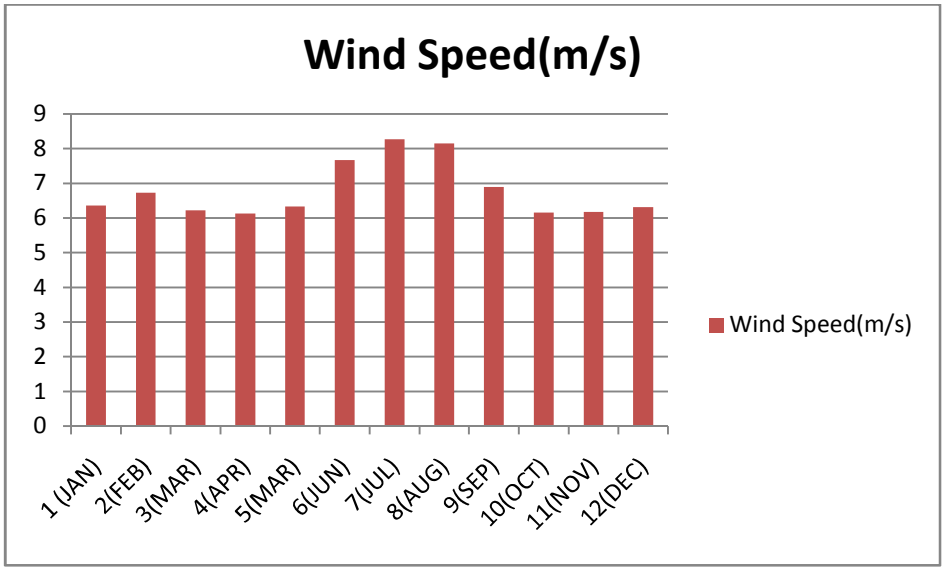

Figure 5.15 Annual average wind speed in m/s

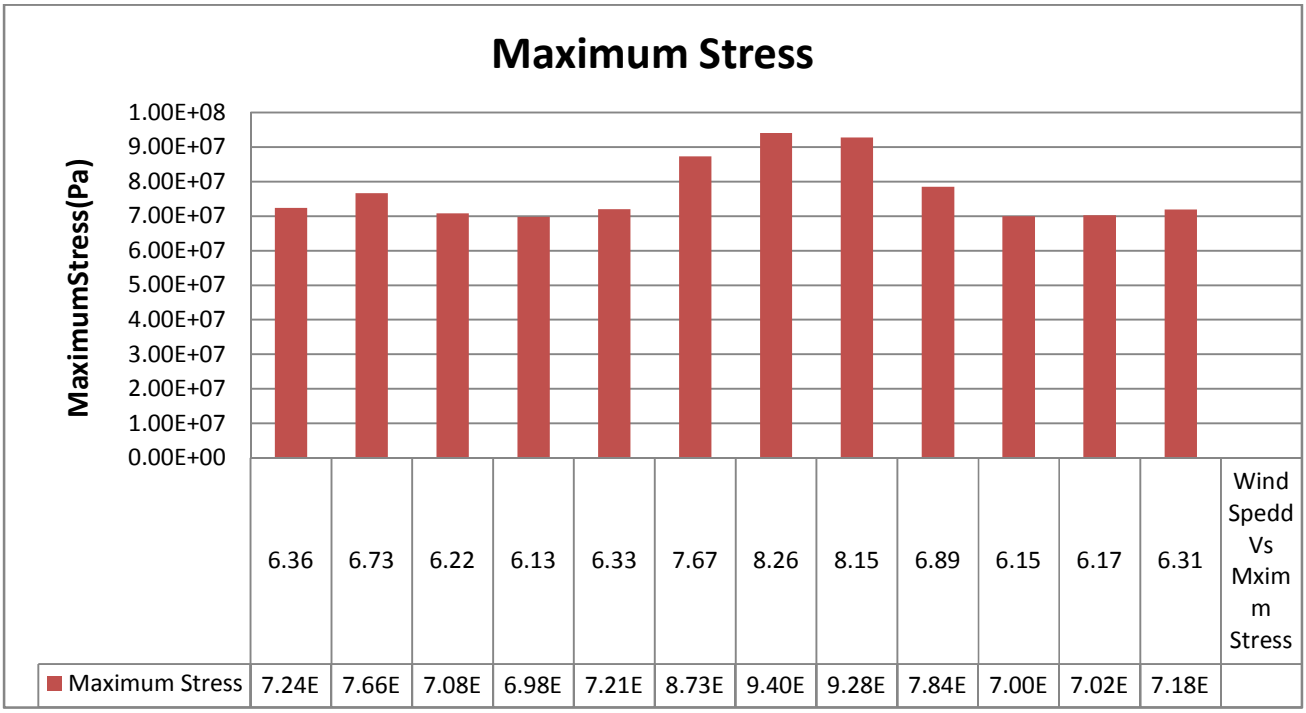

	6.36	6.73	6.22	6.13	6.33	7.67	8.26	8.15	6.89	6.15	6.17	6.31	Wind Speed Vs Maximum Stress
Maximum Stress	7.24E	7.66E	7.08E	6.98E	7.21E	8.73E	9.40E	9.28E	7.84E	7.00E	7.02E	7.18E	

Figure 5.16 Maximum Stress Results at different Annual wind speed

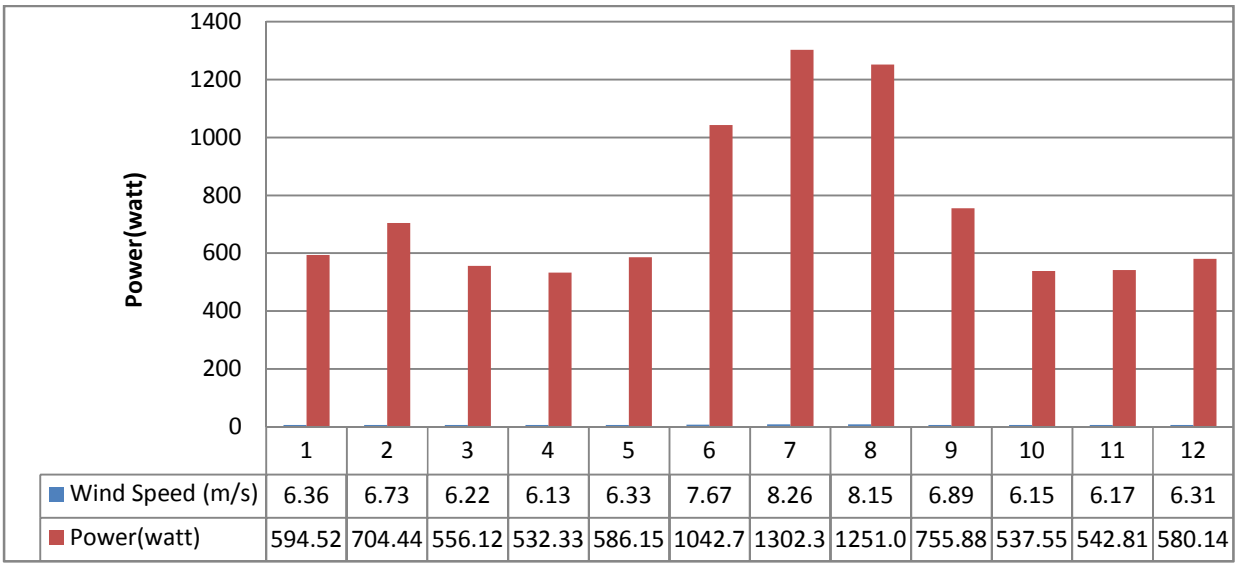

	1	2	3	4	5	6	7	8	9	10	11	12
Wind Speed (m/s)	6.36	6.73	6.22	6.13	6.33	7.67	8.26	8.15	6.89	6.15	6.17	6.31
Power(watt)	594.52	704.44	556.12	532.33	586.15	1042.7	1302.3	1251.0	755.88	537.55	542.81	580.14

Figure 5.17 Output Power Results at different Annual wind speed

In the above figure5.9 to figure5.17 the maximum mean average wind speed V= 8.26m/s created a resultant load of 3270.05N is applied in the positive x- direction. It is possible to apply forces in the local direction specified by the user. The output power at this wind speed is 1302.38watt. This amount of power is produced from a single turbine blades and can operate 39.466 number of lamps for three hours per day of working time but the power consumption of each lump is 11watt.

In the Table 5.3listed all results after applying displacement and load boundary conditions and computing, the analysis can be run. The resulting Von Misses stress, Directional Deformation, Maximum Principal Stress, Maximum Shear Stress, Maximum Principal Elastic Strain and Maximum Shear Elastic Strain are displayed above, are displayed above, the maximum Von Misses stress value in ANSYS 15 Workbench is 94.0224MPa and the maximum deformation is 0.088698m.

In both above cases the stresses on the blade which are below the yield strength of the selected material.

The maximum stress from the ANSYS 15 workbench is obtained 94.0224MPa. As previously done, the ANSYS 15 workbench value is compared with the analytical value. The calculated value is found 99.5MPa. The percentage error is 5.5%. This percentage error is found because of a 1.3979mm element size mesh to minimize the memory size of the computer.

5.3 Modal Shape:

Table 5.4 Modal Shape analysis at workbench

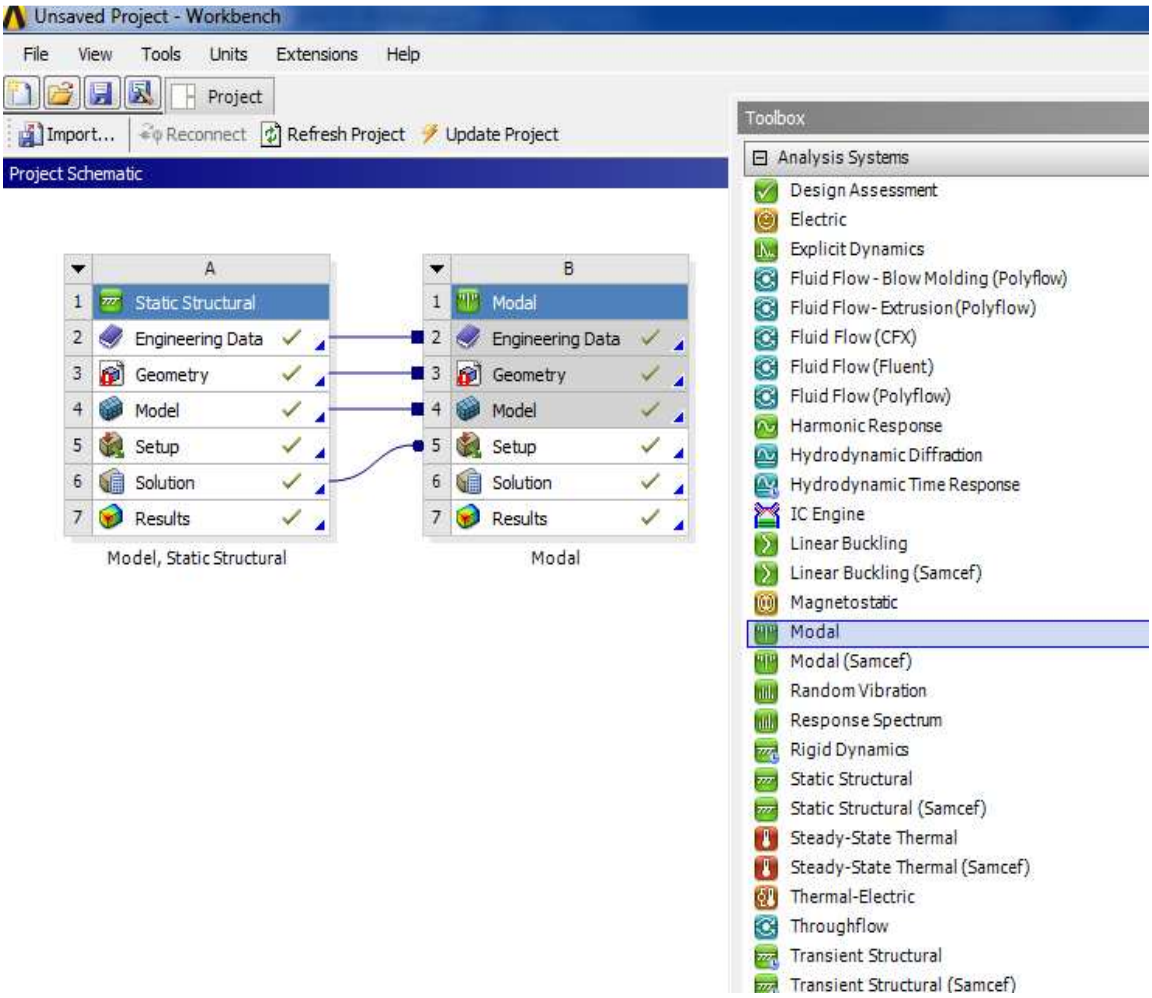

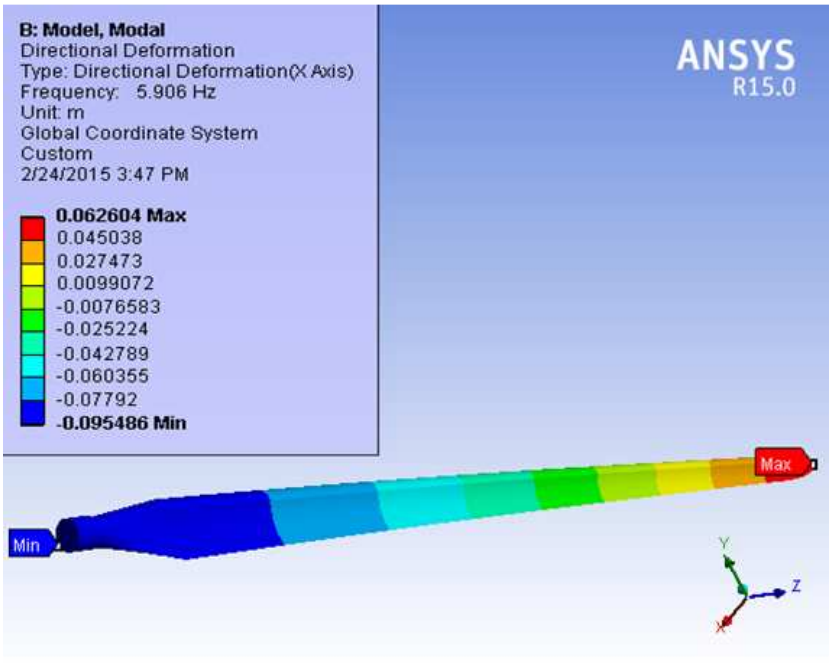

Figure 5.18 First natural mode of the blade at frequency of 5.906Hz.

Table 5.5 Modal Shape analysis at workbench

Modal	Frequency Hz.
1	5.906
2	7.214
3	21.425
4	27.146
5	54.835
6	77.374

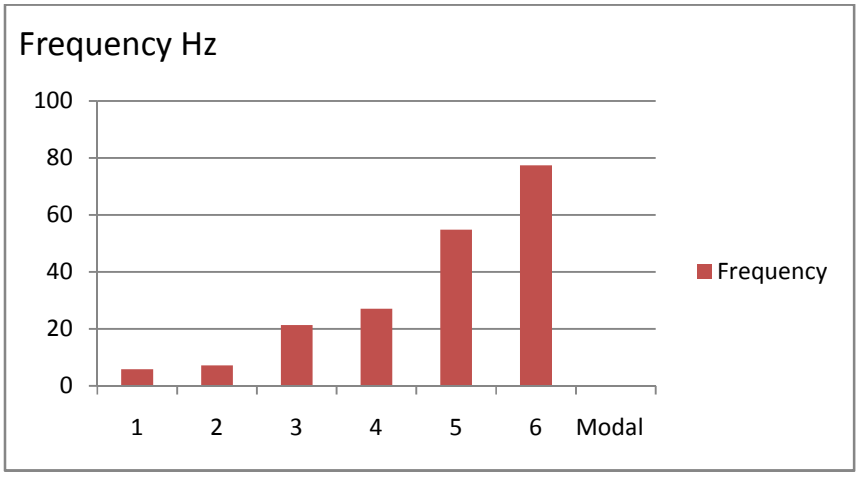

Figure 5.19 Values of frequency at different Modals.

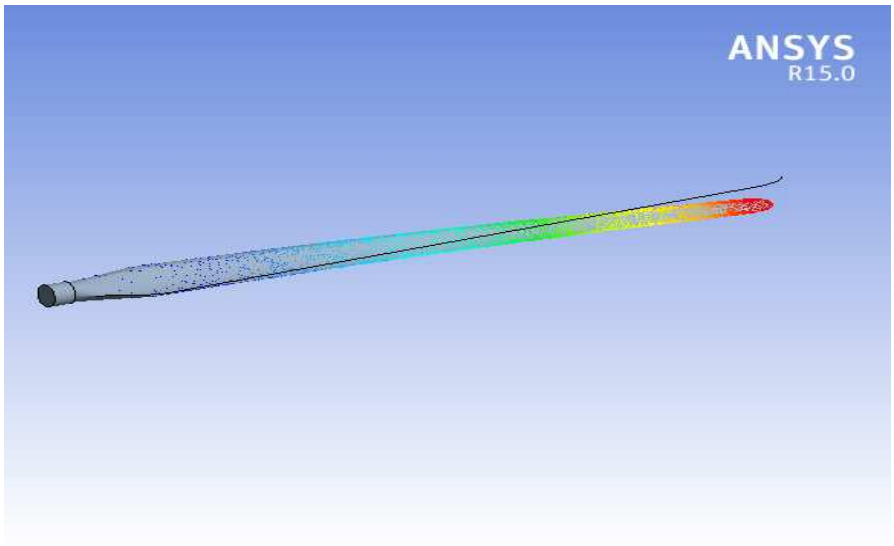

Figure 5.20 Second natural mode of the blade at frequency of 7.214.

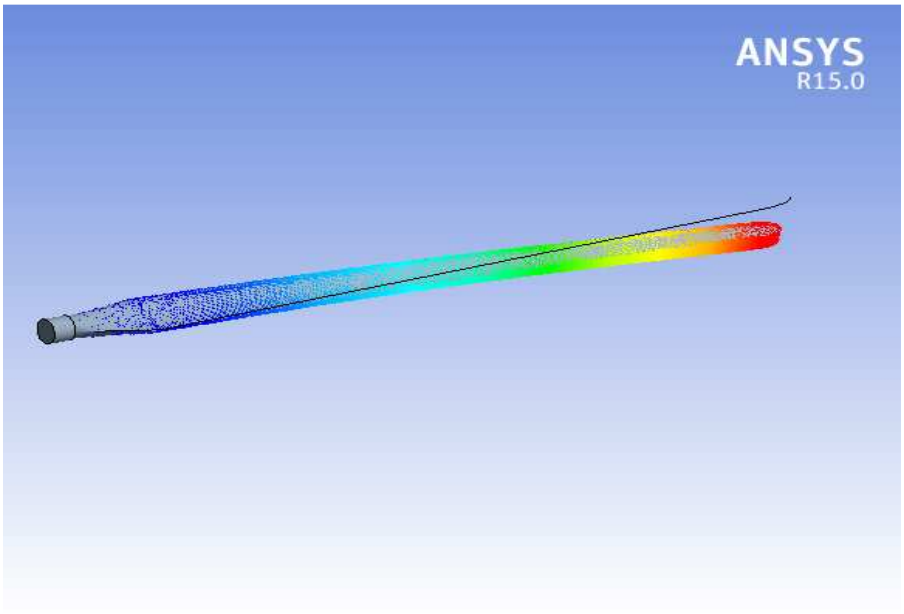

Figure 5.21 Third natural mode of the blade at frequency of 21.425.

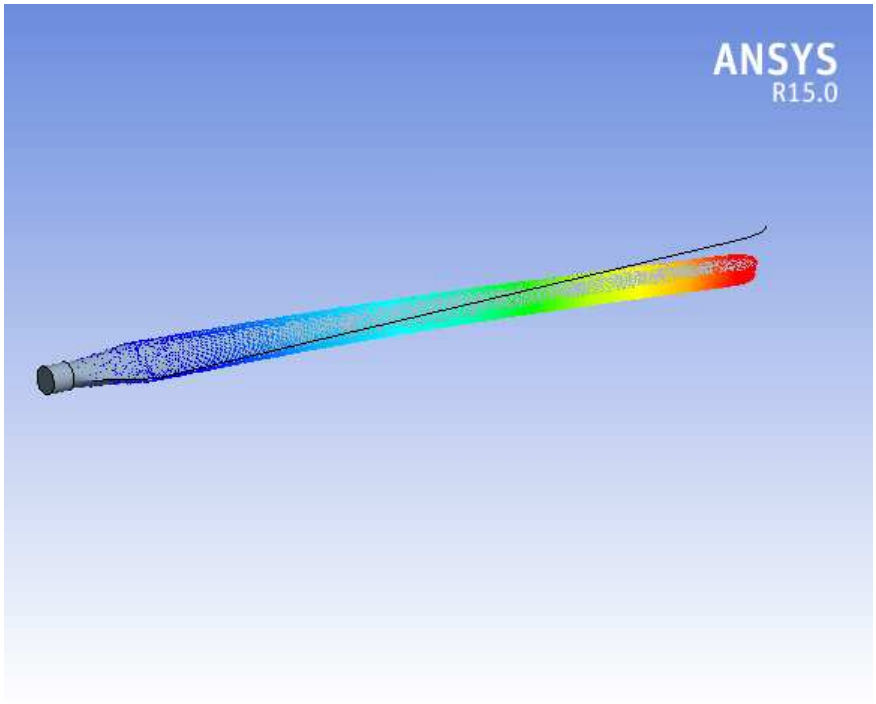

Figure 5.22 Fourth natural mode of the blade at frequency of 27.146.

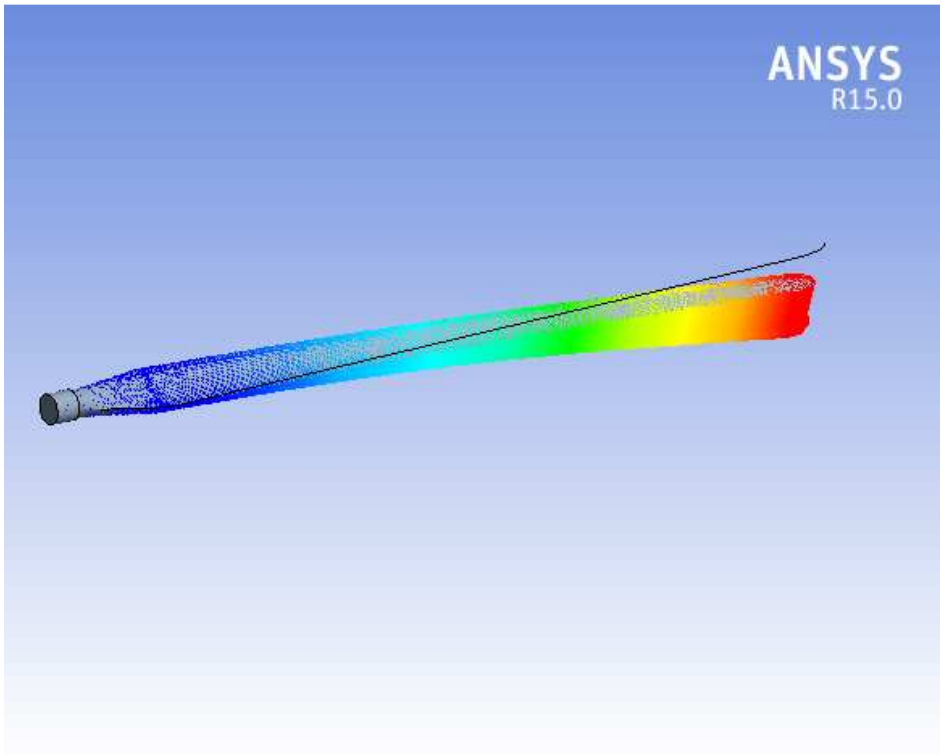

Figure 5.23 Fifth natural mode of the blade at frequency of 54.835.

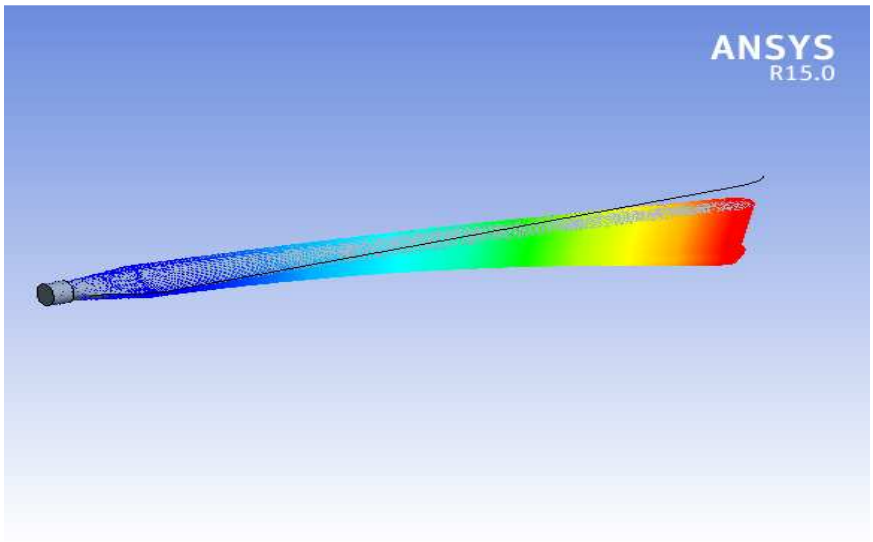

Figure 5.24 Sixth natural mode of the blade at frequency of 77.374.

Results of the modal analysis are presented in figure5.18 to figure5.24 and Table 5.5. The ANSYS Workbench modal frequencies provide satisfactory correlation of the result for first six natural frequencies. However, for higher frequencies the deformation also different. This can be explained by the fact that higher frequencies are more influenced by structural deviations. Usually for small turbine blades evaluations of natural frequencies are of interest. Therefore, in general it can be concluded that the ANSYS Workbench model is validated for modal shape of blade.

5.4 Assembly blade:

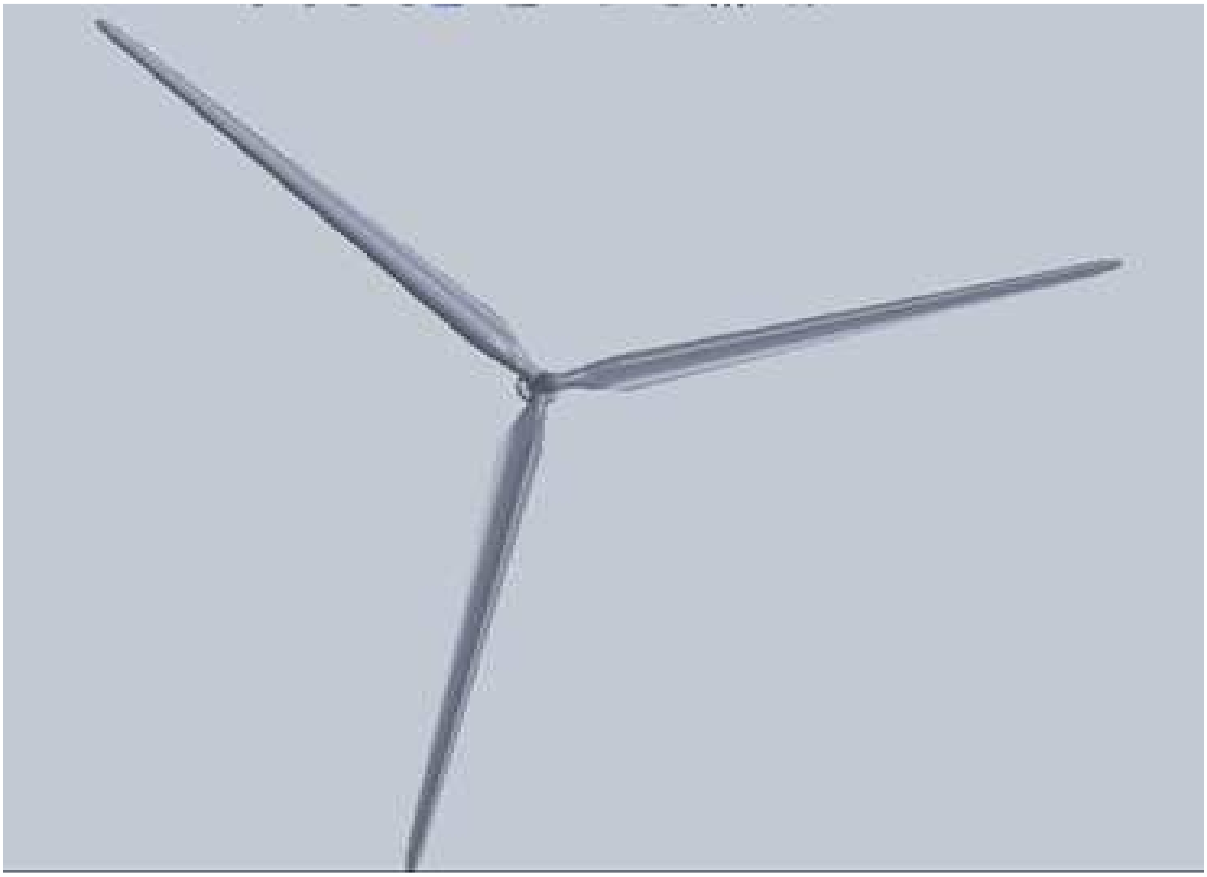

Figure 5.25 Solid work Model of Assembly Blades

Figure 5.26 Solid work Model of Assembly at rotor

The above figure5.25 and figure5.36 are the assembly models by Solid work software, to show the assembly of the three blades within the hub and the center to center angle of each consecutive blades is 120^0.

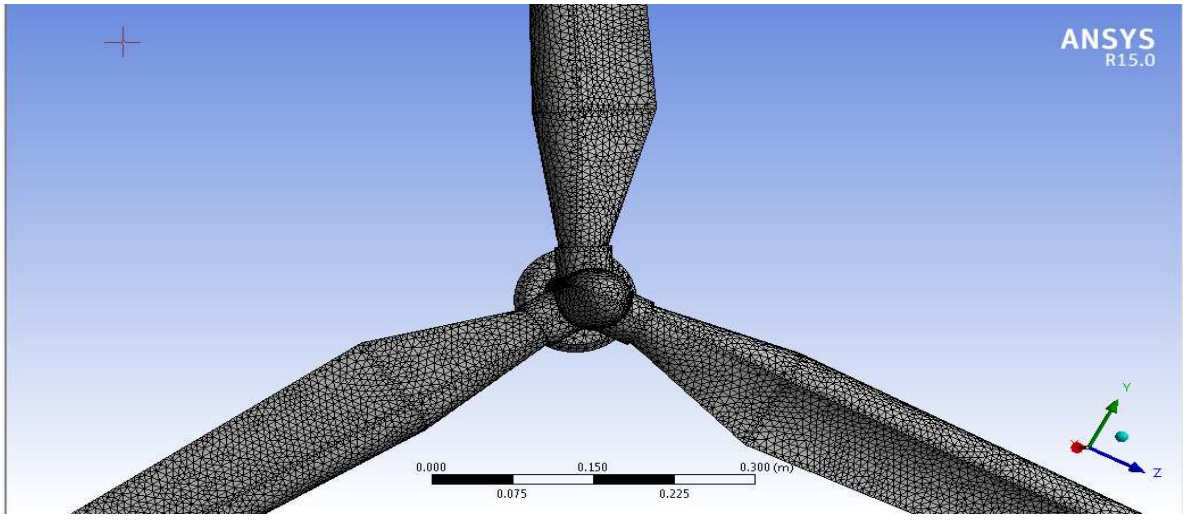

Figure 5.27 A 1.3979mm element size mesh on Assembly blade

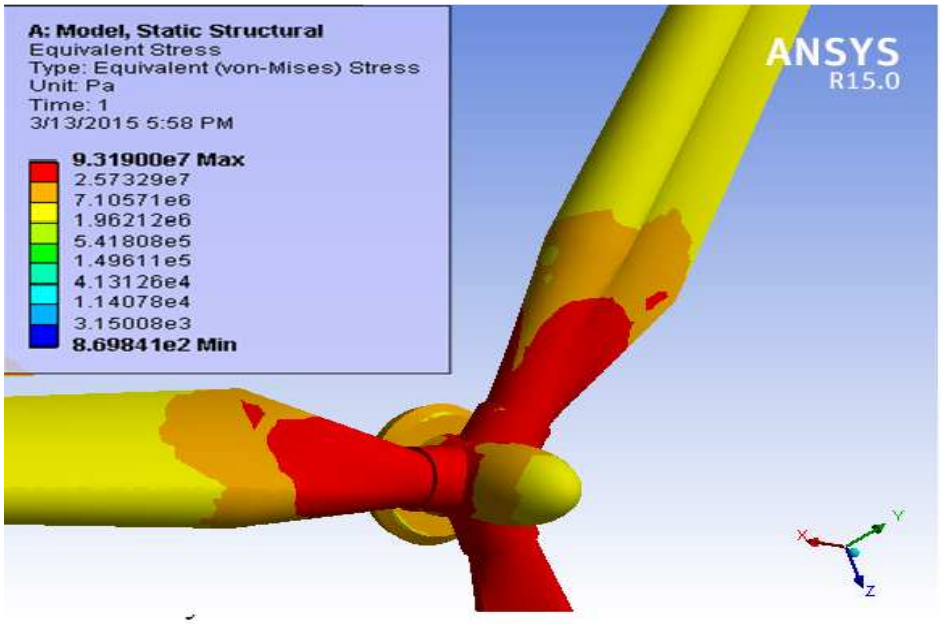

Figure 5.28 Stress on Assembly blade

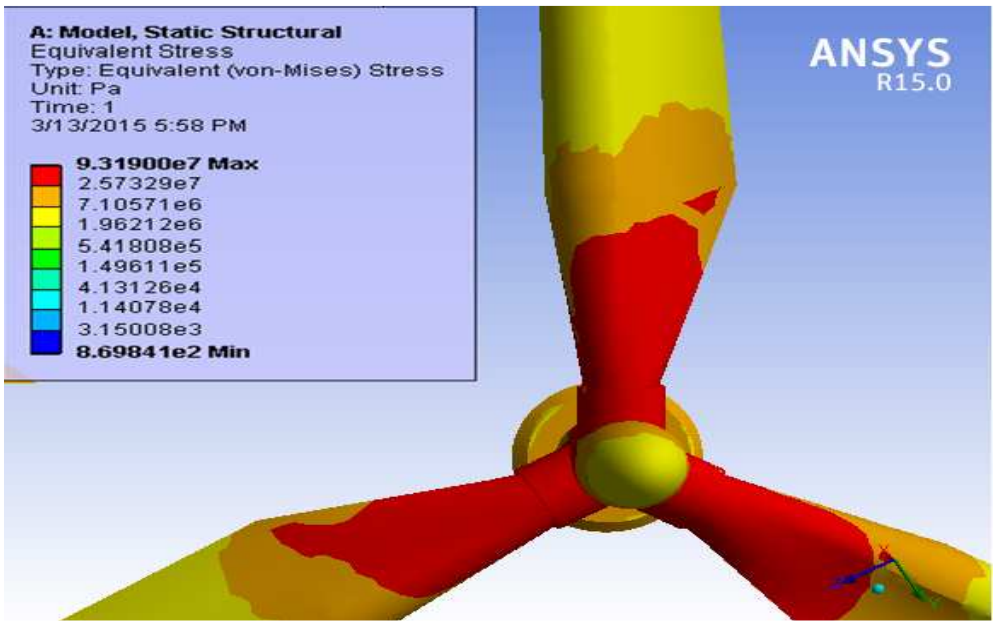

Figure 5.29 Maximum Stress on Assembly blades

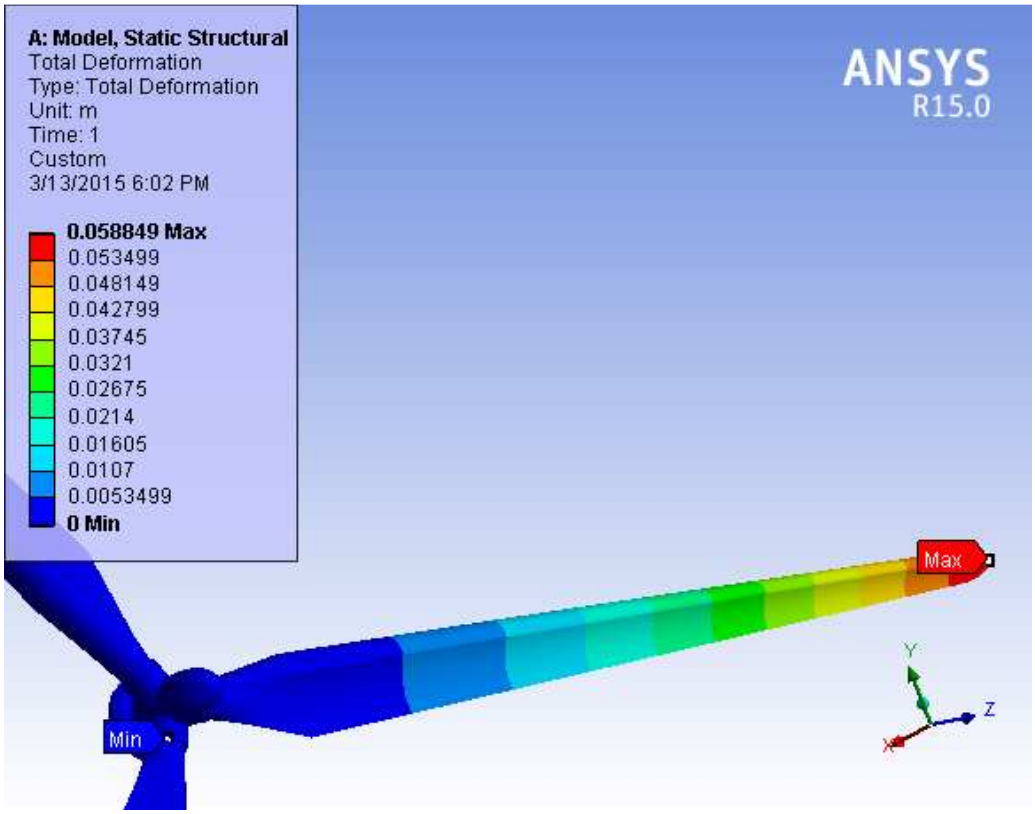

Figure 5.30 Maximum Deformation on Assembly blades

In the above figure5.37 to figure5. 30, the analysis of stress and deformation done by ANSYS15 WORKBANCH software, to show the positions of maximum stresses and deformations when a different an aerodynamics loads, wind speeds and maximum pressures are applied on the faces of the blades the maximum stresses at the root parts of the blades and the maximum deformations at the tip parts of the blades because of the pressure distribution on the three blades are varies with the pressure on single blade so that the maximum stress and maximum deformation also different.

CHAPTER 6
CONCIUSION AND RECOMMENDATION

6.1 CONCLUTION:

In this study, design and stress analysis of small scale horizontal-axis wind turbine blade was investigated . Wind turbine blades are the pivot of the other parts of a wind turbine in electricity production since they extract the energy from the wind and carry this energy to generators which produce electricity. The interaction between the wind and the blades is related to the aerodynamic, gravitational and centrifugal forces acting on the blades. While the wind is passing through the area swept by a rotor it leaves its some part of energy on the blades resulting from these forces interaction. Hence it is limited to the aerodynamic aspect during the study of HAWT blade design. From the literature and background of this thesis, when a resultant loading or pressure is applied on the wind blade body, since the blade considered as a cantilever beam that is support at the root part (hub), the general idea and the analysis shows as follow.

1. Based on the collected wind speed date from Negele Borana and gathering of information from literatures, developing of mathematical model for a single and assembly wind blade that produced power that can be used electrification for all communities has been analyzed and designed for Laga-Gula kebele.

2. For a mean average wind speed data of 6.13m/s, because of this minimum wind speed, the loads are minimum, pressure is minimum, stress at root , blade deformation is at tip and the minimum amount of power is produced. This shows that the probability of failures decrease but insufficient power is produced. More over this, the thesis shows that the output power produced by this wind speed can operate only 16.1312 number of lamps per day for only three hours i.e. the power consumption of each lamp is 11W.

3. For a maximum wind speed data of 8.26m/s, because of this maximum wind speed, the loads are maximum, pressure is maximum, maximum stress at root , maximum blade deformation is at tip and the maximum amount of power is produced. This shows that the probability of failures

increase and sufficient power is produced. More over this, the thesis also shows that the output power of 1302.38watt produced by this wind speed can operate 39.466 lamps per day for three hours i.e. the power consumption of each lamp is 11W.

Those points show us how wind speed varies the stress, deformation and power . This helps us how we should treat wind speed behaviors during design. It also helps to determine blade dimension and airfoil selection during design, blade investigation after manufacturing and during maintenance to investigate the position of maximum stress and deformation on blade. According to the results the maximum stresses occur at the support and the maximum deformation occur at the tip of the blade.

To get sufficient power for the Laga-Gula rural communities i.e. for 193 number of households design a number of turbines for example the number of turbines is twelve the output power will be 6387.96watt per day by minimum wind speed. It can operate 193.5745 lamps per day for three hours i.e. the power consumption of each lamp is 11W. If the wind speed is maximum the total output power of all twelve turbines will be 15628.56watt. It can operate 473.5927 lamps per day for three hours i.e. the power consumption of each lamp is 11W.

6.2 Recommendations of Future Work:

As mentioned before, the goal of this dissertation research was the determination design and stress analysis of wind blade parameter for Laga-Gula rural communities . This thesis determined the behaviors of maximum stress, maximum deformation and sufficient power parameters for minimum and maximum average wind speed cases. However, it is easy to conclude that to satisfied the electric power for all Laga-Gula rural communities it needs a least twelve wind turbine blades and the results of the maximum stress at root, maximum deformation at tip and sufficient power produced at maximum average wind speed criterion can be evaluated. However, number suggestion can be made, the following future works can be the initial of similar kinds of research:

- Design and stress analysis of small scale Horizontal axis wind turbine blades by the Actuator disk theory and The Betz limit.
- Experimental testing of small-scale wind turbines.
- Design and stress analysis of small scale Vertical axis wind turbine blades for rural electrification(1−5kW).
- Design and stress analysis of small scale Horizontal axis wind turbine blades by the composite material of Carbon Fiber reinforced plastics.
- Blade Performance Analysis and Design Improvement of small horizontal wind turbine for rural areas.
- Design and characterization of a Small horizontal wind turbine model equipped with a pitching system**.**
- Design and fabrication of a new small horizontal wind turbine blade.
- Design of gearbox and Nacelle for small scale Horizontal axis wind turbine blades.
- Setup and performance test of a small-scale horizontal axis wind turbine.
- Design of wind turbine tower and foundation systems optimization approach.

REFERENCES

1. Spera, D. A., “Wind Turbine Technology”, Asme Press, 1998.
2. Manwell, J. F., McGowan, J. G., Rogers, A. L., “Wind Energy Explained; Theory, Design and Application”, John Wiley & Sons Ltd, 2002
3. World wind report 2008
4. Teferi Tayi," wind energy harnessing- Theory and the Ethiopian experience", Journal of the ESME, Vol. II, No.2, October 1999
5. Hansen, A. and Butterfield, "Aerodynamics of horizontal-axis wind turbines", Annual Review of Fluid Mechanics 1993.
6. Manwell, J. McGowan, and Rogers, "Wind Energy Explained. Theory, Design and Application" John Wiley and Sons, Ltd 2002.
7. Walker, J. and Jenkins, "Wind Energy Technology", John Wiley and Sons, Ltd 1997.
8. S. Desta, S. Tezera, G. Gebru and P. Kristjanson, "Summary of Baseline Household Survey Results in Borana, Ethiopia" December 2011 .
9. Grant Ingram, " Wind Turbine Blade Analysis using the Blade Element Momentum Method" Version 1.1, October 18, 2011.
10. Siraj Ahmed, " Design and Analysis of Horizontal Axis Wind Turbine Rotor", Maulana Azad National Institute of Technology, Bhopal , November 2011.
11. Verónica Cabanillas, "Studied Blade Performance Analysis and Design Improvement of A Small Wind Turbine for Rural Areas", University of Purdue West Lafayette, August 2013.
12. Peter J. Schubel and Richard J. Crossley, "Wind Turbine Blade Design", University of Nottingham, Nottingham NG7 2RD, UK, April 2012.
13. Mulugeta Biadgo, "Computer-aided aerodynamic and structural design of horizontal- axis wind turbine blades", AAU, June 2009.
14. Fadi Abdulhadi, "Design and Characterization of a Small Wind Turbine Model equipped with a Pitching System", REMENA, Feb 2012.
15. Andrew Corbyn" fiber glass wind turbine blade manufacturing guide ", Engineers Without Borders, Version 1.4, 1st May 2008.

16. Ravi Anant Kishore, "Small-scale Wind Energy Portable Turbine (SWEPT)", Virginia Polytechnic Institute and State University, May 06, 2013.
17. Qiyue Song, "Design, Fabrication, and Testing of a New Small Wind Turbine Blade", The University of Guelph, Ontario, Canada, April, 2012.
18. Jason R. Gregg, B.S.M.E, "Design and Experimental Testing of Small-Scale Wind Turbines", Baylor University, May 2011.
19. Student nr: 1333186, "Small Wind Turbines in Kenya", Delft University of Technology, 21 March 2012.
20. F.W. Perkins and D.E. Cromack, "Wind Turbine Blade Stress Analysis And Natural Frequencies", University of Massachusetts Amherst, Massachusetts 01003, August 1978.
21. I. Youm , J. Sarr , M. Sall , A. Ndiaye and M.M. Kane, "Analysis of wind data and wind energy potential along the northern coast of Senegal", Université Cheikh Anta Diop, Dakar-Fann, Sénégal, Rev. Energ. Ren. Vol. 8 (2005) 95 - 108.
22. Jean-Jacques chattot, "Design and analysis of wind turbines using helicoidally vortex model", University of California Davis, Davis, California, December 9, 2001.
23. Xinzi Tang, Ruitao Peng, Xiongwei Liu, Anthony Ian Broad, "Design and Finite Element Analysis of Mixed Aerofoil Wind Turbine Blades", University of Central Lancashire Fylde Road, Preston, UK, August 2011.
24. Hao Wang, Bing Ma, Jiaojiao Ding, Shuaibin Li, "The Modeling and Stress Analysis of Wind Turbine Blade", College of Energy and Mechanical Engineering, Shanghai University, Vol.12, No.6, June 2011.
25. Serhat Duran, "Computer- Aided design of Horizontal- axis wind turbine blades", Middle east technical university, JAN 2005 .
26. J. Selwin Rajadurai" Finite element analysis with an improved failure criterion for composite wind turbine blades", Published online: 3 June 2008.
27. Samia Zekaria" Statistical Reports of the Census for Oromiya Region" Member and Secretary, Population Census Commission,2008.

28. Ma Jiangtao and Zhang Bo " Master Plan Report of Wind and Solar Energy in the Federal Democratic Republic of Ethiopia" Hydrochina Corporation, July 2012
29. U.S. Department of Energy’s, Energy Efficiency and Renewable Energy Information Portal "Small Wind Electric Systems" A U.S. Consumer’s Guide,2002.
30. New Energy Husum " Small Wind World Report 2014 " WWEA Head Office Charles-de-Gaulle-Str. 53113 Bonn, Germany,2014.

Appendices:

The analysis of stresses and deformations by ANSYS 15 WORKBEANCH at different average monthly wind speeds data at Negele Borana town at Gujii zone.

Material Data :

Epoxy-E Glass fiber Reinforced plastic (GRP)

Epoxy-E Glass fiber Reinforced plastic (GRP) > Constants

Density	2000 kg m^-3

Table M1 Epoxy-E Glass fiber Reinforced plastic (GRP) > Orthotropic Elasticity

Temperature C	Young's Modulus X direction MPa	Young's Modulus Y direction MPa	Young's Modulus Z direction MPa	Poisson's Ratio XY	Poisson's Ratio YZ	Poisson's Ratio XZ	Shear Modulus XY (MPa)	Shear Modulus YZ (MPa)	Shear Modulus XZ (MPa)
	3.44e+04	6.53e+003	6.53e+003	0.217	0.336	0.217	2.43e+003	1.7e+003	2.43e+003

Table M2 Epoxy-E Glass fiber Reinforced plastic (GRP) > Orthotropic Strain Limits

Temperature C	Tensile X direction	Tensile Y direction	Tensile Z direction	Compressive X direction	Compressive Y direction	Compressive Z direction	Shear XY	Shear YZ	Shear XZ
	2.44e-002	3.5e-003	3.5e-003	-1.5e-002	-1.2e-002	-1.2e-002	1.6e-002	1.2e-002	1.6e-002

Table M3 Epoxy-E Glass fiber Reinforced plastic (GRP) > Orthotropic Stress Limits

Temperature C	Tensile X direction (MPa)	Tensile Y direction (MPa)	Tensile Z direction (MPa)	Compressive X direction (MPa)	Compressive Y direction (MPa)	Compressive Z direction (MPa)	Shear XY (MPa)	Shear YZ (MPa)	Shear XZ (MPa)
	1.1e+003	3.5e+001	3.5e+001	-6.75e+002	-1.2e+002	-1.2e+002	8.e+001	4.6154e+001	8.e+001

Mesh:

Table M4 Model(A4) > Mesh

Object Name	Mesh
Sizing	
Relevance Center	Fine
Element Size	1.3979e-003 m

Appendix A:

V= 6.36 m/s

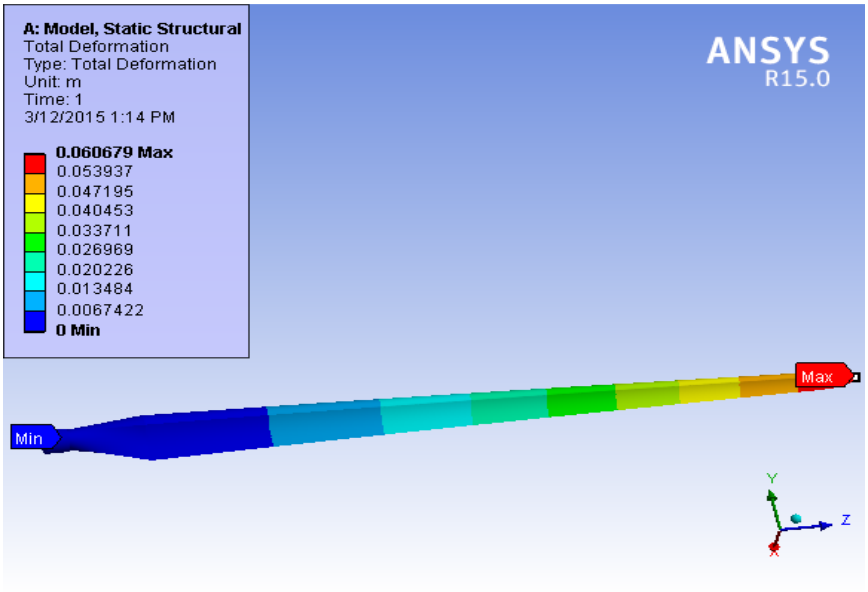

Figure A1 Directional Deformation

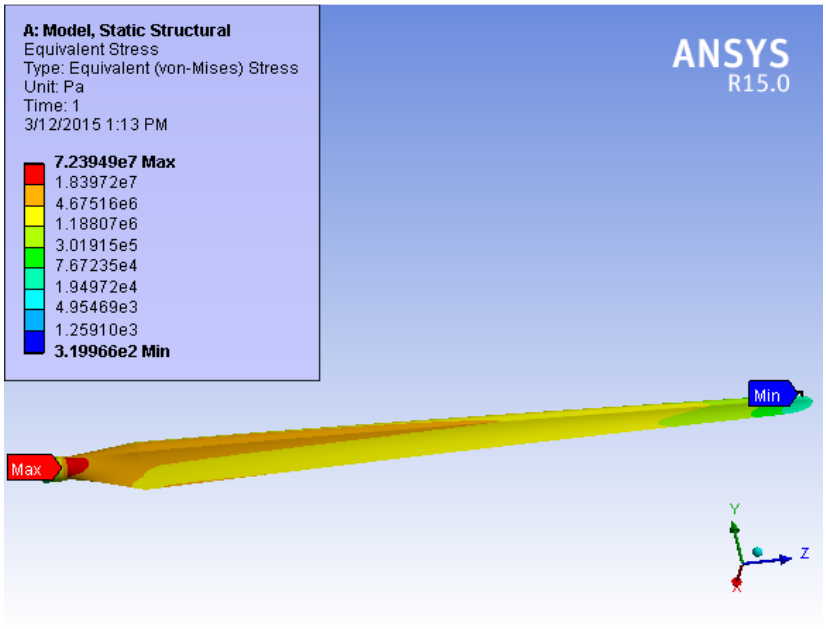

Figure A2 Equivalent Stress at V= 6.36m/s

Solution :

Table A1 Model (A4) > Static Structural (A5) > Solution (A6) > Results

Object Name	*Equivalent Stress*	*Total Deformation*	*Maximum Principal Stress*	*Maximum Shear Stress*	*Maximum Principal Elastic Strain*	*Maximum Shear Elastic Strain*
State	Solved					
Scope						
Scoping Method	Geometry Selection					
Geometry	All Bodies					
Definition						
Type	Equivalent (von-Mises) Stress	Total Deformation	Maximum Principal Stress	Maximum Shear Stress	Maximum Principal Elastic Strain	Maximum Shear Elastic Strain
Integration Point Results						
Display Option	Averaged		Averaged			
Results						
Minimum	319.97 e-006 MPa	0. m	-1.1626e+001 MPa	172.41 e-006 MPa	1.5229e-008 m/m	6.8141e-008 m/m
Maximum	7.2395e+001 MPa	6.0679e-002 m	7.0976e+001 MPa	4.1793e+001 MPa	1.1995e-002 m/m	1.8167e-002 m/m

Appendix B:

V= 6.73m/s

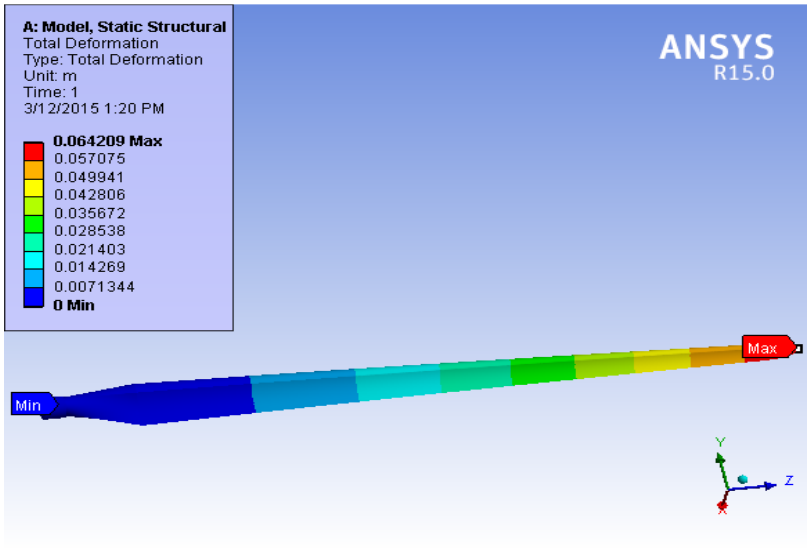

Figure B1 Directional Deformation

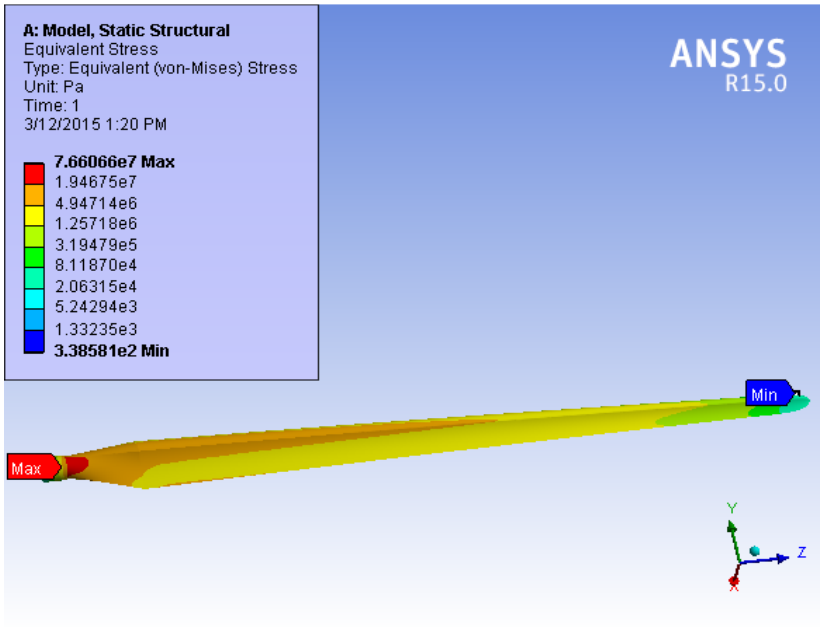

Figure B2 Equivalent Stress at V= 6.73m/s

Solution :

Table B 1 Model (A4) > Static Structural (A5) > Solution (A6) > Results

Object Name	*Equivalent Stress*	*Total Deformation*	*Maximum Principal Stress*	*Maximum Shear Stress*	*Maximum Principal Elastic Strain*	*Maximum Shear Elastic Strain*
State	Solved					
Scope						
Scoping Method	Geometry Selection					
Geometry	All Bodies					
Definition						
Type	Equivalent (von-Mises) Stress	Total Deformation	Maximum Principal Stress	Maximum Shear Stress	Maximum Principal Elastic Strain	Maximum Shear Elastic Strain
Integration Point Results						
Display Option	Averaged		Averaged			
Results						
Minimum	338.58e-006 MPa	0. m	-1.2303e+001 MPa	182.44 e-006 MPa	1.6115e-008 m/m	7.2105e-008 m/m
Maximum	7.6607e+001 MPa	6.4209e-002 m	7.5686e+001 MPa	4.4224e+001 MPa	1.2692e-002 m/m	1.9224e-002 m/m

Appendix C:

V= 6.22m/s

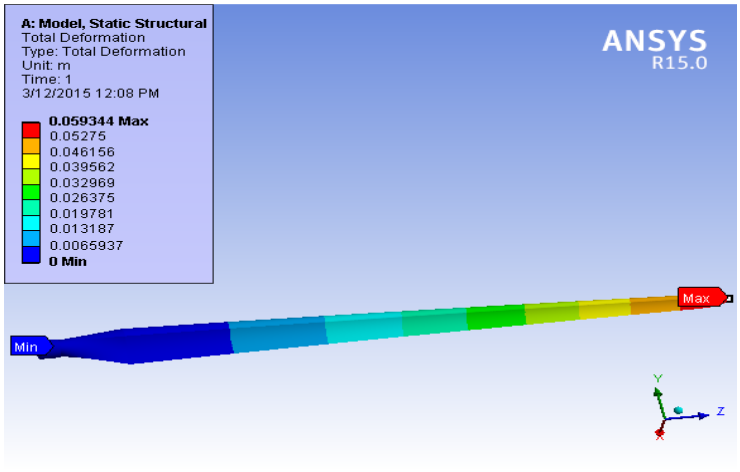

Figure C1 Directional Deformation

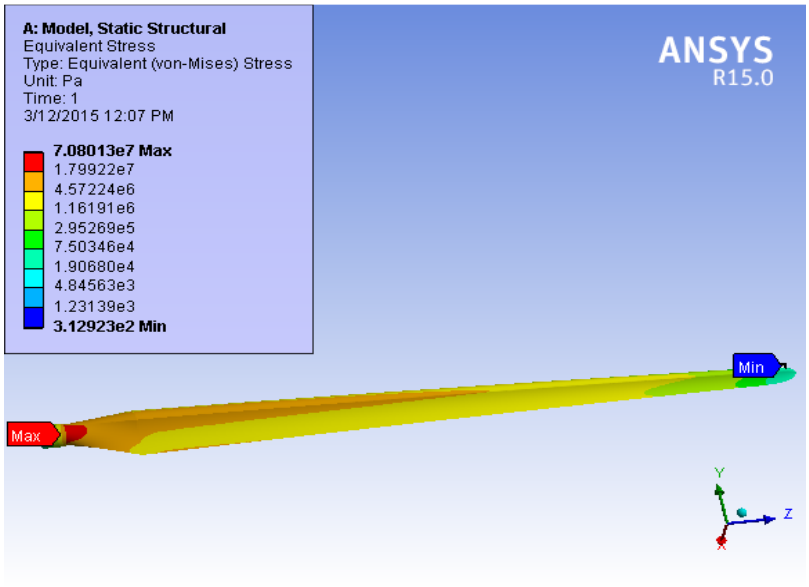

Figure C2 Equivalent Stress at V= 6.22m/s

Solution :

Table C1 Model (A4) > Static Structural (A5) > Solution (A6) > Results

Object Name	*Equivalent Stress*	*Total Deformation*	*Maximum Principal Stress*	*Maximum Shear Stress*	*Maximum Principal Elastic Strain*	*Maximum Shear Elastic Strain*
State	Solved					
Scope						
Scoping Method	Geometry Selection					
Geometry	All Bodies					
Definition						
Type	Equivalent (von-Mises) Stress	Total Deformation	Maximum Principal Stress	Maximum Shear Stress	Maximum Principal Elastic Strain	Maximum Shear Elastic Strain
Integration Point Results						
Display Option	Averaged		Averaged			
Results						
Minimum	312.92 e-006 MPa	0. m	-1.137e+001 MPa	168.61 e-006 MPa	1.4894e-008 m/m	6.6641e-008 m/m
Maximum	7.0801e+001 MPa	5.9344e-002 m	7.9193e+001 MPa	4.0873e+001 MPa	1.1731e-002 m/m	1.7768e-002 m/m

Appendix D:

V= 6.33m/s

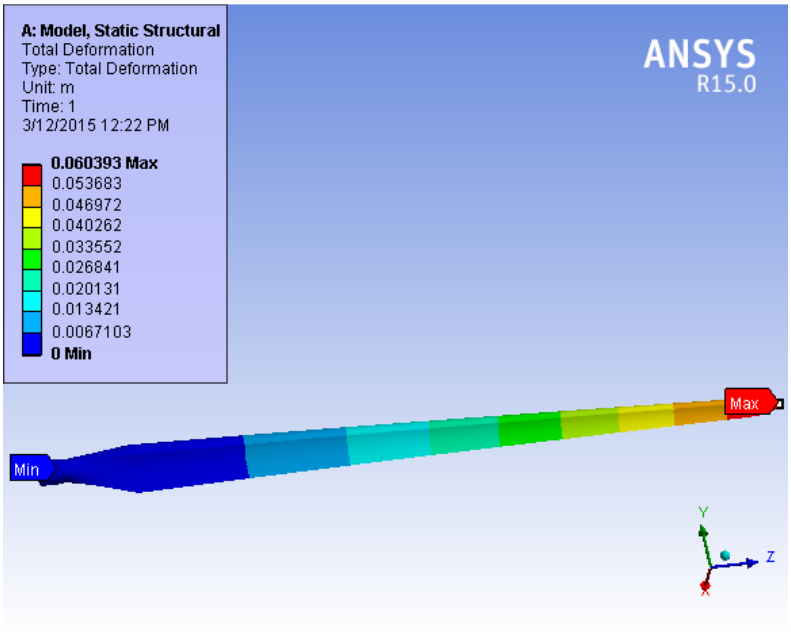

Figure D1 Directional Deformation

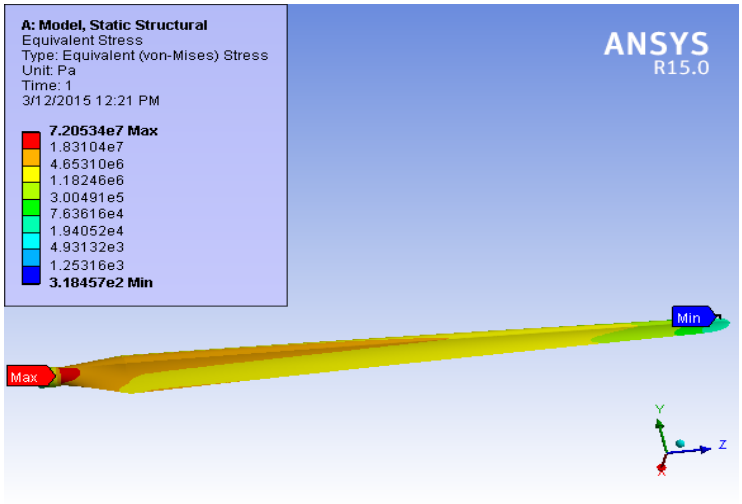

Figure D2 Equivalent Stress V= 6.33m/s

Solution :

Table D1 Model (A4) > Static Structural (A5) > Solution (A6) > Results

Object Name	*Equivalent Stress*	*Total Deformation*	*Maximum Principal Stress*	*Maximum Shear Stress*	*Maximum Principal Elastic Strain*	*Maximum Shear Elastic Strain*
State	Solved					
Scope						
Scoping Method	Geometry Selection					
Geometry	All Bodies					
Definition						
Type	Equivalent (von-Mises) Stress	Total Deformation	Maximum Principal Stress	Maximum Shear Stress	Maximum Principal Elastic Strain	Maximum Shear Elastic Strain
Integration Point Results						
Display Option	Averaged		Averaged			
Results						
Minimum	318.46 e-006 MPa	0. m	-1.1571e+001 MPa	171.59 e-006 MPa	1.5157e-008 m/m	6.7819e-008 m/m
Maximum	7.2053e+001MPa	6.0393e-002 m	7.0594e+001 MPa	4.1596e+001 MPa	1.1938e-002 m/m	1.8082e-002 m/m

Appendix E:

V= 7.67m/s

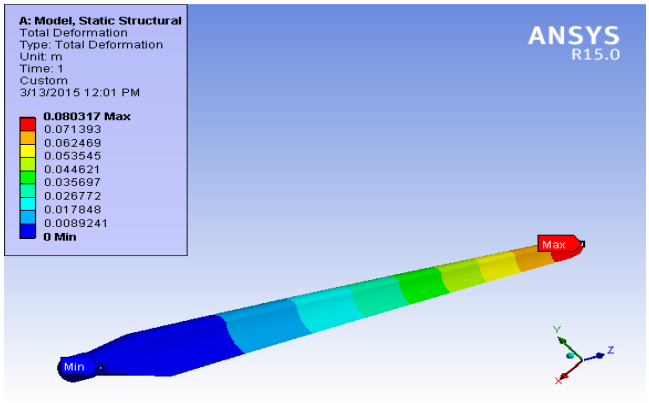

Figure E1 Directional Deformation

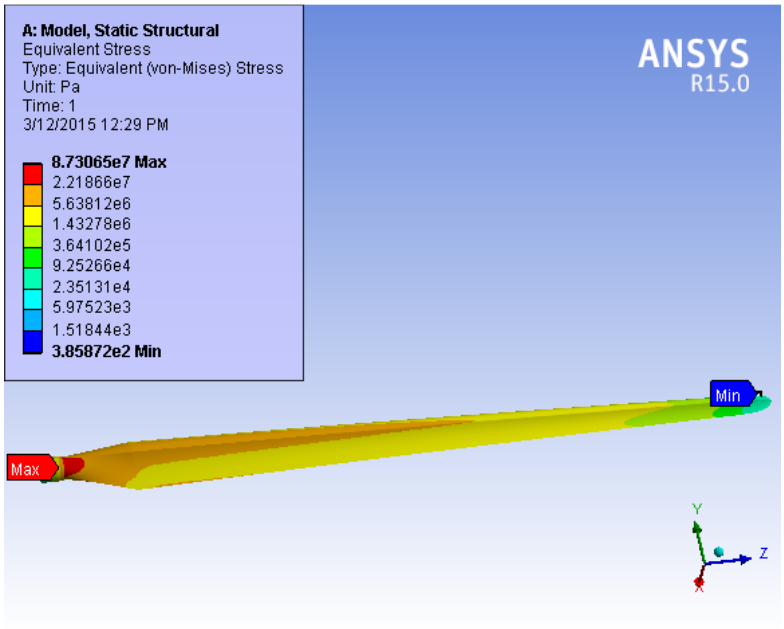

Figure E2 Equivalent Stress at V= 7.67m/s

Solution :

Table E1 Model (A4) > Static Structural (A5) > Solution (A6) > Results

Object Name	*Equivalent Stress*	*Total Deformation*	*Maximum Principal Stress*	*Maximum Shear Stress*	*Maximum Principal Elastic Strain*	*Maximum Shear Elastic Strain*
State	Solved					
Scope						
Scoping Method	Geometry Selection					
Geometry	All Bodies					
Definition						
Type	Equivalent (von-Mises) Stress	Total Deformation	Maximum Principal Stress	Maximum Shear Stress	Maximum Principal Elastic Strain	Maximum Shear Elastic Strain
Integration Point Results						
Display Option	Averaged		Averaged			
Results						
Minimum	385.87 e-006 MPa	0. m	-1.4021e+001 MPa	207.92 e-006 MPa	1.8366e-008 m/m	8.2176e-008 m/m
Maximum	8.7306e+001 MPa	7.3178e-002 m	8.7654e+001 MPa	5.0401e+001 MPa	1.4465e-002 m/m	2.191e-002 m/m

Appendix F:

V= 8.15m/s

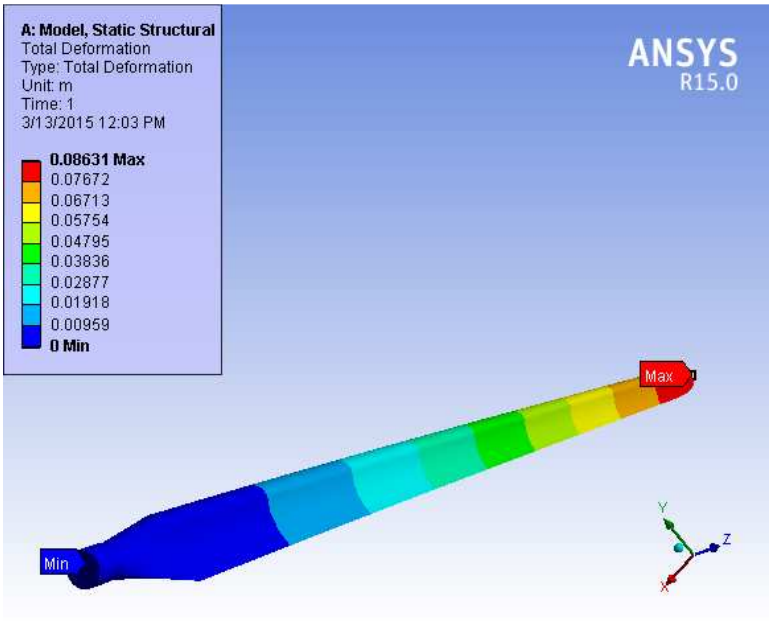

Figure F1 Directional Deformation

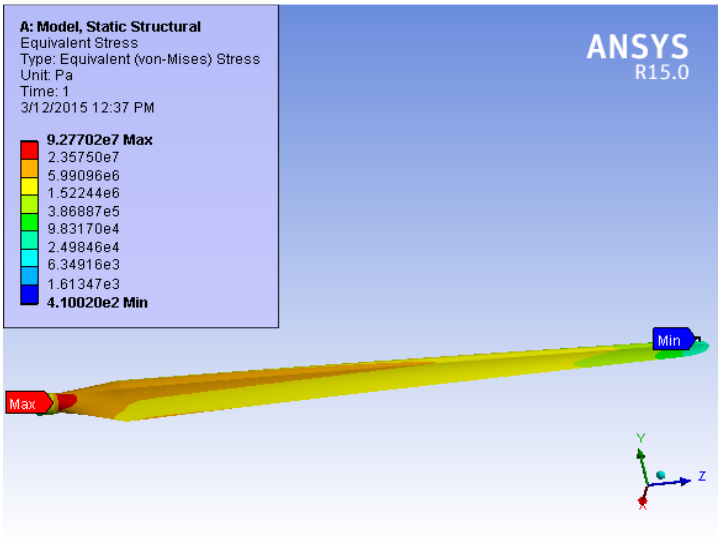

Figure F2 Equivalent Stress at V= 8.15m/s

Solution :

Table F1 Model (A4) > Static Structural (A5) > Solution (A6) > Results

Object Name	*Equivalent Stress*	*Total Deformation*	*Maximum Principal Stress*	*Maximum Shear Stress*	*Maximum Principal Elastic Strain*	*Maximum Shear Elastic Strain*
State	Solved					
Scope						
Scoping Method	Geometry Selection					
Geometry	All Bodies					
Definition						
Type	Equivalent (von-Mises) Stress	Total Deformation	Maximum Principal Stress	Maximum Shear Stress	Maximum Principal Elastic Strain	Maximum Shear Elastic Strain
Integration Point Results						
Display Option	Averaged		Averaged			
Results						
Minimum	410.02 e-006 MPa	0. m	-1.4898e+001 MPa	220.93 e-006 MPa	1.9515e-008 m/m	8.7319e-008 m/m
Maximum	9.277e+001 MPa	7.7757e-002 m	9.0377e+001 MPa	5.3556e+001 MPa	1.5371e-002 m/m	2.3281e-002 m/m

Appendix G:

V= 6.89m/s

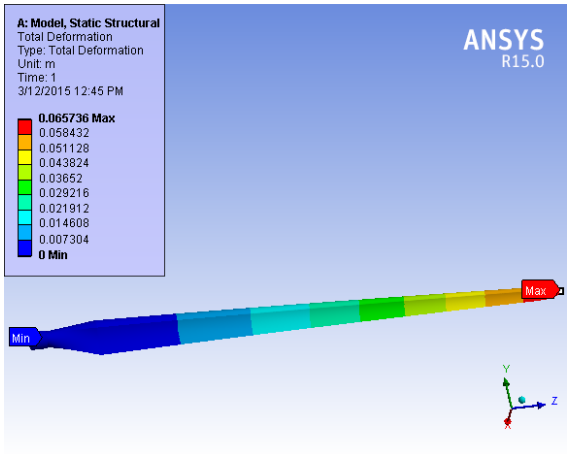

Figure G1 Directional Deformation

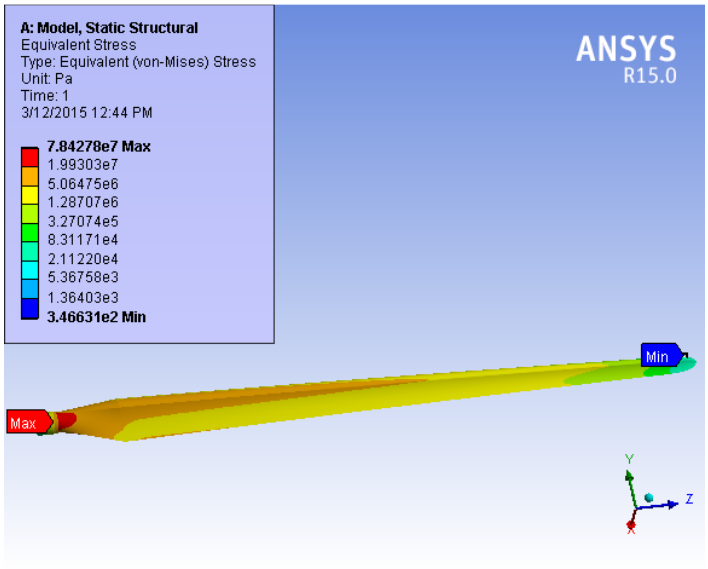

Figure G2 Equivalent Stress at V= 6.89m/s

Solution :

Table G1 Model (A4) > Static Structural (A5) > Solution (A6) > Results

Object Name	*Equivalent Stress*	*Total Deformation*	*Maximum Principal Stress*	*Maximum Shear Stress*	*Maximum Principal Elastic Strain*	*Maximum Shear Elastic Strain*
State	Solved					
Scope						
Scoping Method	Geometry Selection					
Geometry	All Bodies					
Definition						
Type	Equivalent (von-Mises) Stress	Total Deformation	Maximum Principal Stress	Maximum Shear Stress	Maximum Principal Elastic Strain	Maximum Shear Elastic Strain
Integration Point Results						
Display Option	Averaged		Averaged			
Results						
Minimum	346.63 e-006 MPa	0. m	-1.2595e+001 MPa	186.78 e-006 MPa	1.6498e-008 m/m	7.3819e-008 m/m
Maximum	7.8428e+001 MPa	6.5736e-002 m	7.7723e+001 MPa	4.5276e+001 MPa	1.2994e-002 m/m	1.9681e-002 m/m

Appendix H:

V= 6.15m/s

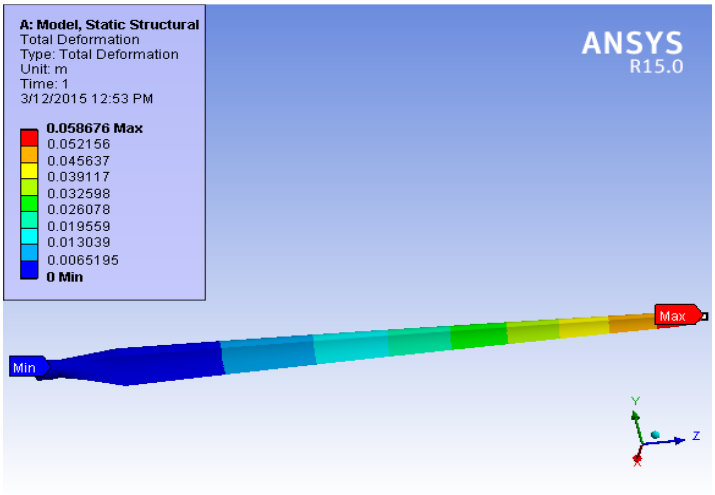

Figure H1 Directional Deformation

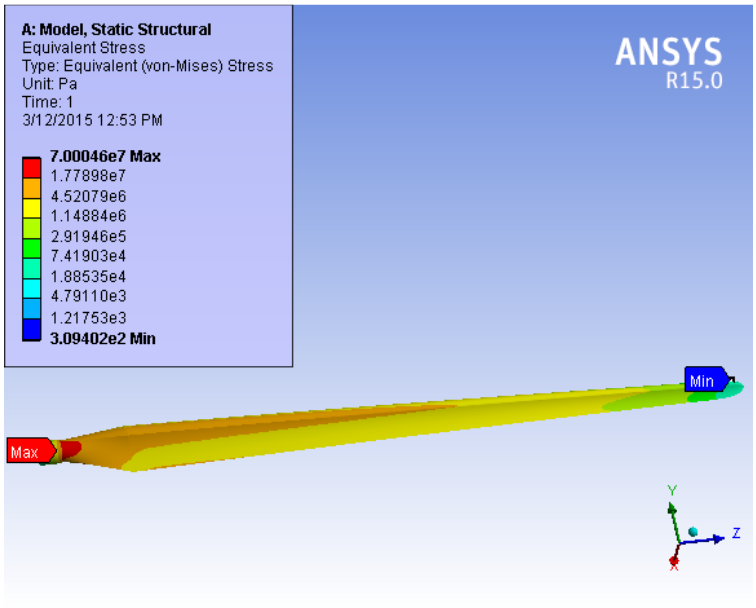

Figure H2 Equivalent Stress at V= 6.15m/s and p=353.44pa

Solution :

Table H1 Model (A4) > Static Structural (A5) > Solution (A6) > Results

Object Name	*Equivalent Stress*	*Total Deformation*	*Maximum Principal Stress*	*Maximum Shear Stress*	*Maximum Principal Elastic Strain*	*Maximum Shear Elastic Strain*
State	Solved					
Scope						
Scoping Method	Geometry Selection					
Geometry	All Bodies					
Definition						
Type	Equivalent (von-Mises) Stress	Total Deformation	Maximum Principal Stress	Maximum Shear Stress	Maximum Principal Elastic Strain	Maximum Shear Elastic Strain
Integration Point Results						
Display Option	Averaged		Averaged			
Results						
Minimum	309.4 e-006 MPa	0. m	-1.1242e+001 MPa	166.71 e-006 MPa	1.4726e-008 m/m	6.5891e-008 m/m
Maximum	7.0005e+001 MPa	5.8676e-002 m	6.8302e+001 MPa	4.0413e+001 MPa	1.1599e-002 m/m	1.7568e-002 m/m

Appendix I:

V= 6.17m/s

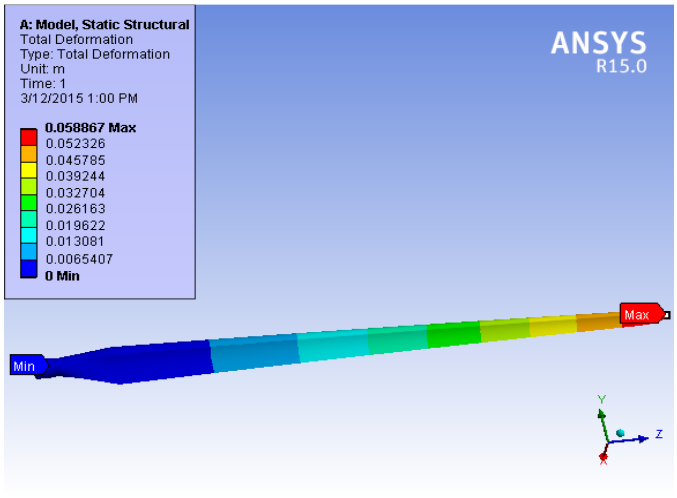

Figure I 1 Directional Deformation

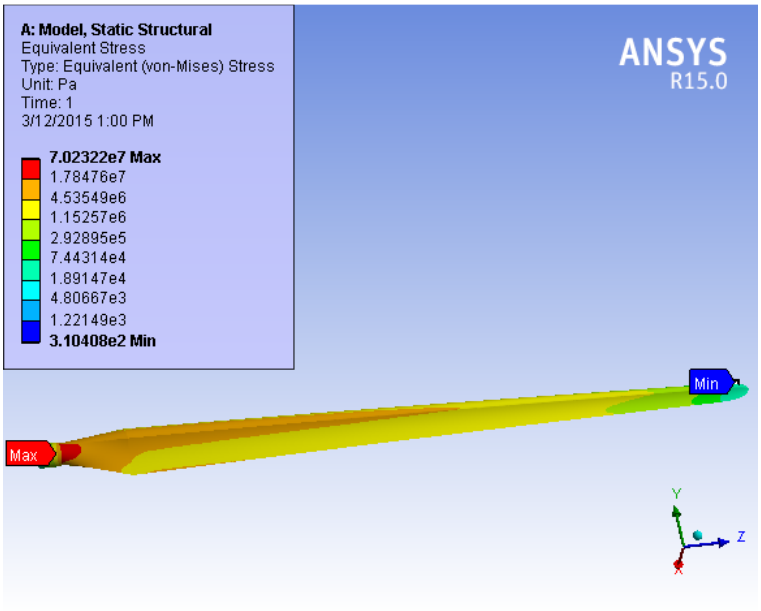

Figure I 2 Equivalent Stress at V= 6.17m/s

Solution :

Table I 1 Model (A4) > Static Structural (A5) > Solution (A6) > Results

Object Name	*Equivalent Stress*	*Total Deformation*	*Maximum Principal Stress*	*Maximum Shear Stress*	*Maximum Principal Elastic Strain*	*Maximum Shear Elastic Strain*
State	Solved					
Scope						
Scoping Method	Geometry Selection					
Geometry	All Bodies					
Definition						
Type	Equivalent (von-Mises) Stress	Total Deformation	Maximum Principal Stress	Maximum Shear Stress	Maximum Principal Elastic Strain	Maximum Shear Elastic Strain
Integration Point Results						
Display Option	Averaged		Averaged			
Results						
Minimum	310.41 e-006 MPa	0. m	-1.1279e+001 MPa	167.26 e-006 MPa	1.4774e-008 m/m	6.6105e-008 m/m
Maximum	7.0232e+001 MPa	5.8867e-002 m	6.8556e+001 MPa	4.0545e+001 MPa	1.1636e-002 m/m	1.7625e-002 m/m

Appendix J:

V= 6.31m/s

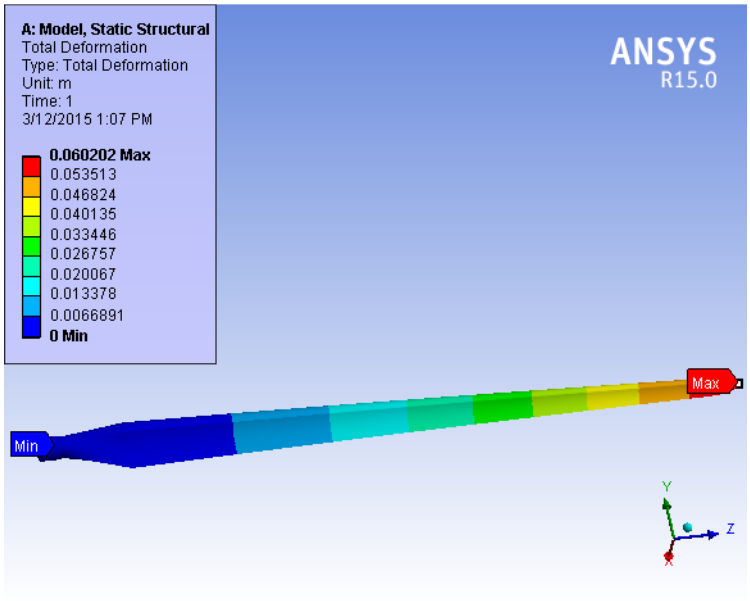

Figure J 1 Directional Deformation

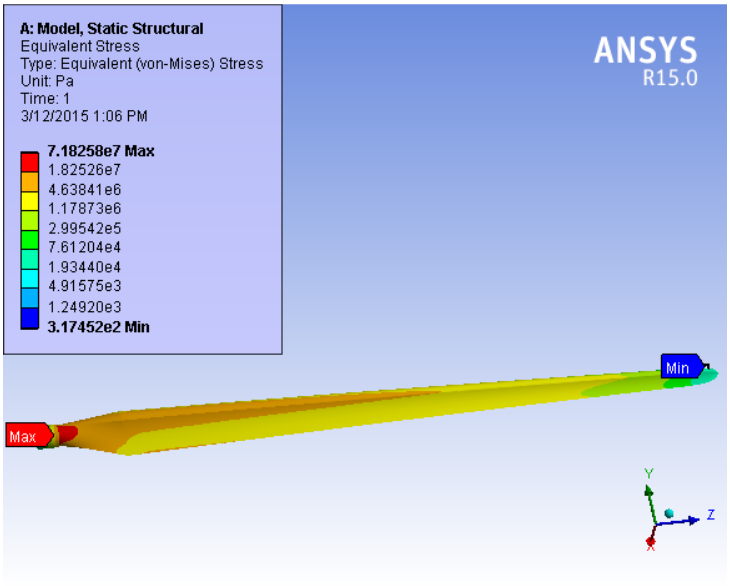

Figure J 2 Equivalent Stress at V= 6.31m/s

Solution :

Table J 1 Model (A4) > Static Structural (A5) > Solution (A6) > Results

Object Name	*Equivalent Stress*	*Total Deformation*	*Maximum Principal Stress*	*Maximum Shear Stress*	*Maximum Principal Elastic Strain*	*Maximum Shear Elastic Strain*
State	Solved					
Scope						
Scoping Method	Geometry Selection					
Geometry	All Bodies					
Definition						
Type	Equivalent (von-Mises) Stress	Total Deformation	Maximum Principal Stress	Maximum Shear Stress	Maximum Principal Elastic Strain	Maximum Shear Elastic Strain
Integration Point Results						
Display Option	Averaged		Averaged			
Results						
Minimum	317.45 e-006 MPa	0. m	-1.1535e+001 MPa	171.05 e-006 MPa	1.5109e-008 m/m	6.7605e-008 m/m
Maximum	7.1826e+001 MPa	6.0202e-002 m	7.0339e+001 MPa	4.1464e+001 MPa	1.19e-002 m/m	1.8025e-002 m/m

Appendix K:

V= 8.26m/s

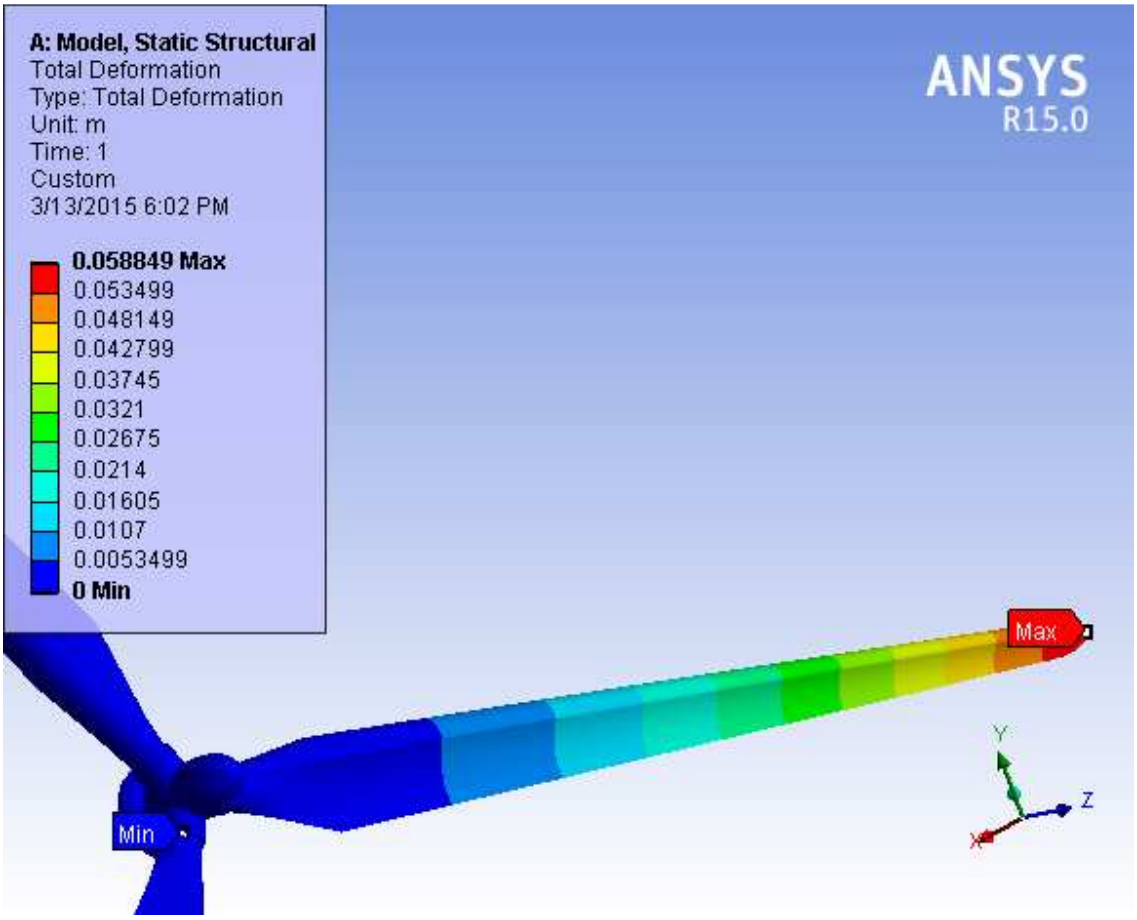

Figure k 1 Directional Deformation at V= 8.26m/s

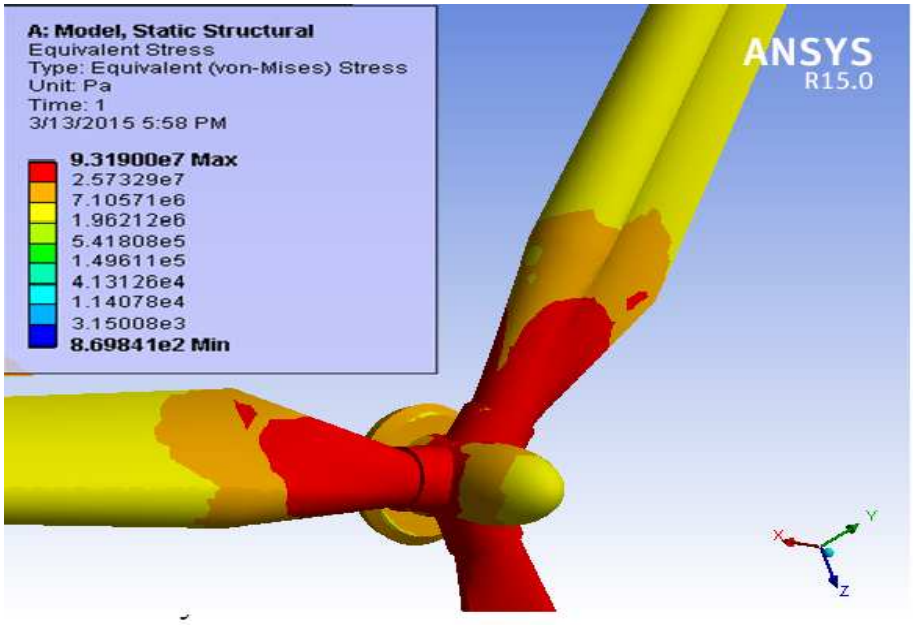

Figure K 2 Equivalent Stress at V= 8.26m/s

Solution :

Table K 1 Model (A4) > Static Structural (A5) > Solution (A6) > Results

Object Name	*Equivalent Stress*	*Total Deformation*
State	Solved	
Scope		
Scoping Method	Geometry Selection	
Geometry	All Bodies	
Definition		
Type	Equivalent (von-Mises) Stress	Total Deformation
Integration Point Results		
Display Option	Averaged	
Results		
Minimum	869.84 e-006 MPa	0. m
Maximum	9.319e+001 MPa	5.8849e-002 m